

DTIC FILE COPY

Technical Report

AD-A223 418

Bistatic Radar Cross Section of a Perfectly Conducting Rhombus-Shaped Flat Plate

DTIC
ELECTE
JUL 02 1990
S D C D

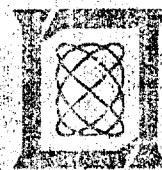
A.J. Koss

2 May 1990

Lincoln Laboratory

MASSACHUSETTS INSTITUTE OF TECHNOLOGY

LINCOLN, MASSACHUSETTS



Prepared for the Department of the Air Force
under Contract F19628-90-C-0002.

Approved for public release; distribution is unlimited.

Best Available Copy

This report is based on studies performed at Lincoln Laboratory, a center for research operated by Massachusetts Institute of Technology. The work was sponsored by the Department of the Air Force under Contract F19628-90-C-0002.

This report may be reproduced to satisfy needs of U.S. Government agencies.

The ESD Public Affairs Office has reviewed this report, and it is releasable to the National Technical Information Service, where it will be available to the general public, including foreign nationals.

This technical report has been reviewed and is approved for publication.

FOR THE COMMANDER

Hugh L. Southall

Hugh L. Southall, Lt. Col., USAF
Chief, ESD Lincoln Laboratory Project Office

Non-Lincoln Recipients

PLEASE DO NOT RETURN

Permission is given to destroy this document
when it is no longer needed.

PAGES _____
ARE
MISSING
IN
ORIGINAL
DOCUMENT

(2)

MASSACHUSETTS INSTITUTE OF TECHNOLOGY
LINCOLN LABORATORY

**BISTATIC RADAR CROSS SECTION OF A PERFECTLY
CONDUCTING RHOMBUS-SHAPED FLAT PLATE**

A.J. FENN
Group 61

DTIC
ELECTE
JUL 02 1990
S D D

TECHNICAL REPORT 880

2 MAY 1990

Approved for public release; distribution is unlimited.

LEXINGTON

MASSACHUSETTS

ABSTRACT

The bistatic radar cross section of a perfectly conducting flat plate that has a rhombus shape (equilateral parallelogram) is investigated. The Ohio State University electromagnetic surface patch code (ESP version 4) is used to compute the theoretical bistatic radar cross section of a 35- x 27-in rhombus plate at 1.3 GHz over the bistatic angles 15° to 142° . The ESP-4 computer code is a method of moments FORTRAN-77 program which can analyze general configurations of plates and wires. This code has been installed and modified at Lincoln Laboratory on a SUN 3 computer network. Details of the code modifications are described. Comparisons of the method of moments simulations and measurements of the rhombus plate are made. It is shown that the ESP-4 computer code provides a high degree of accuracy in the calculation of copolarized and cross-polarized bistatic radar cross section patterns.

Electromagnetic surfaces; Method of moments; Radar cross section; Rhombus

Accession For	
NTIS CRA&I	<input checked="" type="checkbox"/>
DIC TAB	<input type="checkbox"/>
Unannounced	<input type="checkbox"/>
Justification	
By	
Distribution/	
Availability Codes	
Dist	Avail and/or Special
A-1	



TABLE OF CONTENTS

ABSTRACT	iii
LIST OF ILLUSTRATIONS	vii
ACKNOWLEDGEMENTS	ix
1. INTRODUCTION	1
2. ELECTROMAGNETIC SURFACE PATCH CODE (ESP-4) MODIFICATIONS	3
2.1 Modifications to Input Data	4
2.2 Modifications for Fixed Bistatic Angle RCS Patterns	5
3. RESULTS	7
3.1 Rhombus Plate Model	7
3.2 Comparison of Simulated and Measured Bistatic RCS	14
4. CONCLUSION	39
REFERENCES	41
APPENDIX A - REVISED ESP-4 SOFTWARE LISTING	43

LIST OF ILLUSTRATIONS

Figure No.		Page
1-1	Geometry for bistatic radar cross section measurements. The angle β is the bistatic angle, and the angle θ is the target rotation angle.	1
2-1	Block diagram depicting the revisions made to the ESP-4 computer program. The input data have been restructured, and a new option for fixed bistatic angle RCS pattern computation has been added.	3
2-2	Geometry for bistatic radar cross section computation in the ESP-4 computer program.	5
3-1	Geometry for a rhombus flat plate. The rhombus characteristics (side length, interior angles, and area) are readily computed from the diagonal length L and diagonal width W .	7
3-2	Rhombus plate with diagonal length $L = 35$ in and diagonal width $W = 27$ in used both in ESP-4 simulations and in measurements.	8
3-3	Three-dimensional view of rhombus plate in (a) untilted and (b) tilted orientation (rotated 45° about the x axis). All RCS patterns in this report are taken in the xz plane.	9
3-4	Two-dimensional view (looking along the x -axis) of the plate in untilted and tilted configurations.	10
3-5	Bistatic geometry for flat plate. The bistatic angle is fixed and the target aspect angle θ varies. Note that $\theta = 0^\circ$ corresponds to the specular bistatic RCS.	11
3-6	Dual-polarized surface patch layout generated by ESP-4 for the 35×27 -in rhombus plate at 1.3 GHz.	13
3-7	Enlarged view of contiguous rhombus-shaped surface patch monopoles from Figure 3-6.	14
3-8	Three-view plot of the rhombus plate in the untilted orientation.	15
3-9	Three-view plot of the rhombus plate in the 45° tilted orientation.	16
3-10	Comparison of ESP-4 simulations and measurements of the copolarized (HH, VV) bistatic RCS for the 35×27 -in plate at 1.3 GHz. The bistatic angle is $\beta = 15^\circ$ and there is no plate tilt.	18

Figure No.		Page
3-11	Comparison of ESP-4 simulations and measurements of the cross-polarized (HV, VH) bistatic RCS for the 35- × 27-in plate at 1.3 GHz. The bistatic angle is $\beta = 15^\circ$ and there is no plate tilt.	19
3-12	Comparison of ESP-4 simulations and measurements of the copolarized (HH, VV) bistatic RCS for the 35- × 27-in plate at 1.3 GHz. The bistatic angle is $\beta = 45^\circ$ and there is no plate tilt.	20
3-13	Comparison of ESP-4 simulations and measurements of the copolarized (HH, VV) bistatic RCS for the 35- × 27-in plate at 1.3 GHz. The bistatic angle is $\beta = 45^\circ$ and the plate is tilted 45° .	21
3-14	Comparison of ESP-4 simulations and measurements of the cross-polarized (HV, VH) bistatic RCS for the 35- × 27-in plate at 1.3 GHz. The bistatic angle is $\beta = 45^\circ$, and there is no plate tilt.	22
3-15	Comparison of ESP-4 simulations and measurements of the cross-polarized (HV, VH) bistatic RCS for the 35- × 27-in inch plate at 1.3 GHz. The bistatic angle is $\beta = 45^\circ$, and the plate is tilted 45° .	23
3-16	Comparison of ESP-4 simulations and measurements of the copolarized (HH, VV) bistatic RCS for the 35- × 27-in plate at 1.3 GHz. The bistatic angle is $\beta = 90^\circ$, and there is no plate tilt.	24
3-17	Comparison of ESP-4 simulations and measurements of the copolarized (HH, VV) bistatic RCS for the 35- × 27-in plate at 1.3 GHz. The bistatic angle is $\beta = 90^\circ$, and the plate is tilted 45° .	25
3-18	Comparison of ESP-4 simulations and measurements of the cross-polarized (HV, VH) bistatic RCS for the 35- × 27-in plate at 1.3 GHz. The bistatic angle is $\beta = 90^\circ$, and there is no plate tilt.	26
3-19	Comparison of ESP-4 simulations and measurements of the cross-polarized (HV, VH) bistatic RCS for the 35- × 27-in plate at 1.3 GHz. The bistatic angle is $\beta = 90^\circ$, and the plate is tilted 45° .	27
3-20	Comparison of ESP-4 simulations and measurements of the copolarized (HH, VV) bistatic RCS for the 35- × 27-in plate at 1.3 GHz. The bistatic angle is $\beta = 120^\circ$, and there is no plate tilt.	28
3-21	Comparison of ESP-4 simulations and measurements of the copolarized (HH, VV) bistatic RCS for the 35- × 27-in plate at 1.3 GHz. The bistatic angle is $\beta = 120^\circ$, and the plate is tilted 45° .	29

Figure No.		Page
3-22	Comparison of ESP-4 simulations and measurements of the cross-polarized (HV, VH) bistatic RCS for the 35- × 27-in plate at 1.3 GHz. The bistatic angle is $\beta = 120^\circ$, and there is no plate tilt.	30
3-23	Comparison of ESP-4 simulations and measurements of the cross-polarized (HV, VH) bistatic RCS for the 35- × 27-in plate at 1.3 GHz. The bistatic angle is $\beta = 120^\circ$, and the plate is tilted 45° .	31
3-24	Comparison of ESP-4 simulations and measurements of the copolarized (HH, VV) bistatic RCS for the 35- × 27-in plate at 1.3 GHz. The bistatic angle is $\beta = 142^\circ$, and there is no plate tilt.	32
3-25	Comparison of ESP-4 simulations and measurements of the copolarized (HH, VV) bistatic RCS for the 35- × 27-in plate at 1.3 GHz. The bistatic angle is $\beta = 142^\circ$, and the plate is tilted 45° .	33
3-26	Comparison of ESP-4 simulations and measurements of the cross-polarized (HV, VH) bistatic RCS for the 35- × 27-in plate at 1.3 GHz. The bistatic angle is $\beta = 142^\circ$, and there is no plate tilt.	34
3-27	Comparison of ESP-4 simulations and measurements of the cross-polarized (HV, VH) bistatic RCS for the 35- × 27-in plate at 1.3 GHz. The bistatic angle is $\beta = 142^\circ$, and the plate is tilted 45° .	35
3-28	Comparison of ESP-4 simulations and measurements of the specular copolarized (HH, VV) bistatic RCS for the 35- × 27-in plate at 1.3 GHz.	36
3-29	Convergence check of ESP-4 simulations. The figure shows the copolarized (HH, VV) bistatic RCS for the 35- × 27-in plate at 1.3 GHz with two different surface patch sizes. The bistatic angle is $\beta = 142^\circ$, and there is no plate tilt.	37

ACKNOWLEDGEMENTS

The author wishes to express his gratitude to S.E. French for software support and to P. Grubel of the 6585th Test Group at Holloman Air Force Base, New Mexico for supplying the measured data.

1. INTRODUCTION

In radar cross section (RCS) measurements of complex targets it is desirable to make additional measurements of reference targets such as flat plates and cylinders for which the radar cross section is readily computed. These reference targets are used in checking the calibration, target quiet-zone characteristics, and mechanical alignment of the measurements system. This report addresses the simulated RCS of a perfectly conducting flat plate used in bistatic measurements. Depicted in Figure 1-1 is a typical geometry for bistatic RCS measurements. The angle β denotes the bistatic angle which is fixed, and the angle θ denotes the target rotation angle or aspect angle.

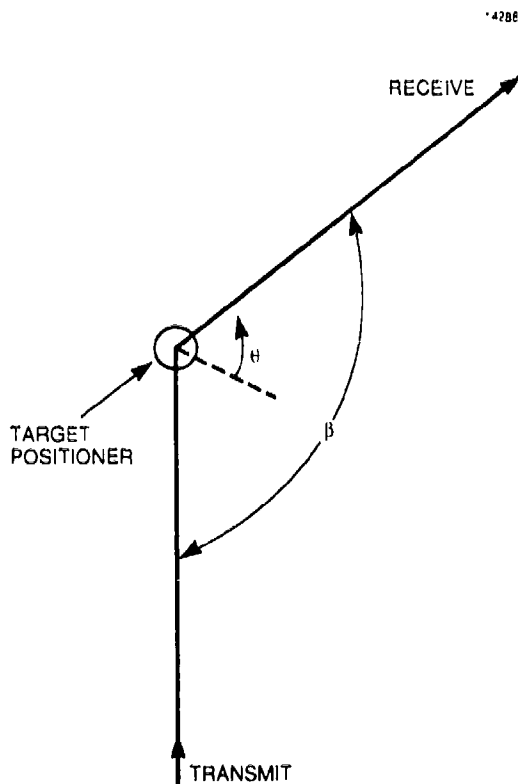


Figure 1-1. Geometry for bistatic radar cross section measurements. The angle β is the bistatic angle, and the angle θ is the target rotation angle.

Except for spheres and cylinders, little published data exist for the far-field bistatic radar cross section of targets [1-3]. The bistatic scattering from a sphere is readily computed [4] and is often used as a primary calibration standard in RCS measurements. Bistatic scattering analyses and measurements for a conducting cylinder of finite length are described in [5-8]. Monostatic scattering from square and circular flat plates is treated thoroughly in [1-3]. A physical optics formulation for the bistatic scattering of a polygonal flat plate is reviewed in [3]. The bistatic RCS

of rectangular and triangular plates has been calculated in [8]. The purpose of this report is to compare simulated and measured data for a rhombus-shaped (equilateral parallelogram) flat plate over a broad range of bistatic angles.

A method of moments code called ESP-4 (electromagnetic surface patch code: version 4) which is capable of analyzing a wide variety of antenna or radar cross section problems has been developed at The Ohio State University [9]. The software can analyze complex geometries involving multiple-connected plates and/or wires and is well-suited to analyzing the scattering from an isolated quadrilateral plate like the rhombus. Many of the subroutines in the ESP-4 code are based on subroutines from an earlier wire-grid RCS/antenna method of moments code developed by Richmond [10]. Wire-grid modeling of a continuous surface, such as a flat plate, is approximated with closely spaced conducting wires [11]. A similar wire-grid moment method computer code is described in [12]. In contrast, surface patch modeling allows a piecewise-continuous approximation to a complicated surface. Surface patch modeling requires fewer unknowns than wire-grid modeling; hence, larger surfaces can be modeled. ESP-4 utilizes the electric field integral equation (EFIE) to enforce the boundary condition of the tangential electric field being zero at the surface of the antenna/target of interest. The EFIE solution allows for either open or closed surfaces. The basis and testing functions used in this code are piecewise sinusoidal. The surface patches (or surface current modes) are assumed to have zero thickness and are quadrilateral dipoles which are useful in modeling an arbitrary-shaped body. For a complete description of the theory and capabilities of the ESP-4 code, the reader is referred to the user's manual [9]. Other moment method codes exist which are based on the magnetic field integral equation (MFIE) for closed surfaces [13,14] and EFIE for arbitrary surfaces [15-17]. The EFIE moment method formulation used in [15-17] differs from the ESP-4 formulation in that triangular-shaped basis functions with pulse weighting are used for the surface current mode vectors.

This report is organized in the following manner: In Section 2, details of the modifications made to the electromagnetic surface patch code ESP-4 are given. The basic modifications of the ESP-4 code are a change in the input data structure and a new option for fixed bistatic angle RCS patterns. A listing of the revised ESP-4 main program is given in the appendix. Bistatic RCS patterns for a 35- x 27-in rhombus flat plate at 1.3 GHz are computed with the ESP-4 code and the results are given in Section 3. Bistatic angles from 15° to 142° have been considered as well as two plate orientations (untilted and tilted). The method of moments simulations are compared against measured data and good agreement is demonstrated.

2. ELECTROMAGNETIC SURFACE PATCH CODE (ESP-4) MODIFICATIONS

The purpose of this section is to describe the modifications made to the main program of The Ohio State University (OSU) electromagnetic surface patch code (ESP-4). This software was obtained in July 1988 from OSU and has since been modified at Lincoln Laboratory. The important modifications are the addition of namelist input data and an option for bistatic radar cross section calculation with a fixed bistatic angle and variable target rotation. A complete description of how to use the ESP-4 code can be found in the user's manual [9]. The revisions to the ESP-4 code are summarized graphically in Figure 2-1 and are described in detail in Sections 2.1 and 2.2.

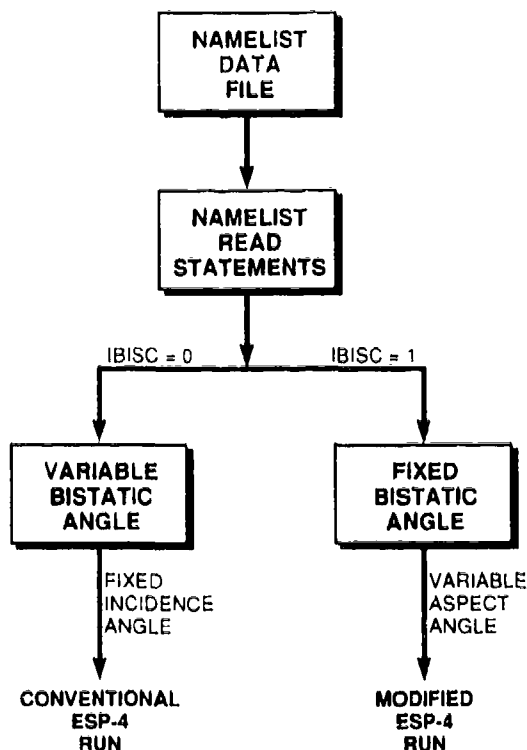


Figure 2-1. Block diagram depicting the revisions made to the ESP-4 computer program. The input data have been restructured, and a new option for fixed bistatic angle RCS pattern computation has been added.

2.1 MODIFICATIONS TO INPUT DATA

The original ESP-4 code defined plate/wire geometries and antenna/RCS pattern cuts through a series of free-format [READ(11.*)] read statements on device 11. There are nearly 80 input parameters in the input data file and the addition of FORTRAN NAMELISTS, where every input quantity is clearly defined, is very attractive. When a NAMELIST is used, the input data are in free format and a typical input parameter, say A, is of the explicit form A=1.0, for example. The NAMELIST data file is helpful in constructing input files for the ESP-4 program that are user-friendly and easily debugged. The present Lincoln Laboratory version of ESP-4 has attempted to keep the definition of the input parameters the same as in the OSU ESP-4 user's manual [9]. The manual should be consulted for the definition of most of the input parameters. Here, only newly defined parameters (input variables) will be defined. Nine namelists have been added to the ESP-4 code and all READ(11.*) statements have been commented. The NAMELIST reads have the form READ(11,NAM) where NAM is the name of the NAMELIST. The added namelist statements (in FORTRAN) are summarized below and follow line ESP01650 of the ESP-4 code.

```
NAMelist /RNCTRL/NGO,NPRINT,NRUNS,NWGS,IWR,IWRZT,INT,INTP,INTD,  
2INWR,IRGM,IFIL,RF,INDZI  
NAMelist /FSWEEP/FMC1,FMC2,DFZI,DFF,IRS12,THRD,PHRD,THRI,PHRI  
NAMelist /PATTRN/IFE,IPFE,FNDFE,PHFE,IFA,IPFA,FNDFA,THFA,  
2ISE,IPSE,FNDSE,PHSE,THIN,PHIN,ISA,IPSA,FNDSA,THSA,  
3AZRANG,ELRANG,AZMIN,ELMIN,IBISC,BETA,NPTBIS,BANGRG  
NAMelist /FWIRET/FMC,CMM,A,NPLTS  
NAMelist /PLATEG/NCNRS,SEGM,IREF,IPN,IGS,ZSHT,XP,YP,ZP  
NAMelist /SAVEZ/IWRZM,IRDZM  
NAMelist /WIREAG/NM,NP,NAT,NFPT,NFS1,NFS2,X,Y,Z,IA,IB  
NAMelist /GENLOD/IFMM,IABB,VLGG,ZLL  
NAMelist /ATTACH/NASAT,IABAT,NFLA,VGA,ZLDA,BDSK
```

The relation between the new namelists and the old read statements is as follows:

- RNCTRL=READ #1
- FSWEEP=READ #1A
- PATTRN=READS # 2,3,4,5 with the addition of parameters AZRANG, ELRANG, AZMIN, ELMIN, IBISC, BETA, NPTBIS, BANGRG described in Section 2.2.
- FWIRET=READ #6 with the addition of the parameter NPLTS (number of plates) from READ #7. Namelist PLATEG (described next) is read NPLTS number of times.
- PLATEG=READS # 7, 8, 9 with the substitution of explicit (XP, YP, ZP) coordinates in array format for the corners of plate NPL. The software then fills in the original three-dimensional PCN arrays (see ESP-4 manual) which contain the plate corner coordinates.

- SAVEZ=READ #10
- WIREAG=READS #11, 12, 13
- GENLOD=READ #14 is executed NFPT times corresponding to the number of feed points.
- ATTACH=READ #15 is executed NAT times corresponding to the number of attachment points between plates and wires.

2.2 MODIFICATIONS FOR FIXED BISTATIC ANGLE RCS PATTERNS

Consider Figure 2-2 which shows the bistatic geometry for an arbitrary target. The pair of angles (θ_i, ϕ_i) denotes the incident direction and, similarly, (θ_s, ϕ_s) denote the scattering direction. The original version of ESP-4 assumed in a bistatic calculation that the angle of incidence was fixed

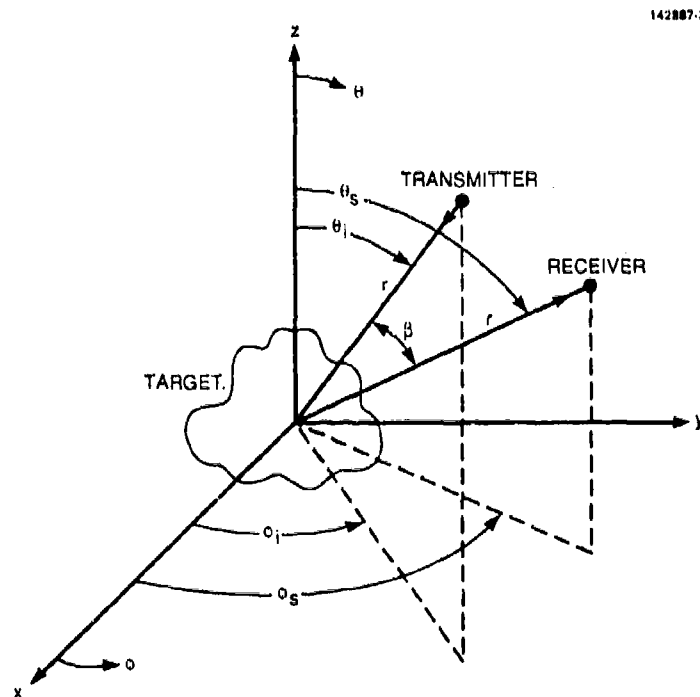


Figure 2-2. Geometry for bistatic radar cross section computation in the ESP-4 computer program.

and the scattering direction (or observation angle) was variable. Thus, the software computes the bistatic RCS pattern as a function of bistatic angle. As described earlier in Figure 1-1, this differs

from a typical bistatic RCS measurement where the bistatic angle is fixed and the target rotation angle varies. The Lincoln Laboratory version of ESP-4 uses a new option, IBISC=1, which fixes the bistatic angle BETA and increments the incident and observation angles appropriately. The implementation of the new option occurs, primarily, following line ESP14200. Note: If IBISC=0 or is not specified, then the code performs in the original bistatic mode where the angle of incidence is fixed and the observation angle varies. When IBISC=1, NPTBIS is the number of target rotation angles and BANGRG is the angular range of target rotation in degrees. BANGRG can be a positive or negative number, as appropriate, to determine the target rotation direction (clockwise or counterclockwise). The original scattering indicators ISE, ISA must be set equal to the appropriate value to invoke bistatic RCS computation in the appropriate elevation or azimuth plane. For example, for scattering in the elevation plane (ϕ is constant) the following three lines of input data are appropriate:

```
ISE=2, IPSE=1, FNDSE=3.0, PHSE=0.0, THIN=90.0, PHIN=0.0, ELRANG=360.,
ISA=0, IPSA=1, FNDSE=3.0, THSA=90.0,
IBISC=1, BETA=120., NPTBIS=121, BANGRG=-360.,
```

ISE is set equal to 2 to indicate that bistatic scattering in the elevation plane is desired. ISA is set equal to 0 to indicate that an azimuth plane scattering pattern is not desired. IBISC is set equal to 1 to invoke the fixed bistatic angle option with BETA=120, the bistatic angle in degrees; NPTBIS=121, the number of target rotation angles for the fixed bistatic angle; and BANGRG=-360, the angular range of target rotation in the counterclockwise direction (+360 would produce clockwise rotation). With IBISC=1, PHIN=0.0 in the first data line is used; however, the value of THIN is computed within the new section of code. The initial value of THIN is equal to $-BETA/2$ and is then uniformly incremented within a new DO LOOP (DO 1920 IBIS=1, NPTBIS) over the target rotation angular range BANGRG. The initial observation angle or scattered angle is initially set equal to $+BETA/2$ and is similarly incremented. If the target is a flat plate located in the xy plane, then the first point computed by the ESP-4 code is the bistatic specular response. This fact is due to the broadside direction being chosen as the bisector of the bistatic angle. This choice is arbitrary and can be changed as desired within the revised ESP-4 code between lines ESP14200 and ESP14240. Note: In the above three data lines if IBISC is set to 0, then the program would compute a bistatic pattern in the elevation plane based on the values given in the first data line above. Thus, the program would run as in the original version of ESP-4.

The original ESP-4 code assumes that azimuth and elevation antenna/RCS patterns cover a full 360° angular range. New parameters, AZRANG, ELRANG have been included in the input data to cover an arbitrary azimuth and elevation range, respectively. Additionally, to start patterns at an arbitrary azimuth or elevation angle, AZMIN and ELMIN, respectively, have been defined. The default values of AZMIN and ELMIN are zero so that they do not have to be defined in the input data file. Further, the line involving IBISC does not have to be defined in the input data since appropriate default values are specified prior to the READ(11, PATTRN) statement. It should be noted that when the new bistatic option is used, the parameters AZRANG and ELRANG are automatically set equal to zero. This effectively forces the number of scattering angles equal to one for a given incident angle. Other minor changes to the code are documented with comments in the modified ESP-4 code listed in the appendix.

3. RESULTS

3.1 RHOMBUS PLATE MODEL

For a general rhombus flat plate, as shown in Figure 3-1, let L and W represent the diagonal

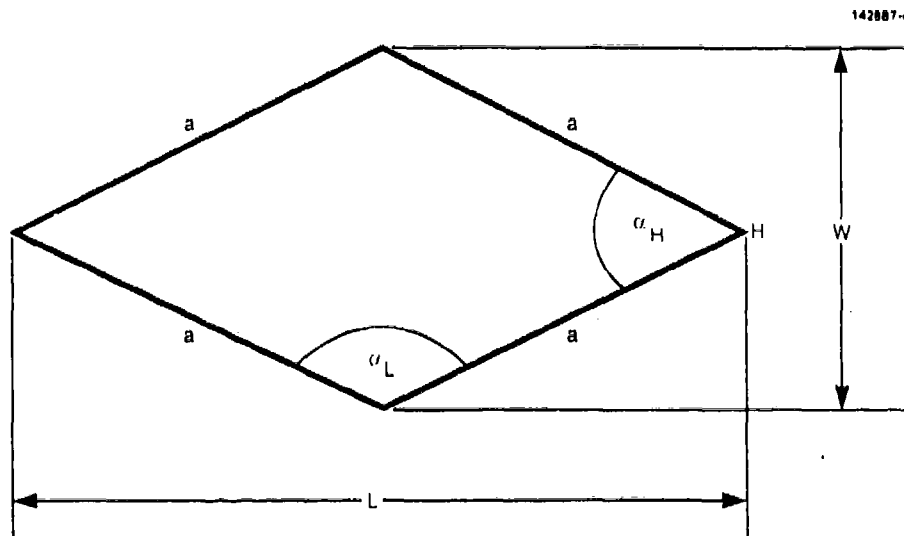


Figure 3-1. Geometry for a rhombus flat plate. The rhombus characteristics (side length, interior angles, and area) are readily computed from the diagonal length L and diagonal width W .

length and diagonal width, respectively, and let a be the side length. The side length of the rhombus is computed according to

$$a = \frac{\sqrt{L^2 + W^2}}{2} \quad (3.1)$$

and the area A , is given by

$$A = \frac{1}{2}LW \quad (3.2)$$

The rhombus interior angles α_L and α_W are computed using

$$\alpha_L = 2 \sin^{-1}\left(\frac{L}{2a}\right) \quad (3.3)$$

$$\alpha_W = 2 \sin^{-1}\left(\frac{H}{2a}\right). \quad (3.4)$$

The specular monostatic radar cross section of the flat plate is given by the well-known equation

$$\sigma = \frac{4\pi A^2}{\lambda^2}. \quad (3.5)$$

A sketch of the rhombus flat plate target under consideration is shown in Figure 3-2. The plate has a diagonal length $L = 35$ in and a diagonal width $W = 27$ in. The length of each of the

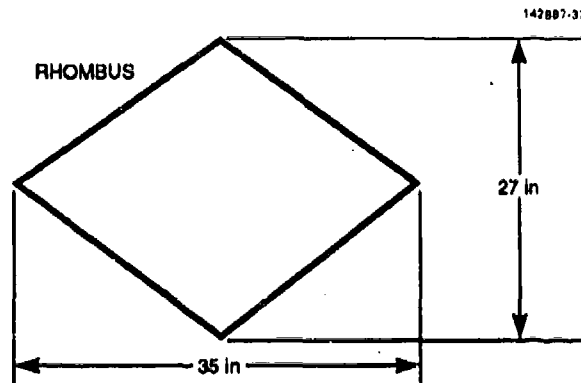
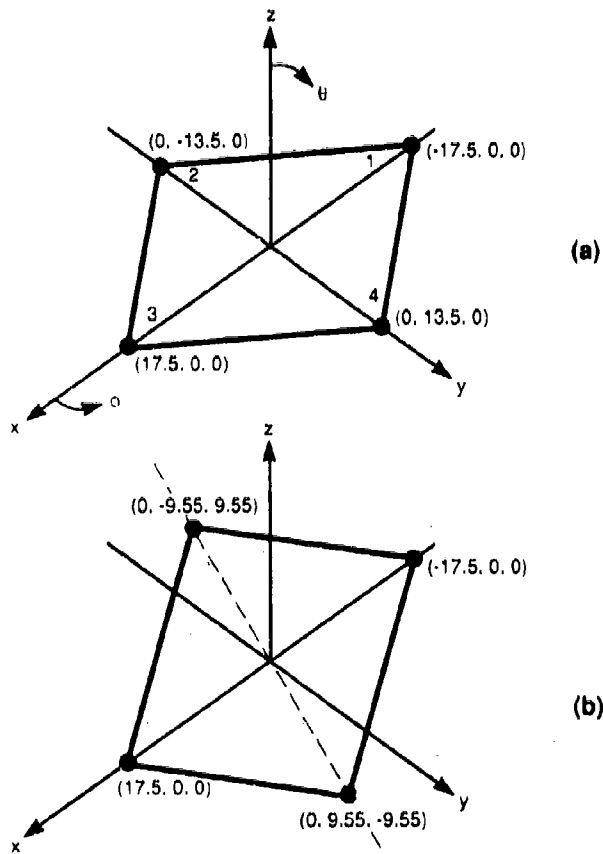


Figure 3-2. Rhombus plate with diagonal length $L = 35$ in and diagonal width $W = 27$ in used both in ESP-4 simulations and in measurements.

four sides is approximately 22.1 in. The acute angles of this plate are $\alpha_W = 75.3^\circ$ and the obtuse angles are $\alpha_L = 104.7^\circ$. In terms of wavelength, at the frequency of interest 1.3 GHz, the electrical dimensions of the plate are $L = 3.85\lambda$ and $W = 2.97\lambda$ and the plate area is 5.74 square wavelengths. The thickness of the experimental plate is 0.5 in or 0.055λ and the plate is simulated using zero thickness. For the given plate dimensions, the specular monostatic radar cross section is computed (using Equations 3.2 and 3.5) to be 13.4 dBsm at the desired frequency 1.3 GHz. Figure 3-3 shows a three-dimensional view of the plate located in the rectangular coordinate system for two plate orientations. In Figure 3-3(a), the plate is in the xy plane and in Figure 3-3(b), the plate has been rotated by 45° with respect to the y axis. In this report, the RCS pattern cuts are always taken in the xz plane. Notice that the long dimension of the plate (35 in) is oriented in the x direction. A two-dimensional view (looking along the x -axis) of the plate in untilted and tilted configurations is shown in Figure 3-4. The bistatic geometry for the plate is depicted in Figure 3-5. Note that the



NOTE: ALL DIMENSIONS ARE IN INCHES

Figure 3-3. Three-dimensional view of rhombus plate in (a) untilted and (b) tilted orientation (rotated 45° about the x axis). All RCS patterns in this report are taken in the xz plane.

angle θ represents the effective target rotation angle for the fixed bistatic angle β . When $\theta = 0^\circ$, the perpendicular direction to the plate is at the bisector of the bistatic angle.

The ESP-4 code was used to analyze the bistatic scattering patterns of the rhombus plate. Bistatic angles of 15° , 45° , 90° , 120° , and 142° were considered corresponding to available 35×27 -in rhombus flat plate measured RCS data collected in 1987 at the US Air Force Radar Target Scatter Facility (RATSCAT)[18]. The important input data for the ESP-4 RCS simulations are listed below with a description of the parameters.

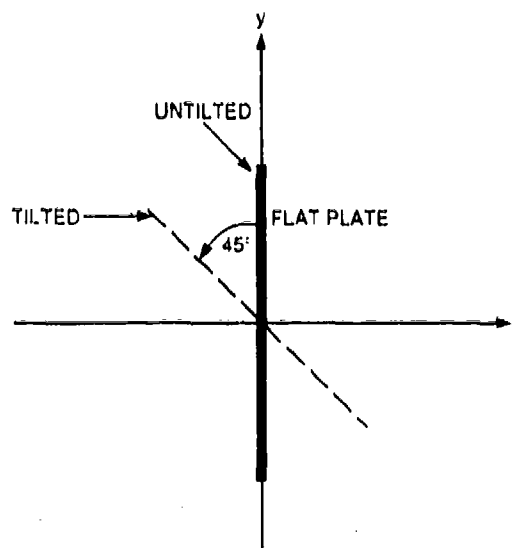


Figure 3-4. Two-dimensional view (looking along the x-axis) of the plate in untitled and tilted configurations.

```
&RNCTRL (Run control parameters)
  NGO=1,NPRINT=2,NRUNS=1,NWGS=1,IWR=0,IWRZT=0,INT=4,INTP=6,INTD=18,
  INWR=0,IRGM=1,IFIL=0,RF=-1.0,INDZI=0,
&
```

In NAMELIST RNCTRL, the parameter NGO=1 runs the ESP-4 program from start to finish. Printout of input parameters and target geometry is implemented with NPRINT=2. The program is executed one time (NRUNS=1) and NWGS is not used. The parameters IWR and IWRZT are both set to zero which means that the induced modal currents and impedance matrix elements, respectively, are not printed out. The parameter INT is not used. The number of Simpson's rule integration intervals used in integrating over the surface patch monopoles is specified by INTP=6. The parameter INTD is not used and INWR=0 means that there are no wires in the target geometry. The parameter IRGM is not used. The parameter IFIL=0 means that full surface patch test modes are used, and RF=-1 performs a far-field computation. The parameter INDZI is set to zero which means do not perform a frequency sweep computation.

```
&PATRN (Pattern specifications)
  IFE=0,IPFE=1,FNDFE=3.0,PHFE=90.0,
  IFA=0,IPFA=1,FNDFFA=3.0,THFA=90.0,
  ISE=2,IPSE=1,FNDSE=3.0,PHSE=0.0,THIN=90.0,PHIN=0.0,ELRANG=0.,
```

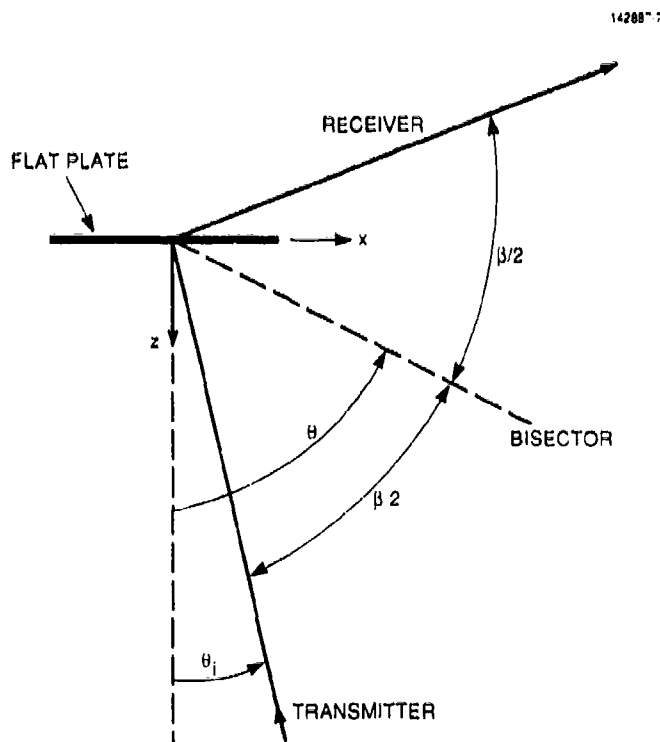


Figure 3-5. Bistatic geometry for flat plate. The bistatic angle is fixed and the target aspect angle θ varies. Note that $\theta = 0^\circ$ corresponds to the specular bistatic RCS.

```
ISA=0,IPSA=1,FNDSA=3.0,THSA=90.0,
IBISC=1,BETA=120.,NPTBIS=121,BANGRG=-360.,
```

The third and fifth lines of the PATTRN NAMELIST indicate that a bistatic scattering elevation pattern (ISE=2) with the new fixed bistatic angle option (IBISC=1) is used. The bistatic angle is defined by BETA=120 (degrees). The azimuth cut angle (ϕ) is PHSE=0 (degrees), which produces a pattern in the xz plane. The incident wavefront azimuth angle (ϕ_i) is PHIN=0 (degrees). The number of target rotation angles is NPTBIS=121, and the range of target rotation is BANGRG=-360 (counter clockwise rotation). Lines 1, 2, and 4 of PATTRN indicate that no other pattern cuts are desired.

```
&FWIRET (Frequency, wire type, and number of plates)
FMC=1300.0,CMM=38.0,A=0.001,NPLTS=1,
```

The frequency has been set to 1.3 GHz (FMC=1300, frequency in MHz) and CMM and A are not used. The number of plates is NPLTS=1.

```

&PLATEG (Plate geometry)
  NCNRS(1)=4,SEGM(1)=0.2,IREC(1)=0,IPN(1)=3,IGS(1)=0,ZSHT(1)=(0.0,0.0),
  XP(1)=-.4445,0.,.4445,0.,
  YP(1)=0.,-.3429,0.,.3429,
  ZP(1)=0.0,0.0,0.0,0.0,
&

```

There are 4 corners on the plate [NCNRS(1)=4], and the maximum surface patch segment size is 0.2λ . The parameter IREC(1)=0 means that the plate is polygonal rather than rectangular. The parameter IPN(1)=3 means that two polarizations are used in the surface patch currents. The parameter IGS=0 means that ESP-4 selects a reference side of the plate. A perfectly conducting plate is defined by the complex sheet impedance ZSHT(1)=(0.0,0.0). The four corners of the plate are described in rectangular coordinates by the data arrays XP, YP, and ZP in meters and correspond to the coordinates shown in Figure 3-3(a).

```

&SAVEZ (Save or reuse impedance matrix)
  IWRZM=1,IRDZM=0,
&

```

The program saves the impedance matrix for additional runs using the parameter IWRZM=1.

After performing an initial run and storing the impedance matrix, a second run is made in which the impedance matrix is read-in using the following input data:

```

&SAVEZ
  IWRZM=0,IRDZM=3,
&

```

For the case of the 45° tilted rhombus plate [Figure 3-3(b)] the input plate geometry NAMELIST is given by

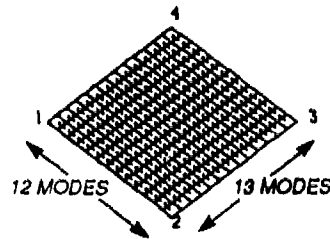
```

&PLATEG
  NCNRS(1)=4,SEGM(1)=0.2,IREC(1)=0,IPN(1)=3,IGS(1)=0,ZSHT(1)=(0.0,0.0),
  XP(1)=-.4445,0.,.4445,0.,
  YP(1)=0.,-.2425,0.,.2425,
  ZP(1)=0.0,.2425,0.0,-.2425,
&

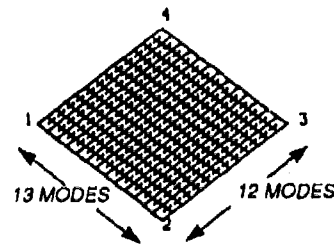
```

The first step in running the ESP-4 code is to verify the target (flat plate) input geometry. This is done by specifying NGO=0 in the input data file. After running the ESP-4 program, an output file is generated which contains the input geometry information. Geometry plotting software called ESP4GM was included with the ESP-4 software and was used to generate visual information about the plate simulation. ESP4GM is a FORTRAN 77 program which utilizes GKS (Graphic Kernel System) software. The results are summarized in Figures 3-6 to 3-9. Figure 3-6 shows the layout of the overlapping piecewise-sinusoidal surface patch modes for both polarizations. For

35 x 27 inch plate



156 MODES FOR
SECOND POLARIZ.



156 MODES FOR
FIRST POLARIZ.

312 TOTAL MODES ON PLATE

NOTE: COMPUTER OUTPUT; ITALICS ADDED BY AUTHOR

Figure 3-6. Dual-polarized surface patch layout generated by ESP-4 for the 35- x 27-in rhombus plate at 1.3 GHz.

each polarization there are 156 modes arranged in a 12×13 grid. In terms of the plate surface area ($5.74\lambda^2$) there are approximately 27 modes (of one polarization) per square wavelength. Each dipole surface patch mode is a parallelogram, and two of these modes arranged side by side form a rhombus, which is similar to the rhombus plate. A detailed (enlarged) view of two contiguous patches of each polarization is depicted in Figure 3-7. The polarization vectors of the two different modes (which are not quite orthogonal) make an obtuse angle with respect to each other that is 104.7° as determined from Equation (3.4). One of the dipole surface patches is made up of two monopole surface patches, each of which has a rhombus shape. In this figure, the side of one of the rhombus-shaped monopole surface patches has a length of 0.187λ . This is found by dividing the side of the rhombus plate, which is 2.43λ , into 13 equal segments. Note that the computer program

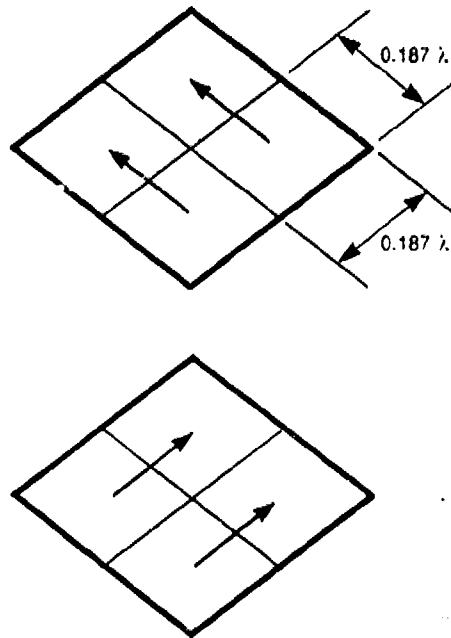


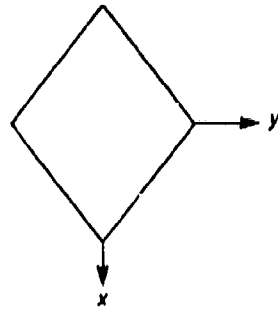
Figure 3-7. Enlarged view of contiguous rhombus-shaped surface patch monopoles from Figure 3-6.

has chosen the size of the patches subject to the maximum patch size specified by the parameter $SEGM(1) \approx 0.2$ (wavelengths). A three-view plot of the rhombus plate geometry is shown in Figure 3-8 for the untilted plate and in Figure 3-9 for the 45° tilted plate.

3.2 COMPARISON OF SIMULATED AND MEASURED BISTATIC RCS

Using the surface patch basis function layout given in Figure 3-6, the bistatic radar cross section of the rhombus plate at 1.3 GHz was computed by setting $NGO=1$. An initial run was made where the method of moments mutual impedance matrix is computed and stored in a disk file for later runs. A collection of simulated (with ESP-4) and measured RCS patterns of the rhombus flat plate covering bistatic angles 15° to 142° are shown in Figures 3-10 to 3-27. For all bistatic angles both plate tilt angles (0° and 45°) were used except for the $\beta = 15^\circ$ case where measurements were available only for the untilted case. For the measured data, the notations H and V refer to horizontal and vertical polarization, respectively. A pair of letters, for example HV, refers to horizontal transmit polarization and vertical receive polarization. In the ESP-4 code,

35 x 27 inch plate



0 WIRE MODES
 312 PLATE MODES
 0 ATTACH. MODES
 312 TOTAL MODES
 SCALE = 1.413λ

Z AXIS VIEW

X AXIS VIEW

Y AXIS VIEW

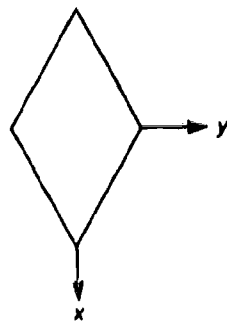
NOTE: COMPUTER OUTPUT; ITALICS ADDED BY AUTHOR

Figure 3-8. Three-view plot of the rhombus plate in the untilted orientation.

spherical components are computed; the θ component is equivalent to H and the ϕ component is equivalent to V. Thus, the relation between the four possible components in the measured and ESP-4 coordinate systems is (HH, VV, HV, VH) \leftrightarrow ($\theta\theta$, $\phi\phi$, $\theta\phi$, $\phi\theta$). For the remainder of the report, the RCS components will be described using the H and V notations.

Consider first Figures 3-10 and 3-11 which show the RCS patterns for the four polarizations (HH, VV, HV, VH) at the bistatic angle 15° . Notice in Figure 3-10 that the simulated copolarized (HH, VV) components are in good agreement with the measurements. The simulated specular bistatic RCS (13.1 dBsm) agrees closely with the theoretical specular monostatic RCS (13.5 dBsm) computed earlier. In Figure 3-11, the simulated cross-polarized RCS (HV, VH) is below the -45 -dBsm level and so the measured data are corrupted by the polarization isolation and background clutter in the measurements. For all the bistatic angles, when the plate is not tilted the simulated

35 x 27 inch tilted plate

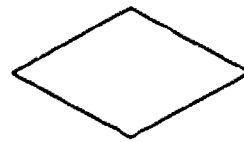


Z AXIS VIEW

0 WIRE MODES
 312 PLATE MODES
 0 ATTACH. MODES
 312 TOTAL MODES
 SCALE = 1.413 λ



X AXIS VIEW



Y AXIS VIEW

NOTE: COMPUTER OUTPUT; ITALICS ADDED BY AUTHOR

Figure 3-9. Three-view plot of the rhombus plate in the 45° tilted orientation.

cross-polarized RCS is very low, and so the measurements are dominated by isolation/clutter-induced errors. These cross-polarized data appear in Figures 3-14, 3-18, 3-22, and 3-26 and will not be discussed further.

A series of patterns for bistatic angles 45° to 142° are shown in Figures 3-12 to 3-27, where both plate tilt angles are considered. For example, Figure 3-12 is for the HH and VV RCS components at the 45° bistatic angle with no target tilt, while Figure 3-13 is for a plate tilt angle of 45°. Notice that the effect of the plate tilt is to break up the main lobe in both HH and VV components. Good agreement between the measurements and simulations is evident for the copolarized components for this case. Next, in Figures 3-14 and 3-15 the cross-polarized RCS is shown for the untilted and tilted plate, respectively. The effect of tilting the plate is to raise the theoretical cross-polarized response; thus, the measured data bear a resemblance to the simulations as in Figure 3-15. The basic lobing structure is the same for the measurements and the simulations, but the amplitude of individual lobes differs by as much as 10 dB. Next, for the 90° bistatic angle case shown in Figure 3-16 there is a clear broadening of the main beamwidth in HH and VV polarizations, and

the simulations and measurements are in good agreement. Good agreement is also achieved in Figures 3-17 and 3-19 for the tilted plate. Figures 3-20 to 3-23 show the $\beta = 120^\circ$ case results. The main lobe continues to broaden for HH and VV components as shown in Figure 3-20. There is a somewhat better agreement between simulations and measurements for HH compared to VV in Figures 3-20 and 3-21. This discrepancy is likely due to a higher background for VV compared to HH. Finally, Figures 3-24 to 3-27 show the results at the 142° bistatic angle. In Figure 3-24, the specular RCS HH component drops by approximately 6 dB compared to the 120° bistatic case, while the VV component is relatively unchanged. There is a difference of several decibels in the simulated and measured specular responses in both HH and VV components. It is further noted in Figure 3-24 that the HH main lobe has broken up into three, while the VV main lobe continues to broaden compared to the $\beta = 120^\circ$ case. There are significant differences between the simulated and measured lobe amplitudes in both Figures 3-24 and 3-25, but the general shapes are in good agreement. The differences are attributed to an increase in the background level. In Figure 3-27 the agreement between the cross-polarized measured data and simulated data is good. A mirror symmetry between HV and VH components is evident here as should be the case for a symmetric target [19].

The specular response of the copolarized RCS for the untilted plate is summarized in Figure 3-28. The simulated data indicate that the specular response decreases monotonically with increasing bistatic angle and the decrease is more rapid for HH compared to VV. The measured data track the simulated curves very well with the exception of the VV component for $\beta = 142^\circ$ where the measured RCS differs from the simulation by about 2 dB. To check the accuracy or convergence of the ESP-4 simulated RCS patterns at the $\beta = 142^\circ$ case, the rhombus plate was modeled using a finer grid of patches with a maximum segment length equal to 0.15λ . With this maximum patch size, the ESP-4 software generated a 17×16 grid of 272 patches for each polarization with an actual patch segment length equal to 0.143λ . The total number of modes is 544, which is 1.74 times the number of modes used with the 0.2λ maximum patch size simulations. A comparison of the copolarized RCS for HH and VV components with 0.187λ and 0.143λ patches (rounded to 0.19λ and 0.14λ , respectively) for the $\beta = 142^\circ$ untilted plate is made in Figure 3-29. The simulated specular values agree to within 0.1 dB, and the overall good agreement between the patterns indicates an insensitivity to the patch size. Thus, the differences between the measured and simulated specular responses (as well as the responses at other angles) observed in Figure 3-28 are attributed to measurement error.

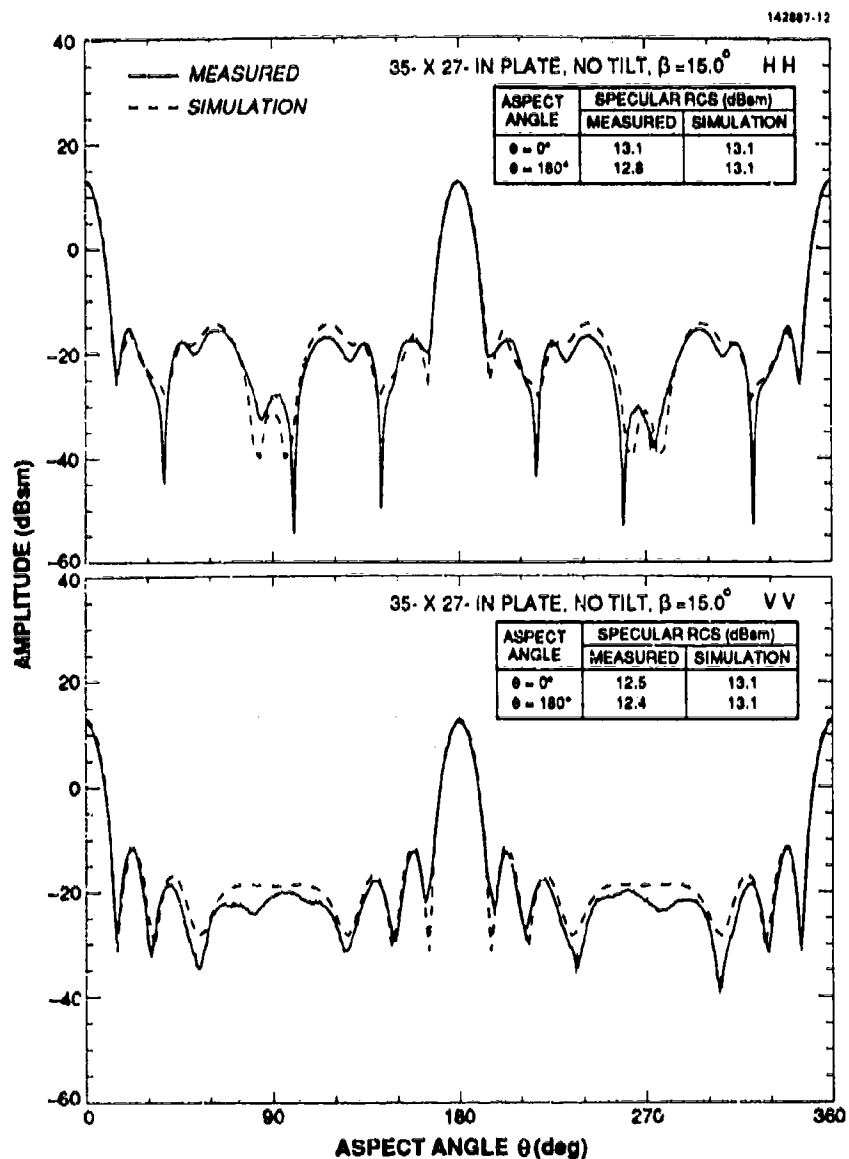


Figure 3-10. Comparison of ESP-4 simulations and measurements of the copolarized (HH, VV) bistatic RCS for the 35- x 27-in plate at 1.3 GHz. The bistatic angle is $\beta = 15^\circ$ and there is no plate tilt.

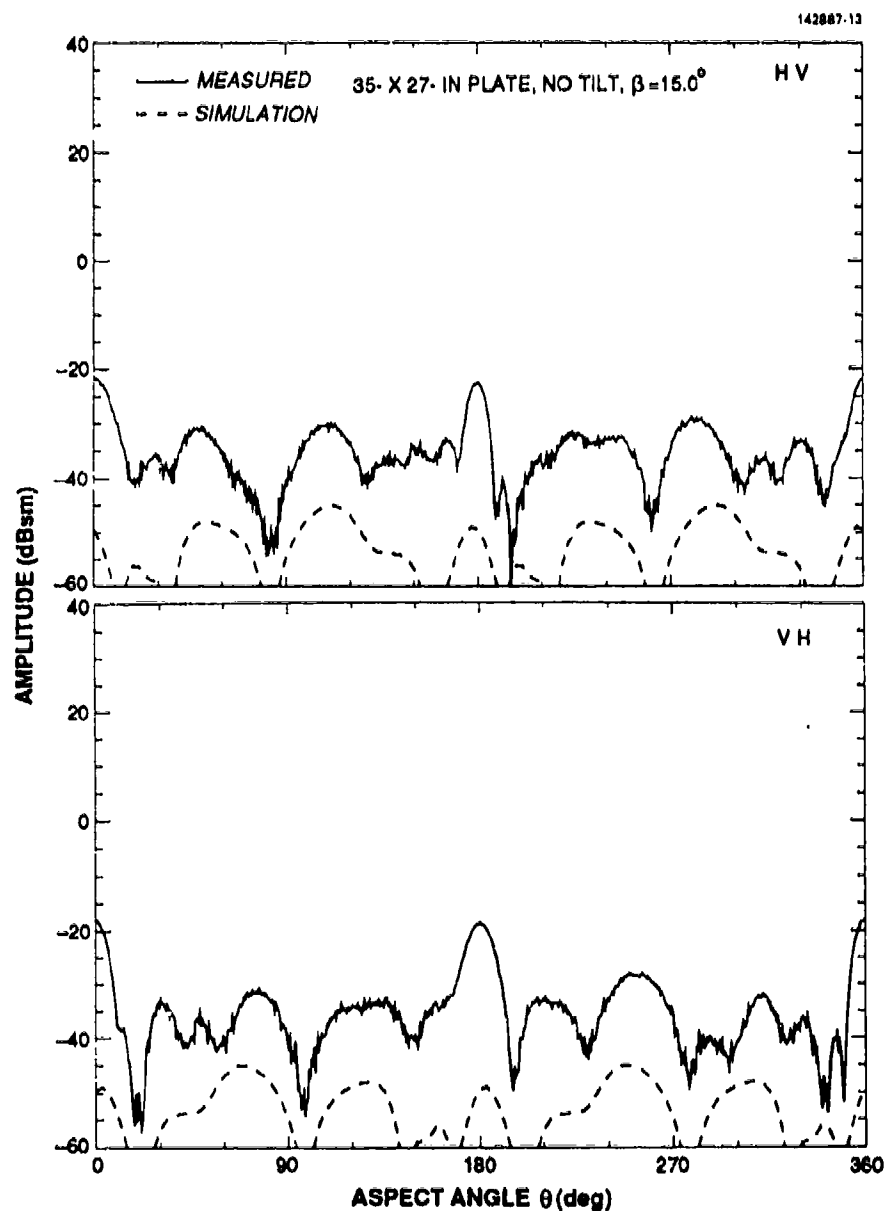


Figure 3-11. Comparison of ESP-4 simulations and measurements of the cross-polarized (HV, VH) bistatic RCS for the 35- \times 27-in plate at 1.3 GHz. The bistatic angle is $\beta = 15^\circ$ and there is no plate tilt.

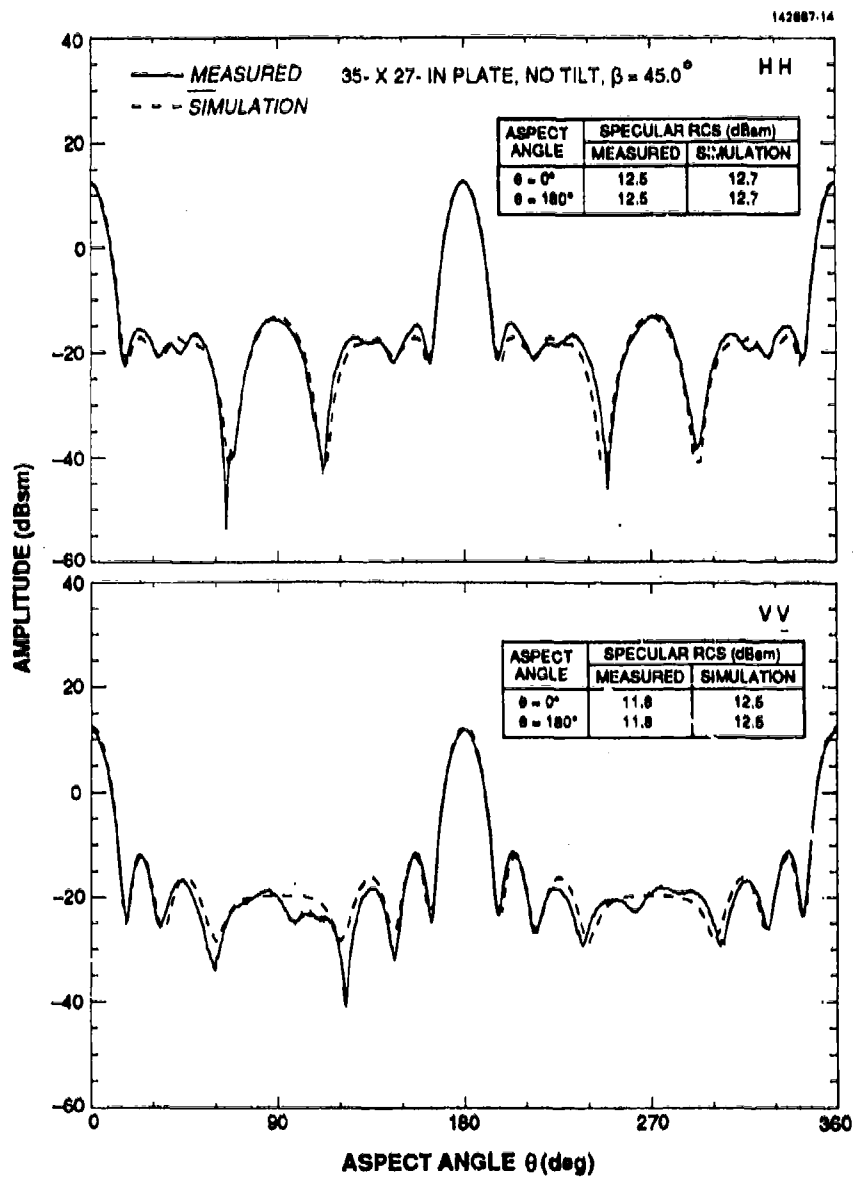


Figure 3-12. Comparison of ESP-4 simulations and measurements of the copolarized (HH, VV) bistatic RCS for the 35- x 27-in plate at 1.3 GHz. The bistatic angle is $\beta = 45^\circ$ and there is no plate tilt.

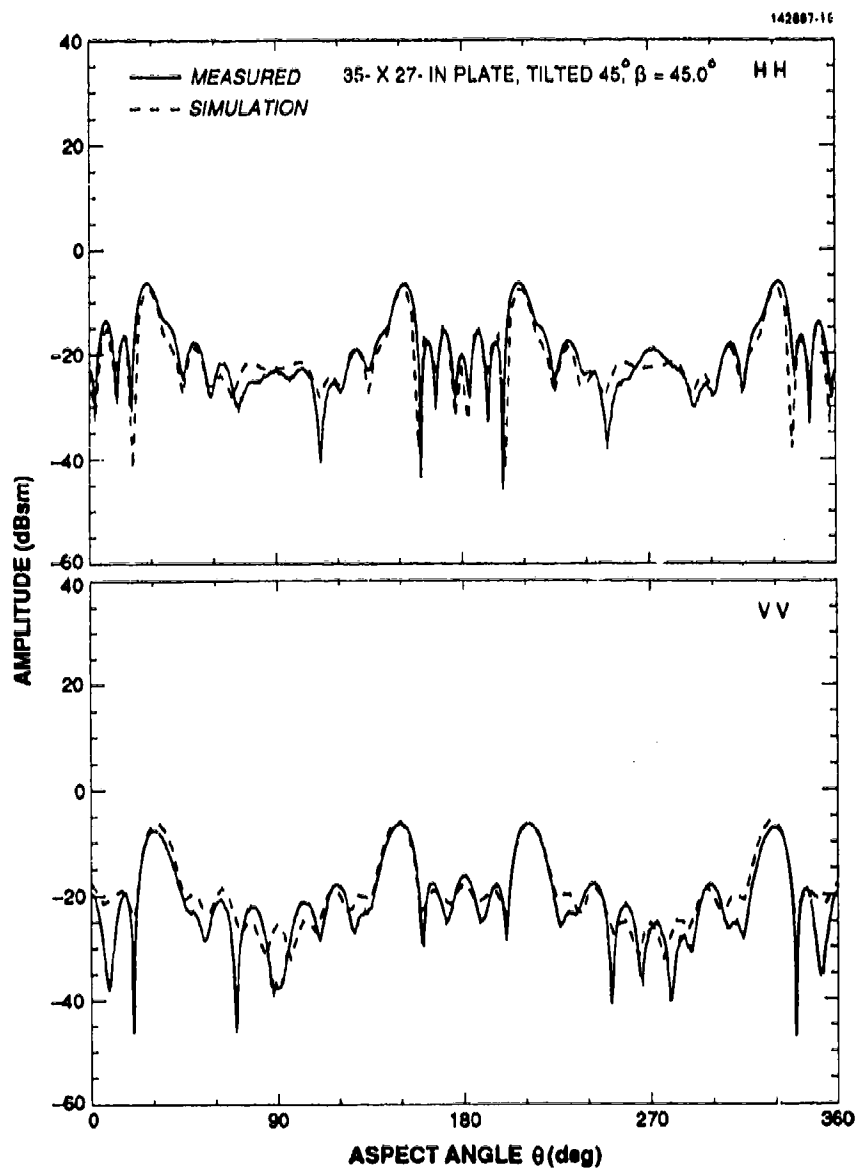


Figure 3-13. Comparison of ESP-4 simulations and measurements of the copolarized (HH, VV) bistatic RCS for the 35- \times 27-in plate at 1.3 GHz. The bistatic angle is $\beta = 45^\circ$ and the plate is tilted 45° .

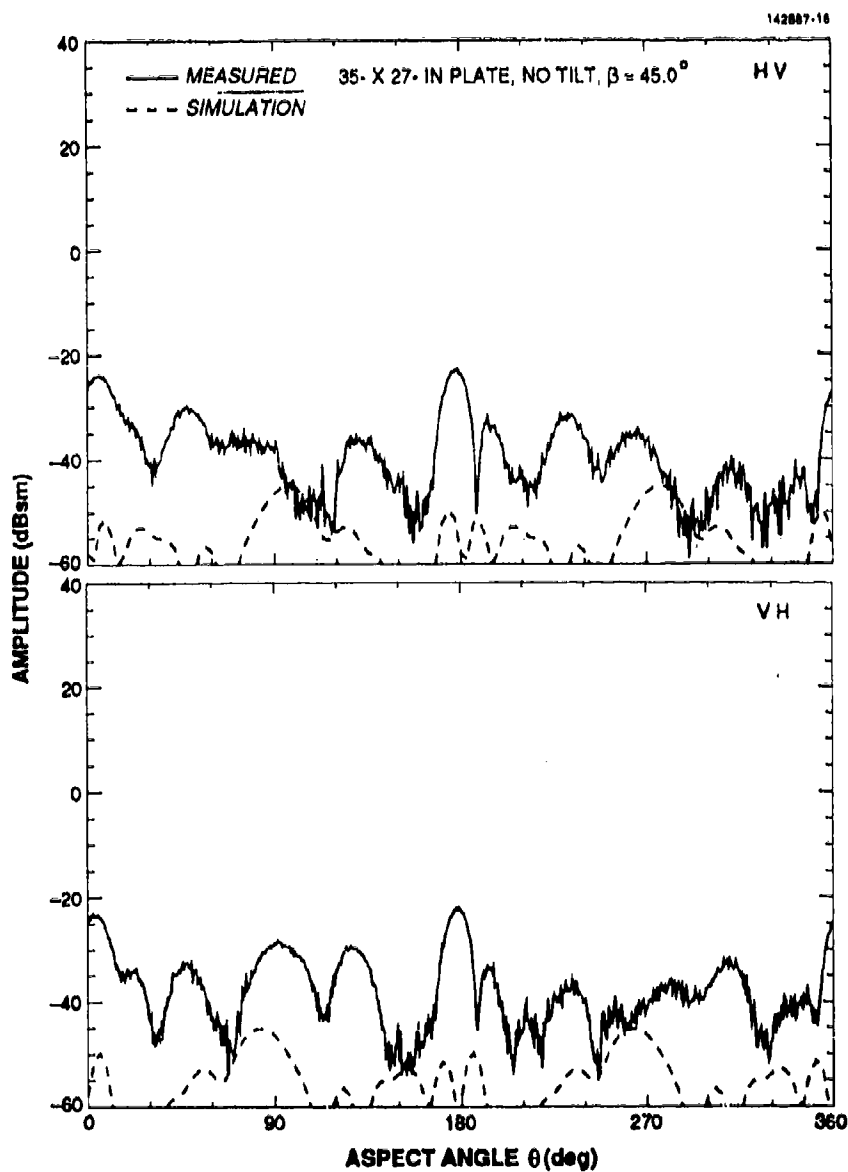


Figure 3-14. Comparison of ESP-4 simulations and measurements of the cross-polarized (HV, VH) bistatic RCS for the 35- \times 27-in plate at 1.3 GHz. The bistatic angle is $\beta = 45^\circ$, and there is no plate tilt.

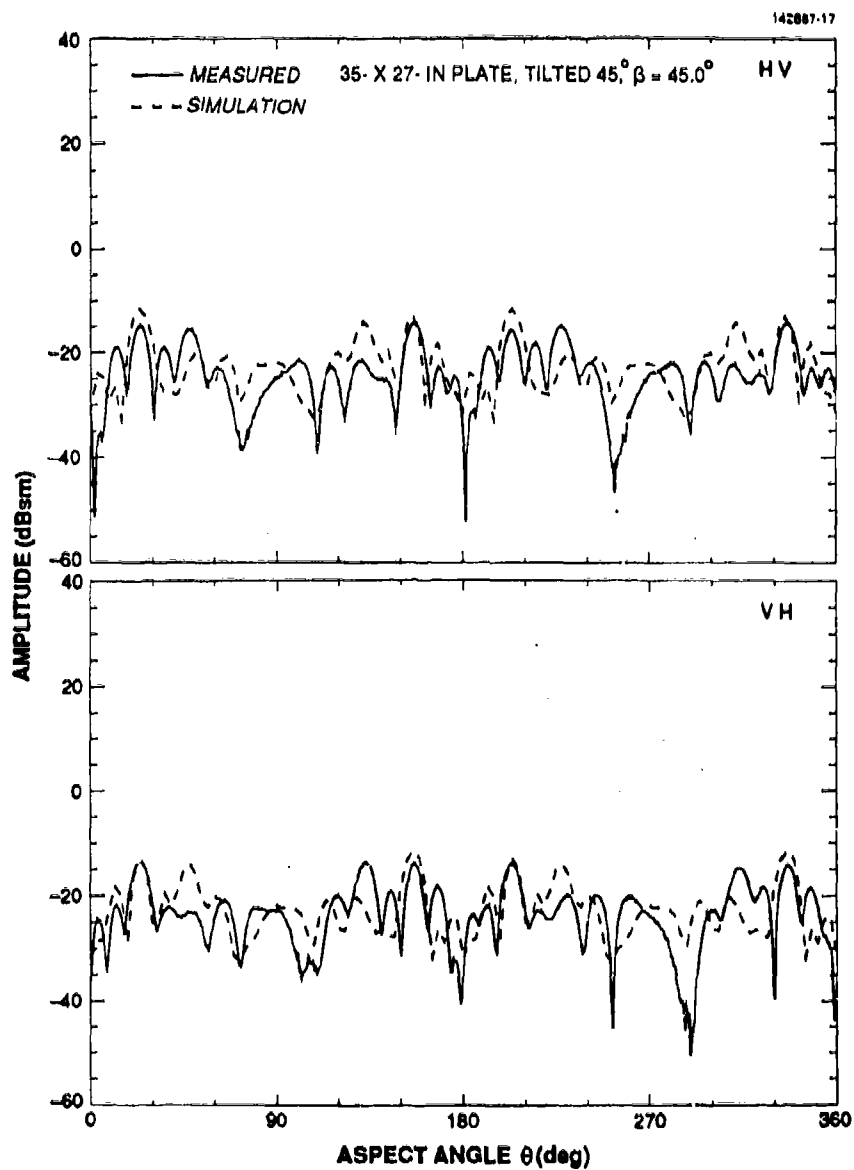


Figure 3-15. Comparison of ESP-4 simulations and measurements of the cross-polarized (HV, VH) bistatic RCS for the 35- x 27-in inch plate at 1.3 GHz. The bistatic angle is $\beta = 45^\circ$, and the plate is tilted 45° .

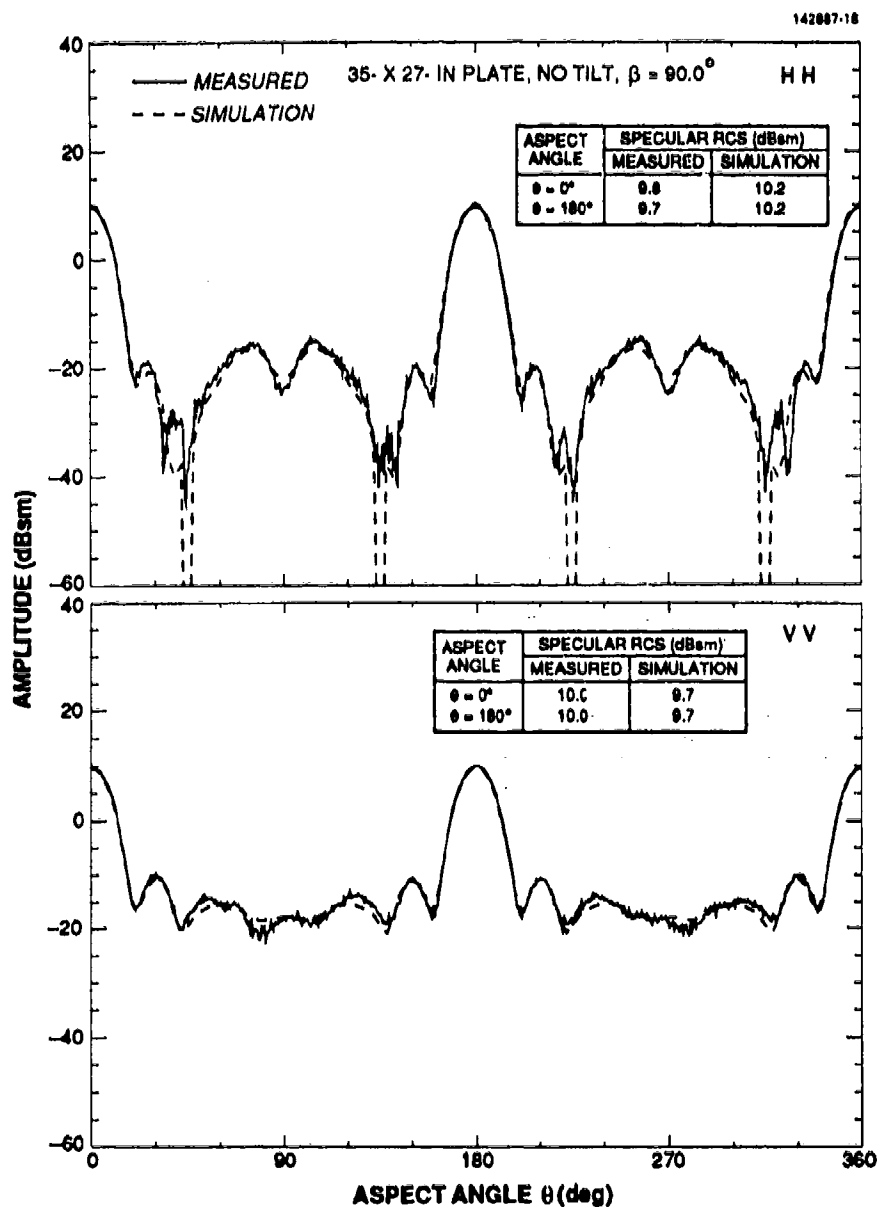


Figure 3-16. Comparison of ESP-4 simulations and measurements of the copolarized (HH, VV) bistatic RCS for the 35- x 27-in plate at 1.3 GHz. The bistatic angle is $\beta = 90^\circ$, and there is no plate tilt.

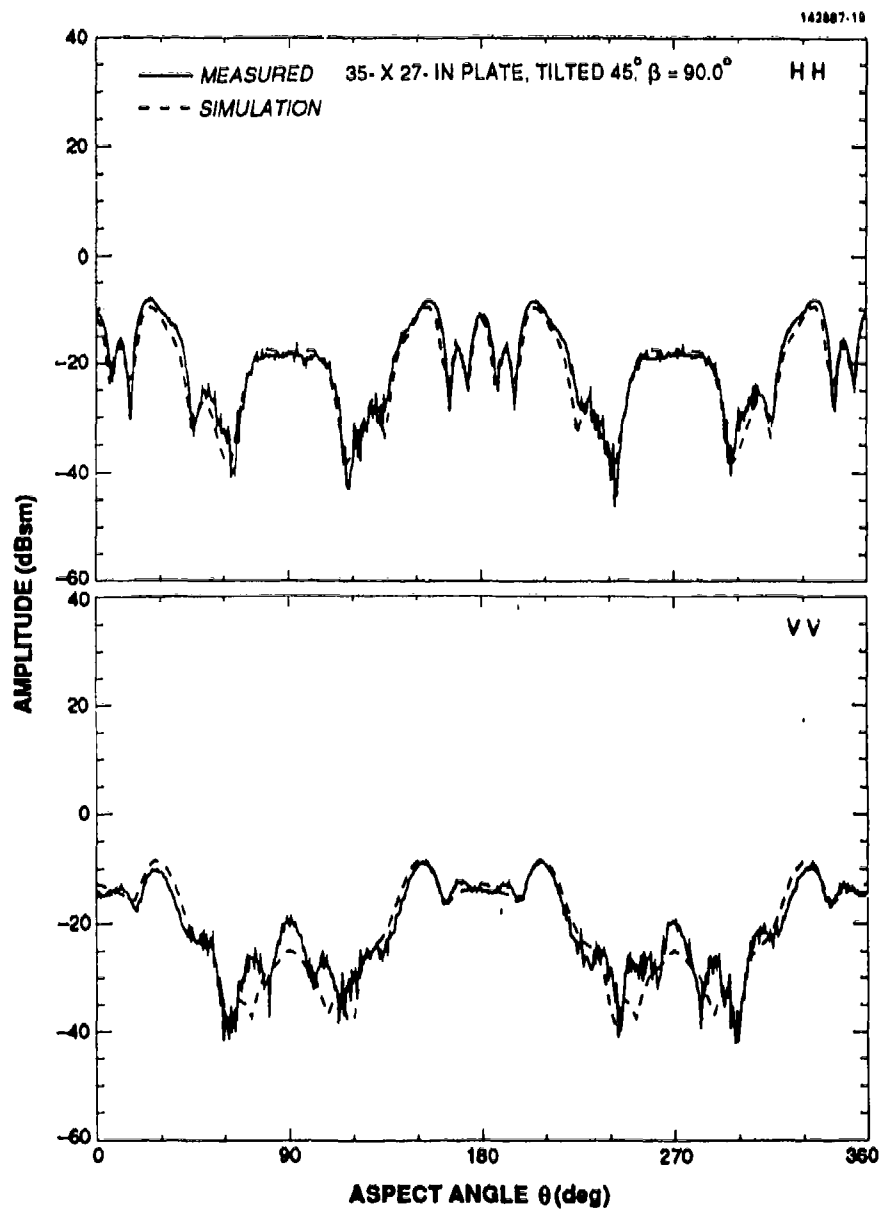


Figure 3-17. Comparison of ESP-4 simulations and measurements of the copolarized (HH, VV) bistatic RCS for the 35- \times 27-in plate at 1.3 GHz. The bistatic angle is $\beta = 90^\circ$, and the plate is tilted 45° .

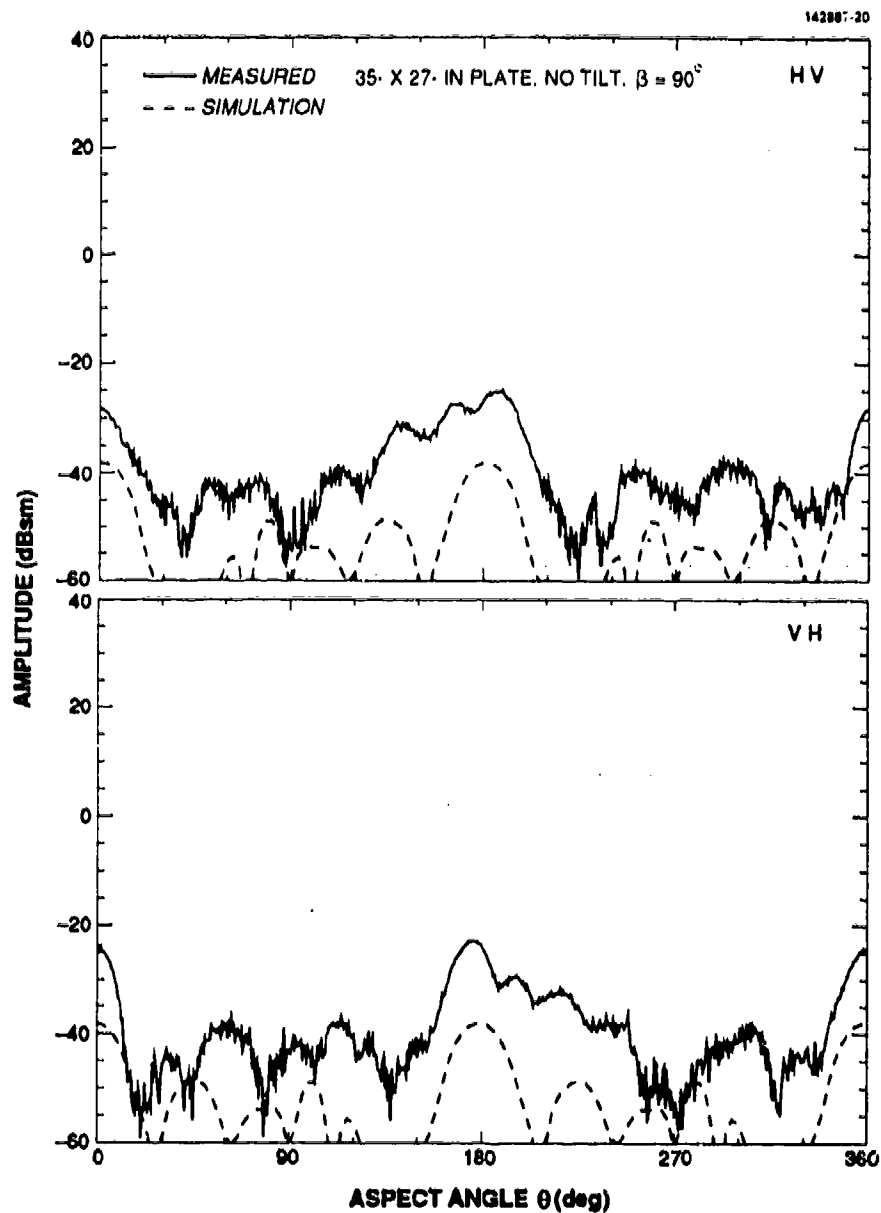


Figure 3-18. Comparison of ESP-4 simulations and measurements of the cross-polarized (HV, VH) bistatic RCS for the 35- \times 27-in plate at 1.3 GHz. The bistatic angle is $\beta = 90^\circ$, and there is no plate tilt.

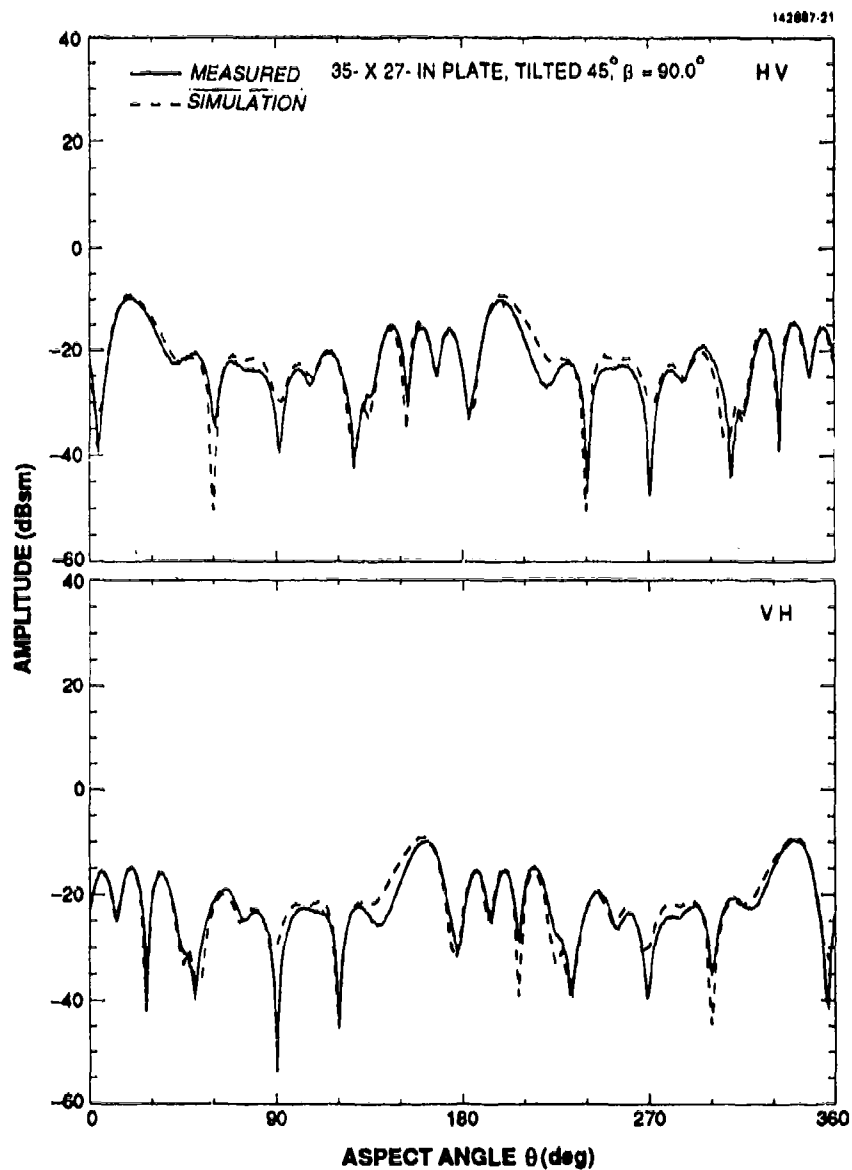


Figure 3-19. Comparison of ESP-4 simulations and measurements of the cross-polarized (HV, VH) bistatic RCS for the 35- x 27-in plate at 1.3 GHz. The bistatic angle is $\beta = 90^\circ$, and the plate is tilted 45° .

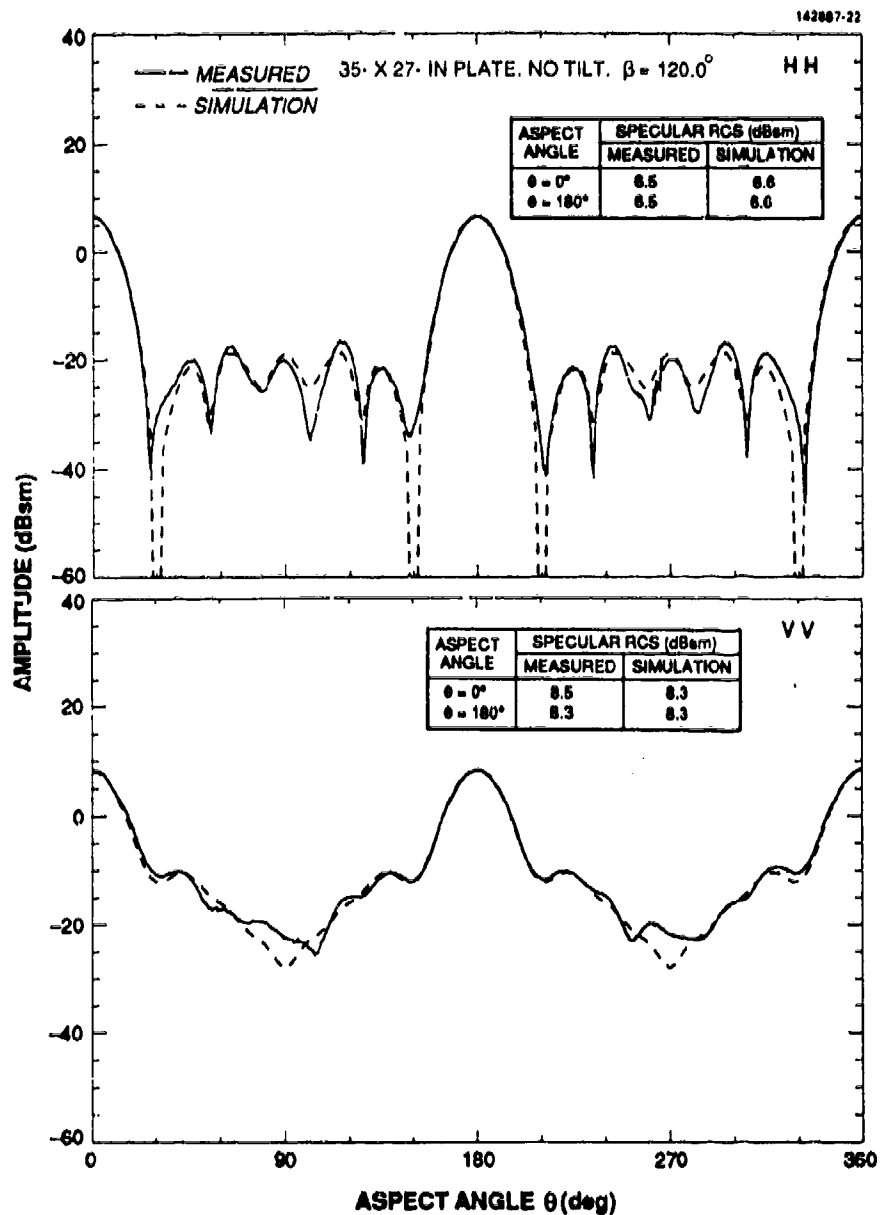


Figure 3-20. Comparison of ESP-4 simulations and measurements of the copolarized (HH, VV) bistatic RCS for the 35- x 27-in plate at 1.3 GHz. The bistatic angle is $\beta = 120^\circ$, and there is no plate tilt.

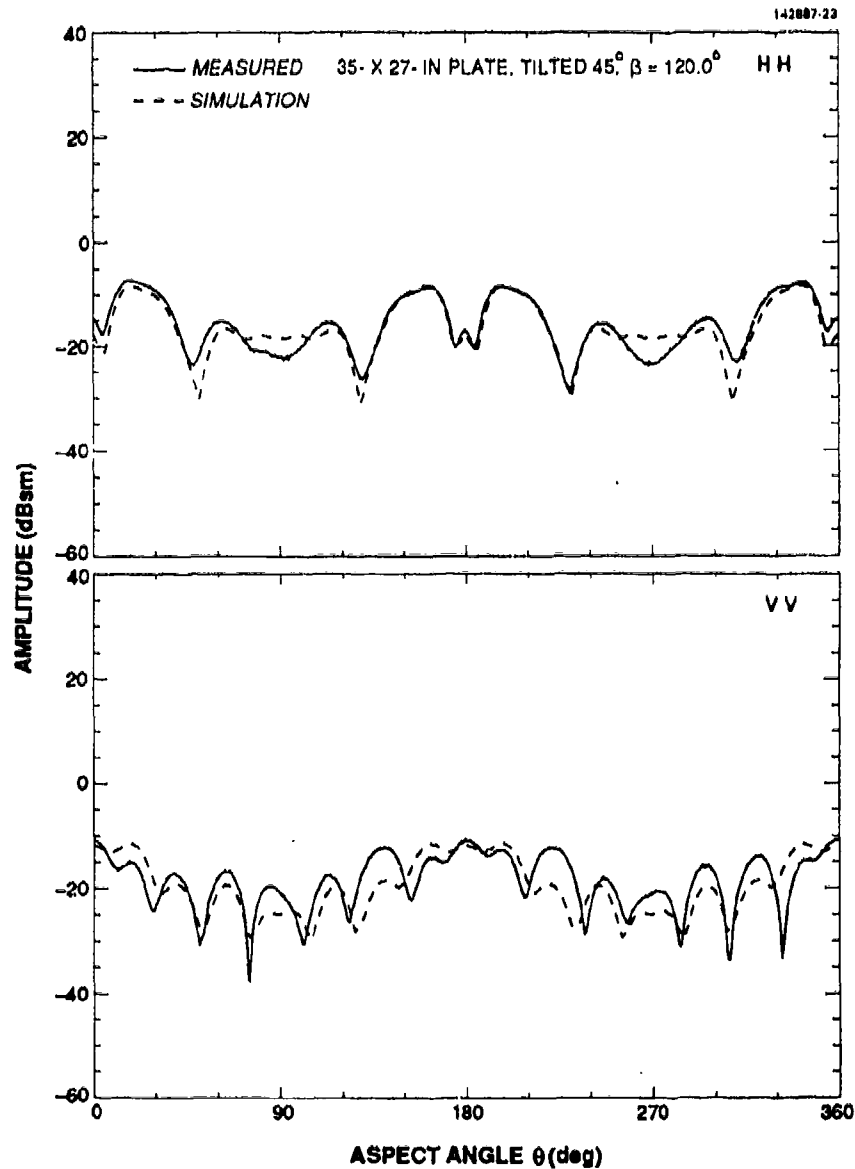


Figure 3-21. Comparison of ESP-4 simulations and measurements of the copolarized (HH, VV) bistatic RCS for the 35- x 27-in plate at 1.3 GHz. The bistatic angle is $\beta = 120^\circ$, and the plate is tilted 45° .

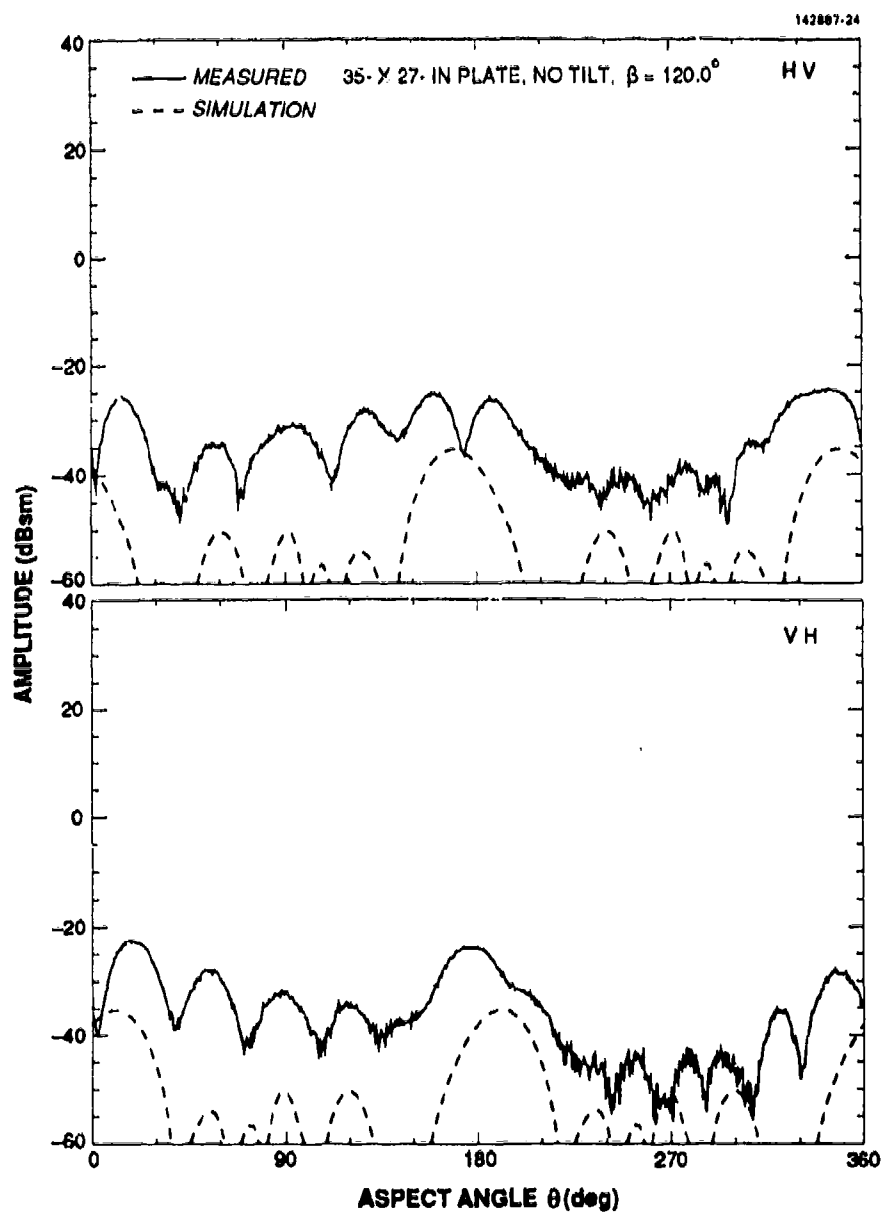


Figure 3-22. Comparison of ESP-4 simulations and measurements of the cross-polarized (HV, VH) bistatic RCS for the 35- x 27-in plate at 1.3 GHz. The bistatic angle is $\beta = 120^\circ$, and there is no plate tilt.

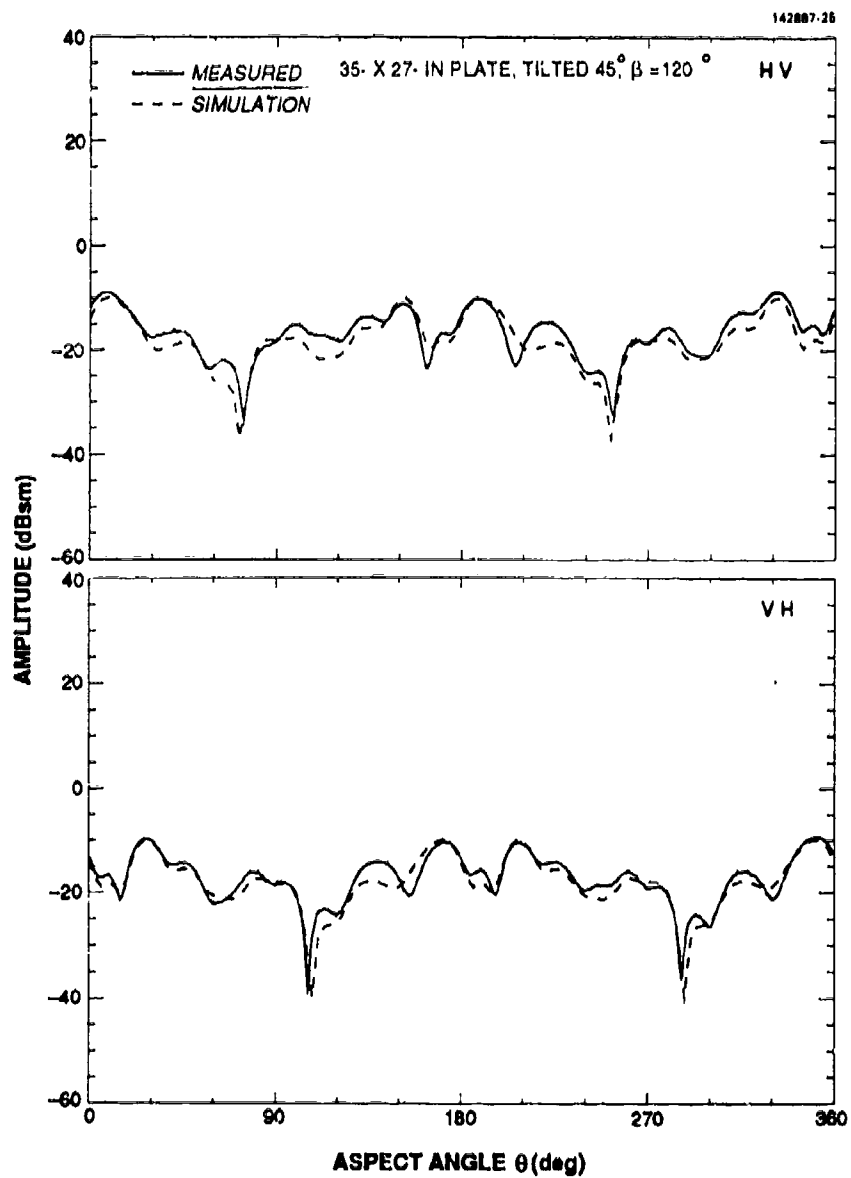


Figure 3-23. Comparison of ESP-4 simulations and measurements of the cross-polarized (HV, VH) bistatic RCS for the 35- \times 27-in plate at 1.3 GHz. The bistatic angle is $\beta = 120^\circ$, and the plate is tilted 45° .

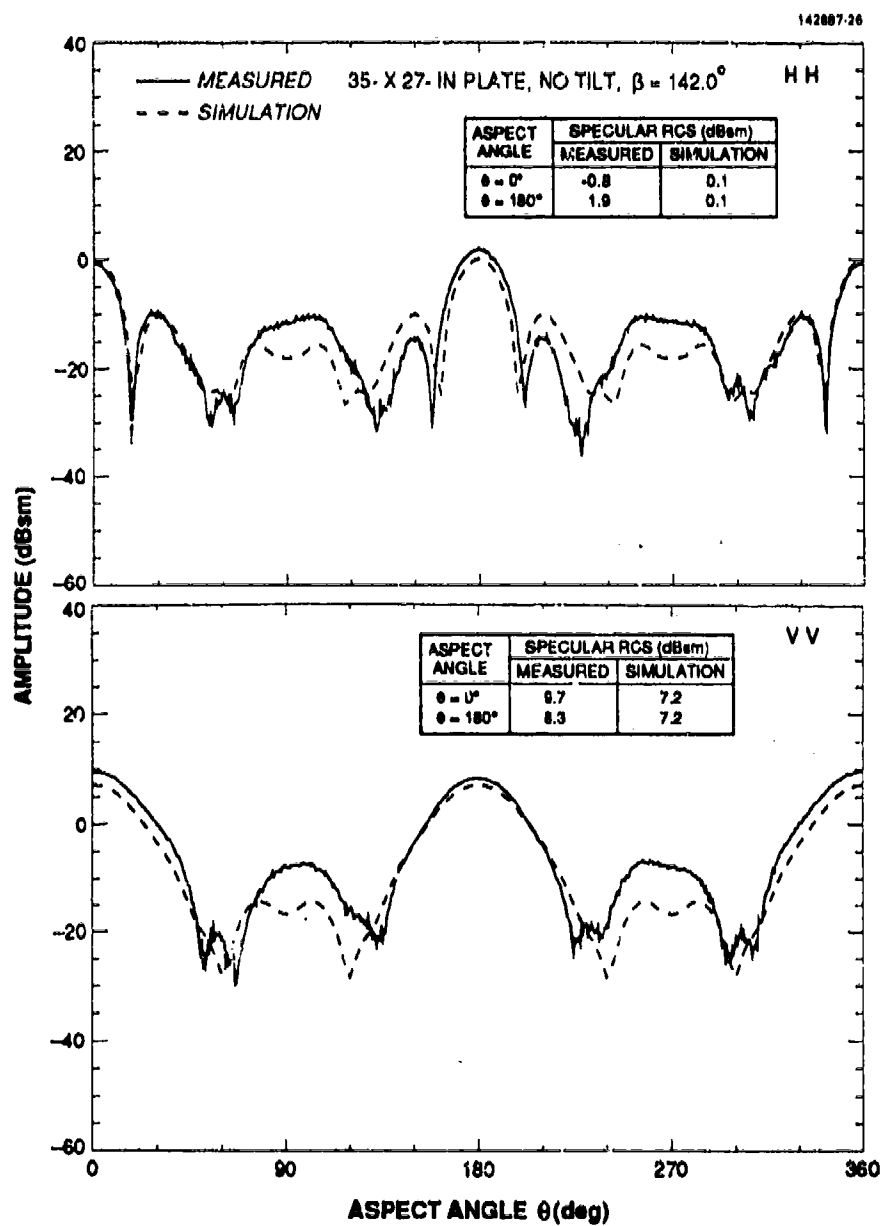


Figure 3-24. Comparison of ESP-4 simulations and measurements of the copolarized (HH, VV) bistatic RCS for the 35- x 27-in plate at 1.3 GHz. The bistatic angle is $\beta = 142^\circ$, and there is no plate tilt.

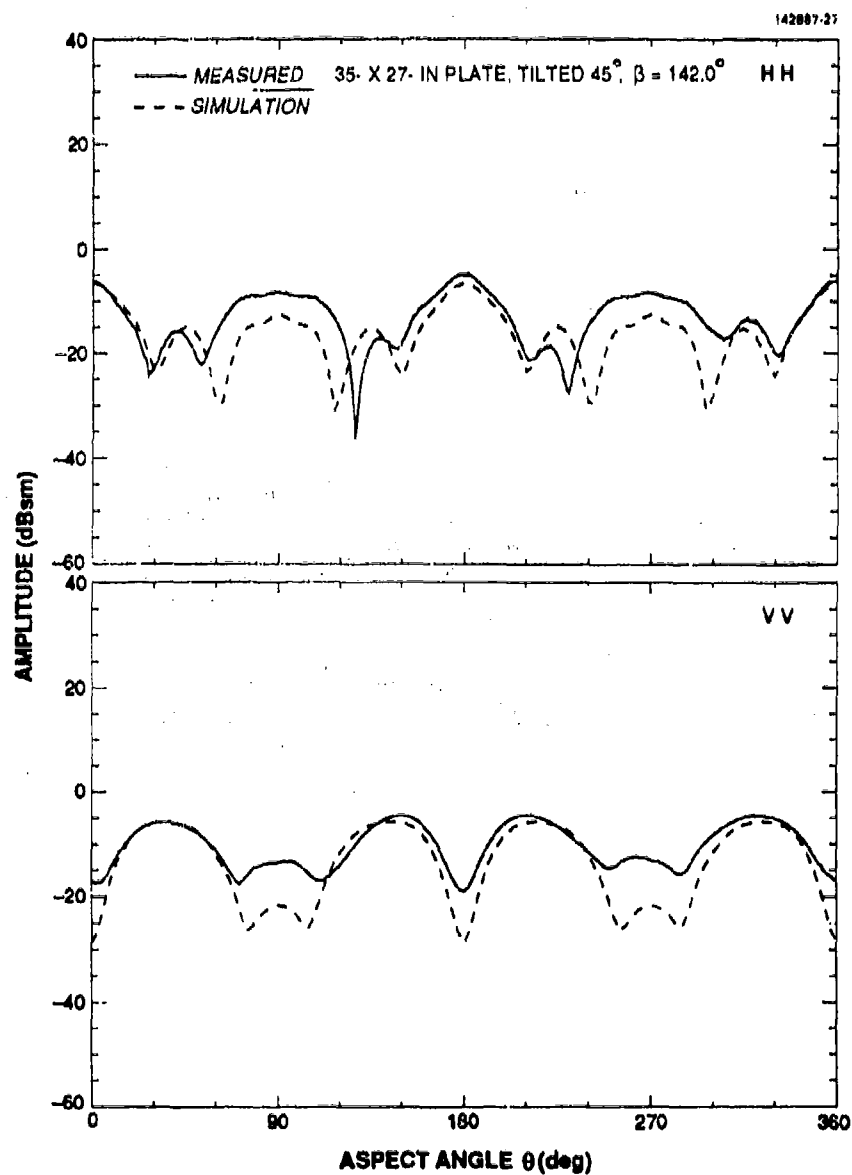


Figure 3-25. Comparison of ESP-4 simulations and measurements of the copolarized (HH, VV) bistatic RCS for the 35- \times 27-in plate at 1.3 GHz. The bistatic angle is $\beta = 142^\circ$, and the plate is tilted 45° .

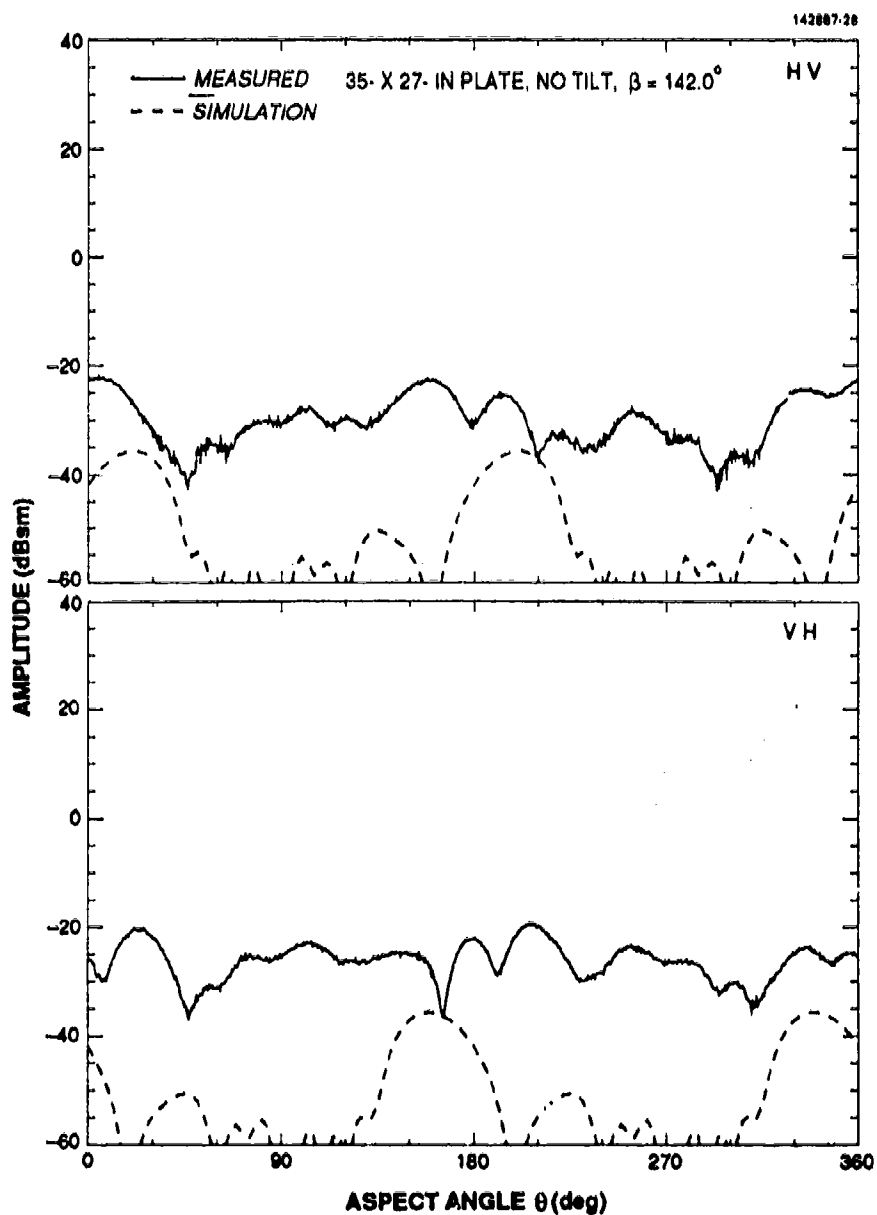


Figure 3-26. Comparison of ESP-4 simulations and measurements of the cross-polarized (HV VH) bistatic RCS for the 35- \times 27-in plate at 1.3 GHz. The bistatic angle is $\beta = 142^\circ$, and there is no plate tilt.

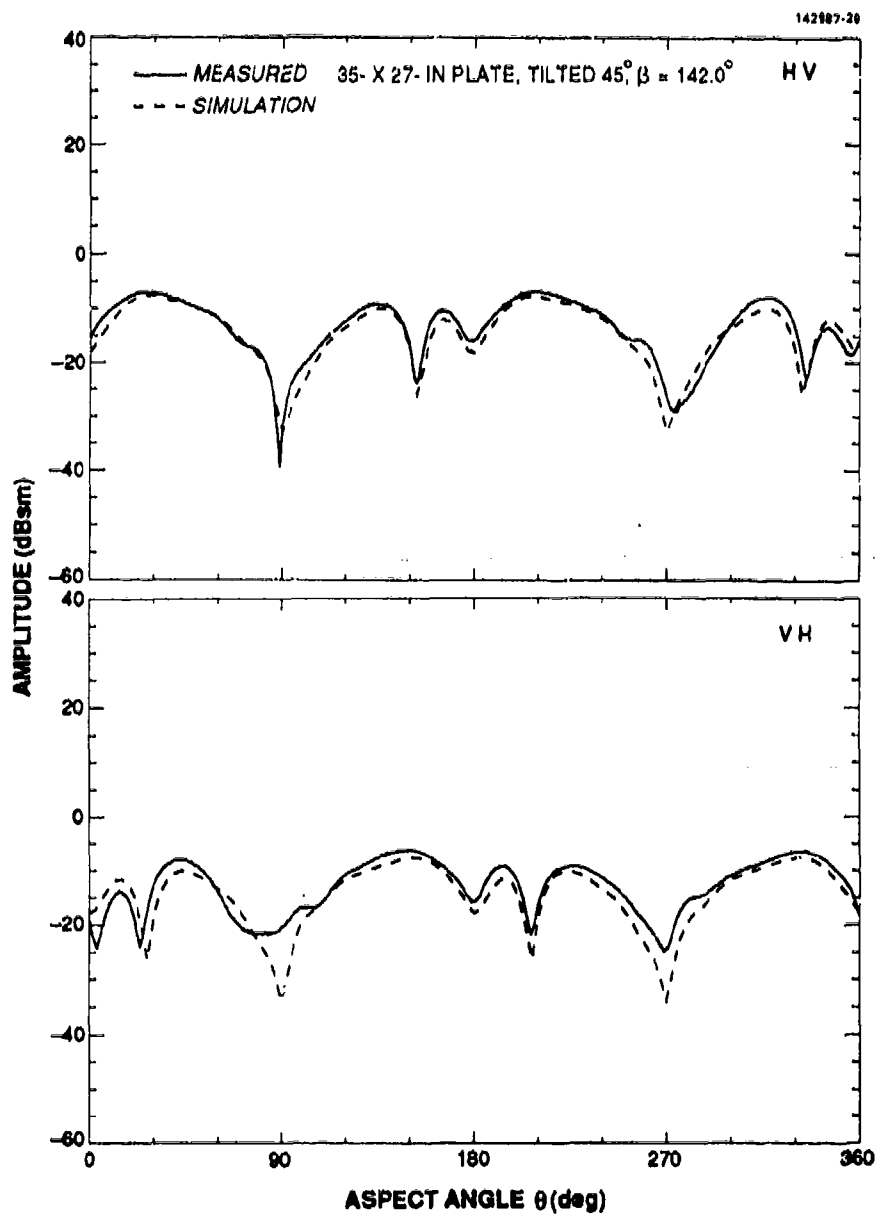


Figure 3-27. Comparison of ESP-4 simulations and measurements of the cross-polarized (HV, VH) bistatic RCS for the 35- x 27-in plate at 1.3 GHz. The bistatic angle is $\beta = 142^\circ$, and the plate is tilted 45° .

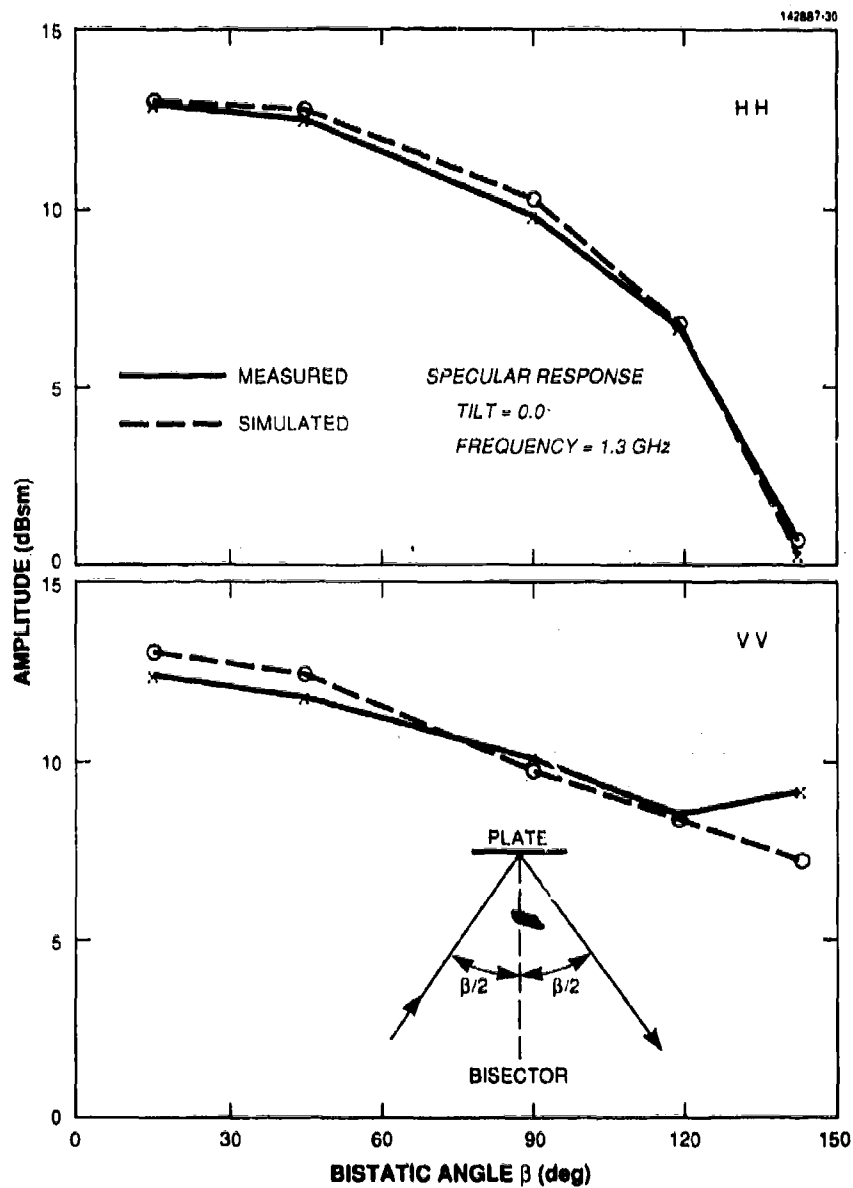


Figure 3-28. Comparison of ESP-4 simulations and measurements of the specular copolarized (HH, VV) bistatic RCS for the 35- x 27-in plate at 1.3 GHz.

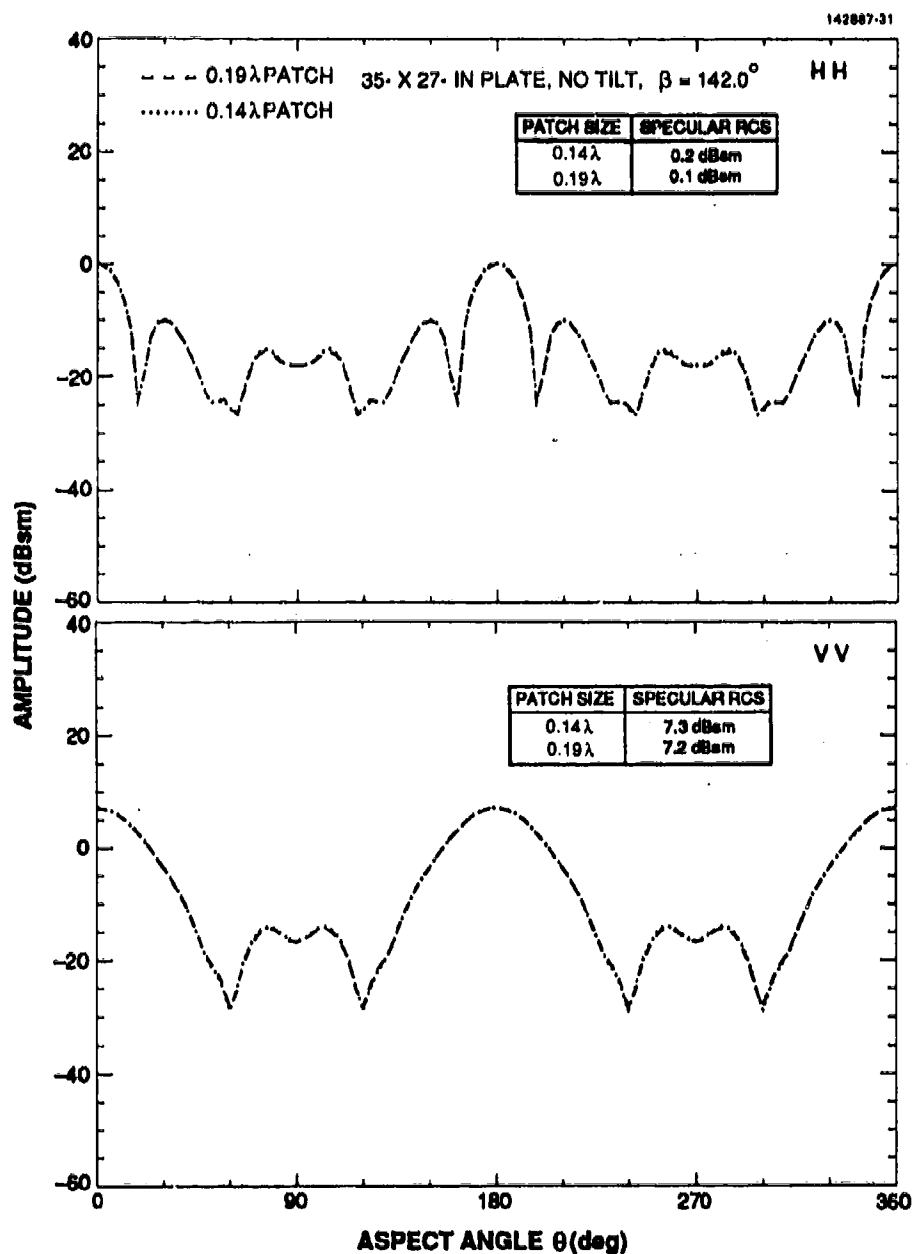


Figure 3-29. Convergence check of ESP-4 simulations. The figure shows the copolarized (HH, VV) bistatic RCS for the 35- \times 27-in plate at 1.3 GHz with two different surface patch sizes. The bistatic angle is $\beta = 142^\circ$, and there is no plate tilt.

4. CONCLUSION

This report has described modifications made at Lincoln Laboratory to The Ohio State University electromagnetic surface patch code version 4 (ESP-4) and its utilization in the computation of the bistatic radar cross section of a rhombus-shaped flat plate. The modifications are the restructuring of the input data statements and the addition of a new option for bistatic radar cross section computation with a fixed bistatic angle. A listing of the revised software is given in the appendix.

Comparisons of the ESP-4 method of moments simulations with far-field measurements over bistatic angles 15° to 142° have been made at 1.3 GHz for a 35×27 -in rhombus plate in untilted and tilted configurations and good agreement is observed. From these simulations, it is concluded that both the copolarized and cross-polarized bistatic RCS of arbitrarily oriented flat plates can be accurately predicted with this software.

REFERENCES

1. J.W. Crispin, Jr., and K.M. Siegel, *Methods of Radar Cross-Section Analysis*, New York: Academic Press (1968).
2. G.T. Ruck, *Radar Cross Section Handbook, Volume 2*, New York: Plenum Press (1970).
3. E.F. Knott, J.F. Shaeffer, and M.T. Tuley, *Radar Cross Section*, Dedham, Mass.: Artech House, Inc. (1985).
4. J.P. DiBeneditto, "Bistatic Scattering from Conducting Calibration Spheres," Rome, N.Y.: Rome Air Development Center, RADC-TR-84-93, April 1984, AD-A154173.
5. K. Chiang and R.J. Marhefka, "Bistatic Scattering from a Finite Circular Cylinder," The Ohio State University ElectroScience Laboratory, Columbus, Ohio, Technical Rep. 714614-4 (July 1984).
6. V.J. DiCaudo and W.W. Martin, "Approximate Solution to Bistatic Radar Cross Section of Finite Length, Infinitely Conducting Cylinder," *IEEE Trans. Antennas Propag.* AP-14, 668-669 (1966).
7. F.C. Paddison, J.W. Follin, Jr., F. Mitchell, and A.L. Maffett, "Large Bistatic Angle Radar Cross Section of a Right Circular Cylinder," *Electromagnetics* 5, 63-77 (1985).
8. J.I. Glaser, "Bistatic RCS of Complex Objects Near Forward Scatter," *IEEE Trans. Aerosp. Electron. Syst.*, AES-21, 70-78 (1985).
9. E.H. Newman, "A User's Manual for an Electromagnetic Surface Patch Code: ESP Version IV," The Ohio State University ElectroScience Laboratory, Columbus, Ohio, Rep. 716199-11 (August 1988).
10. J. H. Richmond, "Radiation and Scattering by Thin-Wire Structures in a Homogeneous Conducting Medium (Computer Program Description)," *IEEE Trans. Antennas Propag.* AP-22, 365 (1974).
11. J.H. Richmond, "A Wire-Grid Model for Scattering by Conducting Bodies," *IEEE Trans. Antennas Propag.* AP-14, 782-786 (1966).
12. D. Kuo and B.J. Strait, "Improved Programs for Analysis of Radiation and Scattering by Configurations of Arbitrarily Bent Thin Wires," Syracuse, N.Y.: Syracuse University, Scientific Rep. 15, AFCRL-72-0051, (15 January 1972).
13. N.C. Albertsen, J.E. Hansen, and N.E. Jensen, "Computation of Radiation from Wire Antennas on Conducting Bodies," *IEEE Trans. Antennas Propag.* AP-22, 200-206 (1974).

14. G.J. Burke and A.J. Poggio, "Numerical Electromagnetic Code - Method of Moments," San Diego, Calif.: Naval Ocean Systems Center, Technical Doc. 116, AFWL-TR-76-320 (July 1977).
15. S.M. Rao, D.R. Wilton, and A.W. Glisson, "Electromagnetic Scattering by Surfaces of Arbitrary Shape," *IEEE Trans. Antennas Propag.* AP-30 409-418 (1982).
16. S. Lee, D.A. Shnidman, and F.A. Lichauco, "Numerical Modeling of RCS and Antenna Problems: Part I - Theory. Part II - Verification," MIT Lincoln Laboratory, Lexington, Mass.: Technical Rep. 785 (21 December 1987).
17. S. Lee, D.A. Shnidman, and F.A. Lichauco, "Numerical Modeling of RCS and Antenna Problems: Part III - User's Guide," MIT Lincoln Laboratory, Lexington, Mass.: Technical Rep. 785 (28 December 1987).
18. J. Lutz, "Bistatic Radar Cross Section Measurement Considerations," Alamogordo, N. Mex.: DynCorp Radar Backscatter Division, RATSCAT Project No. 87-07, TR-AD-88-003 (September 1988).
19. G.E. Heath, "Bistatic Scattering Reflection Asymmetry, Polarization Reversal Asymmetry, and Polarization reversal Reflection Symmetry," *IEEE Trans. Antennas Propag.* AP-29, 429-434 (1981).

APPENDIX A

REVISED ESP-4 SOFTWARE LISTING

The purpose of this appendix is to list the main program of a modified version of the electromagnetic surface patch code (ESP-4). This software was obtained in July 1988 from The Ohio State University and has since been modified at Lincoln Laboratory. The important modifications are the addition of namelist input data and the option for bistatic radar cross section calculation with a fixed bistatic angle and variable target rotation. Other minor changes to the code are documented with comments in the modified ESP-4 code listed below. The main program contains nearly 1700 lines of code and is listed in its entirety. The ESP-4 subroutines contain an additional 7000 lines of code and are not listed here. However, in the subroutines no changes other than a global conversion from (ARCOS, ARSIN, ARTAN) to (ACOS, ASIN, ATAN) have been made. Following the listing are two data files corresponding to the untilted and tilted plate configurations.

*****Modified ESP-4 FORTRAN 77 code listing (SUN 3 computer system).

```

****Main program      filename:  esp4nam.f   at Lincoln Laboratory

C
C
C      OHIO STATE UNIVERSITY ELECTROSCIENCE LAB MOMENT METHOD, SURFACE PATCH CODE. BASED UPON PIECEWISE SINUSOIDAL REACTION FORMULATION. TREATS:
C      THIN WIRES
C      RECTANGULAR OR POLYGONAL PLATES
C      WIRE/PLATE ATTACHMENTS (AT LEAST 0.1-WAVE FROM EDGE)
C      PLATE/PLATE ATTACHMENTS
C      OPEN OR CLOSED SURFACES
C
C      REFERENCE "A USER'S MANUAL FOR AN ELECTROMAGNETIC SURFACE PATCH CODE: ESP VERSION IV," BY E.H. NEWMAN, OSU/FSL REPORT 716199-11, AUGUST 1988.
C
C      ALSO "A USER'S MANUAL FOR ELECTROMAGNETIC SURFACE PATCH CODE: VERSION III - POLYGONAL PLATES AND WIRES" BY E.H. NEWMAN AND R.L. DILSAVO, OSU/ESL REPORT 716148-19, APRIL 1987.
C
C      ANY COMMENTS CAN BE REFERRED TO:
C
C      EDWARD H. NEWMAN
C      ELECTROSCIENCE LABORATORY
C      1320 KINNEAR ROAD
C      COLUMBUS, OHIO 43212
C      PHONE: (614) 292-4999
C
C      FILENAME esp4nam.f  SUN 3 COMPUTER SYSTEM at MIT LINCOLN LABORATORY.
C      MODIFIED FOR NAMELIST INPUT DATA AND FIXED BISTATIC ANGLE WITH VARIABLE TARGET ROTATION.
C      ALL LINCOLN LABORATORY MODIFICATIONS ARE MADE EVIDENT BY THE ABSENCE OF ESP LINE NUMBERS.
C      THE SUBROUTINES USED BY esp4nam.f HAVE BEEN DIVIDED INTO TWO FILES esp4suba1.f AND esp4subs2.f WHICH ARE THE ORIGINAL ESP4 SUBROUTINES (I.E. NO MODIFICATIONS).
C
C      DATE: 3 JANUARY 1990
C
C
C      DIMENSION INDICATORS:
C      THE FOLLOWING ARE DEFINED BY THE USER:
C
C      IDFIL: INDICATOR TO DIMENSION FOR FILAMENT TESTING
C      = 1 IMPLIES DIMENSION FOR FILAMENT TESTING
C      = 0 IMPLIES DO NOT DIMENSION FOR FILAMENT TESTING
C      IDSUR: INDICATOR TO DIMENSION FOR FULL SURFACE TESTING
C      = 1 IMPLIES DIMENSION FOR FULL SURFACE TESTING
C      = 0 IMPLIES DO NOT DIMENSION FOR FULL SURFACE TESTING
C      IDWR= MAX. NUMBER OF WIRE POINTS, WIRE SEGMENTS, AND WIRE MODES
C      IPL= MAX. NUMBER PLATES
C      ICM= MAX. NUMBER OF CORNERS ON POLYGONAL PLATES
C      IAT= MAX. NUMBER WIRE/PLATE ATTACHMENT POINTS
C      ITOT= MAX. TOTAL NUMBER OF MODES (WIRE+PLATE+ATTCH.)
C      IDMZI = INDICATOR FOR MAKING FREQUENCY SWEEP COMPUTATION
C      = 1 IMPLIES SET UP Z ARRAY FOR INTERPOLATION
C      = 0 NO FREQUENCY SWEEP
C      IERSR = MAX. I FOR THE ERSR(IAT,I) ARRAY USED IN SUB. ZTOTZ

```

C		ESP00460
C	THE FOLLOWING ARE COMPUTED BY THE CODE:	ESP00470
C		ESP00480
C	IDZT= MAX. LENGTH OF 1-D IMPEDANCE ARRAY ZT	ESP00490
C	IDZTF=MAX. INDICATOR FOR 2-D ARRAY ZTF USED FOR FILAMENT TESTING	ESP00500
C	IDWR2= 2*IDWR	ESP00510
C	ITW2= THE LARGER OF IDWR2 AND ITOT	ESP00520
C		ESP00530
C	DEFINE DIMENSION INDICATORS	ESP00540
C		ESP00550
	PARAMETER (IDFIL=1)	ESP00560
	PARAMETER (IDSUR=1)	ESP00570
	PARAMETER (IDWR=30)	ESP00580
	PARAMETER (IPL=20)	ESP00590
	PARAMETER (ICN=8)	ESP00600
	PARAMETER (IAT=4)	ESP00610
C	PARAMETER (ITOT=200)	ESP00620
	PARAMETER (ITOT=500)	
	PARAMETER (IDMZI = 1)	ESP00630
	PARAMETER (IERVSR = 200)	ESP00640
C	****THE FOLLOWING LINE ADDED FOR NAMELIST MODIFICATION	
	PARAMETER (INFPT=50)	
C		ESP00650
C	THE FOLLOWING IS EQUIVALENT TO:	ESP00660
C	PARAMETER (IDZT=MAXO((IDWR**2+IDWR)/2,IDSUR*(ITOT**2+ITOT)/2,1))	ESP00670
C		ESP00680
	PARAMETER (NUM1=1+(IDWR**2+IDWR)/2)	ESP00690
	PARAMETER (NUM2=1+IDSUR*(ITOT**2+ITOT)/2)	ESP00700
	PARAMETER (MLT1=((NUM1/NUM2)*NUM2)/(1.0*NUM1))+0.99999)	ESP00710
	PARAMETER (MLT2=((NUM2/NUM1)*NUM1)/(1.0*NUM2))+0.99999)	ESP00720
	PARAMETER (NUM3=1+1+(MLT1*NUM1+MLT2*NUM2)/(MLT1+MLT2))	ESP00730
	PARAMETER (NUM4=1+1)	ESP00740
	PARAMETER (MLT3=((NUM3/NUM4)*NUM4)/(1.0*NUM3))+0.99999)	ESP00750
	PARAMETER (MLT4=((NUM4/NUM3)*NUM3)/(1.0*NUM4))+0.99999)	ESP00760
	PARAMETER (IDZT=-1+(MLT3*NUM3+MLT4*NUM4)/(MLT3+MLT4))	ESP00770
C		ESP00780
C	THE FOLLOWING IS EQUIVALENT TO:	ESP00790
C	PARAMETER (IDZTF=MAXO(IDFIL*ITOT,1))	ESP00800
C		ESP00810
	PARAMETER (NUM5=1+IDFIL*ITOT)	ESP00820
	PARAMETER (NUM6=1+1)	ESP00830
	PARAMETER (MLT5=((NUM5/NUM6)*NUM6)/(1.0*NUM5))+0.99999)	ESP00840
	PARAMETER (MLT6=((NUM6/NUM5)*NUM5)/(1.0*NUM6))+0.99999)	ESP00850
	PARAMETER (IDZTF=-1+(MLT5*NUM5+MLT6*NUM6)/(MLT5+MLT6))	ESP00860
C		ESP00870
	PARAMETER (IDWR2=2*IDWR)	ESP00880
C		ESP00890
C	THE FOLLOWING IS EQUIVALENT TO:	ESP00900
C	PARAMETER (ITW2=MAXO(ITOT,IDWR2))	ESP00910
C		ESP00920
	PARAMETER (NUM7=1+ITOT)	ESP00930
	PARAMETER (NUM8=1+IDWR2)	ESP00940
	PARAMETER (MLT7=((NUM7/NUM8)*NUM8)/(1.0*NUM7))+0.99999)	ESP00950
	PARAMETER (MLT8=((NUM8/NUM7)*NUM7)/(1.0*NUM8))+0.99999)	ESP00960
	PARAMETER (ITW2=-1+(MLT7*NUM7+MLT8*NUM8)/(MLT7+MLT8))	ESP00970
C		ESP00980
C	IDMI = 1 IF IDMZI = 0	ESP00990
C	= 3 IF IDMZI = 1	ESP01000
	PARAMETER (IDMI=1+IDMZI*2)	ESP01010
	PARAMETER (IDZTI=1+IDMZI*IDZT)	ESP01020

	PARAMETER (IDZTFI=1+IDMZI+IDZTF)	ESPO1030
C		ESPO1040
C		ESPO1050
C	THE FOLLOWING ARE DIMENSIONED BY IDWR:	ESPO1060
C		ESPO1070
	COMPLEXCGD(IDWR),SGD(IDWR)	ESPO1080
	DIMENSIOND(IDWR),IA(IDWR),IB(IDWR),ND(IDWR),ISC(IDWR),MD(IDWR,4)	ESPO1090
	DIMENSIONI1(IDWR),I2(IDWR),I3(IDWR),JA(IDWR),JB(IDWR)	ESPO1100
	DIMENSIONX(IDWR),Y(IDWR),Z(IDWR)	ESPO1110
C		ESPO1120
C	THE FOLLOWING ARE DIMENSIONED BY IDWR2 = 2*IDWR:	ESPO1130
C		ESPO1140
	COMPLEXZLD(IDWR2),VG(IDWR2)	ESPO1150
C		ESPO1160
C	THE FOLLOWING ARE DIMENSIONED BY THE LARGER OF ITOT OR IDWR2:	ESPO1170
C		ESPO1180
	COMPLEXCG(ITW2)	ESPO1190
C		ESPO1200
C	THE FOLLOWING ARE DIMENSIONED BY IPL AND ICN:	ESPO1210
C		ESPO1220
	DIMENSIONNM12N(IPL),NM23N(IPL),IPN(IPL),PCN(3,ICN,IPL)	ESPO1230
	DIMENSION XP(ICN),YP(ICN),ZP(ICN)	
	DIMENSIONNCRNS(IPL),SEGM(IPL),PC(3,ICN),NPL11(IPL),NDNPLT(IPL)	ESPO1240
	DIMENSION NPL22(IPL),IREC(IPL),SUBI(IPL),IGS(IPL)	ESPO1250
	COMPLEX ZSHT(IPL),ZSHTF(IPL)	ESPO1260
C		ESPO1270
C	THE FOLLOWING ARE DIMENSIONED BY IAT AND IERSVR:	ESPO1280
C		ESPO1290
	INTEGER NASAT(IAT),IABAT(IAT)	
	DIMENSIONBDSK(IAT),RMIN(IAT),DR(IAT),NPLA(IAT),NSA(IAT),	ESPO1300
2	PDIST(IAT)	ESPO1310
	COMPLEXIERSVR(IAT,IERSVR),ZLDA(IAT),VGA(IAT)	ESPO1320
C		ESPO1330
C	THE FOLLOWING ARE DIMENSIONED BY ITOT:	ESPO1340
C		ESPO1350
	DIMENSIONPA(ITOT,4,3),PB(ITOT,4,3),IQUAD(ITOT)	ESPO1360
	DIMENSIONIOVT(ITOT,4),DOVL(ITOT),ITK(ITOT),OPEP(ITOT,3,2)	ESPO1370
	COMPLEXCJ(ITOT),CJP(ITOT),CJT(ITOT),ETT(ITOT),EPP(ITOT),V(ITOT)	ESPO1380
	COMPLEX EXN(ITOT),EYN(ITOT),EZN(ITOT)	ESPO1390
	DIMENSION MPLA(ITOT),MPLB(ITOT),PSZ(ITOT)	ESPO1400
C		ESPO1410
C	THE FOLLOWING ARE DIMENSIONED BY INFPT *****NAMELIST DATA***	
	INTEGER IFMM(INFPT),IABB(INFPT)	
	COMPLEX VLGG(INFPT),ZLL(INFPT)	
C		
C	THE FOLLOWING ARE DIMENSIONED BY IDZT:	ESPO1420
C		ESPO1430
	COMPLEXIT(IDZT)	ESPO1440
C		ESPO1450
C	THE FOLLOWING ARE DIMENSIONED BY IDZTF:	ESPO1460
C		ESPO1470
	COMPLEX ZTF(IDZTF,IDZTF)	ESPO1480
C		ESPO1490
C	THE FOLLOWING ARRAYS HOLD THE Z MATRICES FOR THE FREQ. SWEEP	ESPO1500
C		ESPO1510
	COMPLEX ZTIN(IDMI,IDZTI),ZTFIN(IDMI,IDZTFI,IDZTFI)	ESPO1520
C		ESPO1530
C	THE FOLLOWING ARE FIXED DIMENSIONED:	ESPO1540
C		ESPO1550
	DIMENSION IZC(3)	ESPO1560

```

COMPLEXETE(1441),EPE(1441),ERE(1441),ETAZ(1441),
2 EPAZ(1441)
DIMENSION PET(1441),PEP(1441),PER(1441)
COMPLEX ERAZ(1441)
COMPLEXETA,GAM,Z11,Y11,ERRS,ETTS,EPPS,ETPS,EPTS,ZS,ZL,VLG,EGD
COMPLEX ZIN,YIN,VIN
COMPLEXICGA,CGB,CGCN,CEXP1,CEXP2,CEXP3,CEXP4,FAC1,FAC2,FAC3,FACK
COMPLEX EXT,EYT,EZT,EXP,EYP,EZP,ETRS,EPRS,XJ,YSHY,YSHYF
COMMON /A/ WV,PI,A,Q,GAM,ETA,XK
C***ADDITION OF NAMELISTS
NAMELIST /RNCRL/NGO,NPRINT,NRUNS,NWGS,IWR,IWRZT,INT,INTP,INTD,
2INWR,IRGM,IFIL,RF,INDZI
NAMELIST /FSWEEP/FMC1,FMC2,DFZI,DFP,IRS12,THRD,PHRD,THRI,PHRI
NAMELIST /PATTRN/IFE,IPFE,FNDFE,PHFE,IFA,IPFA,FNDFA,THFA,
2ISE,IPSE,FNDSE,PHSE,THIN,PHIN,ISA,IPSA,FNDSA,THSA,
3AZRANG,ELRANG,AZMIN,ELMIN,IBISC,BETA,NPTBIS,BANGRG
C**NOTE: AZRANG, ELRANG INCLUDED TO REPLACE FIXED 360 DEG.
C**NOTE: AZMIN,ELMIN INCLUDED TO START PATTERNS AT ARB. POINT
C**NOTE: IBISC=1 USES FIXED BISTATIC ANGLE FEATURE WITH
C BETA THE BISTATIC ANGLE,
C NPTBIS THE NUMBER OF TARGET ROTATION ANGLES,
C BANGRG THE ANGULAR RANGE OF TARGET ROTATION
C NOTE: BANGRG CAN BE >0 OR <0 TO DETERMINE ROTATION DIRECTION
C**WHEN THE BISTATIC OPTION IS USED, ELRANG AND AZRANG ARE SET=0
NAMELIST /FWIRET/FMC,CMM,A,NPLTS
NAMELIST /PLATEG/NCNRS,SEGM,IREC,IPN,IGS,ZSHT,XP,YP,ZP
NAMELIST /SAVEZ/IWRZM,IRDZM
NAMELIST /WIREAG/NM,NP,NAT,NFPT,NFS1,NFS2,X,Y,Z,IA,IB
NAMELIST /GENLOD/IFMM,IABB,VLGG,ZLL
NAMELIST /ATTACH/NASAT,IABAT,NPLA,VGA,ZLDA,BDSK
CHARACTER DATNAM=25,OUTNAM=25
C J(J,I,J,NTOT)=(J-1)*NTOT-(J-J-J)/2+1
C AMP(GAM)=CABS(GAM)
C PHS(GAM)=180.0*ATAN2(AIMAG(GAM),REAL(GAM))/3.1415926
C OPEN(UNIT=6,NAME='OUTFL.DAT',TYPE='UNKNOWN')
C THE MAIN PROGRAM CONTAINS FOUR CALLS TO THE CLOCK FUNCTION
C GETCP(I), WHERE I IS THE CLOCK READING IN HUNDREDTHS OF A
C SECOND. THESE FOUR LINES HAVE BEEN "COMMENTED" OUT. IN ORDER
C FOR THE CODE TO OUTPUT CPU TIMES, THE USER MUST REPLACE THESE
C CALLS TO GETCP BY A COMPARABLE CLOCK FUNCTION ON HIS SYSTEM.
C CALL GETCP2 PERFORMS THE CPU TIME FUNCTION ON THE SUN 3 SYSTEM
C CALL GETCP2(ICPU)
C PI=3.14159265
C I9999=0
C XJ=(0.0,1.0)
C IANT=0
C INM= MAX. NUMBER WIRE SEGMENTS
C ICJ= MAX. NUMBER WIRE MODES
C IPLM= MAX. NUMBER PLATE MODES
C ICC= MAX. SIZE OF 2-D ARRAY ZTF
C INM-IDWR
C ICJ-IDWR
C IPLM-IDTUT
C ICC-IDZTF
C NGO = 0 IMPLIES SET UP GEOMETRY BUT DO NOT RUN.
C NGO = 1 IMPLIES RUN.

```

```

ESP01670
ESP01680
ESP01690
ESP01600
ESP01610
ESP01620
ESP01630
ESP01640
ESP01650
ESP01660
ESP01670
ESP01680
ESP01690
ESP01700
ESP01710
ESP01720
ESP01730
ESP01740
ESP01750
ESP01760
ESP01770
ESP01780
ESP01790
ESP01800
ESP01810
ESP01820
ESP01830
ESP01840
ESP01850
ESP01860
ESP01870
ESP01880
ESP01890
ESP01900
ESP01910
ESP01920
ESP01930

```

C	NPRINT = 0 IMPLIES PRINT INPUT DATA ONLY.	ESP01940
C	NPRINT = 1 IMPLIES PRINT WIRE AND PLATE GEOMETRY.	ESP01950
C	NPRINT = 2 IMPLIES PRINT INPUT DATA AND WIRE/PLATE GEOMETRY.	ESP01960
C	NPRINT = 3 IMPLIES PRINT NEITHER.	ESP01970
C		ESP01980
	WRITE(6,2959)	
2969	FORMAT(1X,'ENTER INPUT DATA FILE NAME (typically esp4nam.datex)')	
	READ(5,*)DATNAM	
	OPEN(11,FILE=DATNAM,FORM='FORMATTED')	
	WRITE(6,3069)	
3969	FORMAT(1X,'ENTER OUTPUT DATA FILE NAME (typ. esp4namfort.8)')	
	READ(5,*)OUTNAM	
	OPEN(8,FILE=OUTNAM,FORM='FORMATTED')	
C	READ(11,*)NGO,NPRINT,NRUNS,NWGS,IWR,IWZT,INT,INTP,INTD,INWR,IRGM,ESP01990	
C	1IFIL,RF,INDZI	ESP02000
	READ(11,RNCTRL)	
C		ESP02010
C	READ IN PARAMETERS OF FREQUENCY SWEEP COMPUTATION	ESP02020
C		ESP02030
	12468=0	ESP02040
	IF(INDZI.NE.0)THEN	ESP02050
	IF(IDMZI.EQ.0)THEN	ESP02060
	WRITE(6,3215)	ESP02070
3215	FORMAT(3X,'DIMENSION INDICATOR IDMZI MUST BE SET TO 1 IF INOZI'/ESP02080	
2	3X,'IN READ 1 IS SET TO 1 OR 2')	ESP02090
	STOP	ESP02100
	ENDIF	ESP02110
C	READ(11,*)FMC1,FMC2,DFZI,DFI,IRS12,THRD,PHAD,THINC,PHINC	ESP02120
	READ(11,FSWEEP)	

DFTOT=(FMC2-FMC1)	ESP02130
NFZI=0.99*DFTOT/DFZI	ESP02140
IF(NFZI.LT.2)NFZI=2	ESP02150
DFZI=DFTOT/NFZI	ESP02160
NFZI=NFZI+1	ESP02170
NFF=0.99*DFTOT/DFF	ESP02180
IF(NFF.LT.1)NFF=1	ESP02190
DFF=DFTOT/NFF	ESP02200
NFF=NFF+1	ESP02210
IF(NGO.NE.0)WRITE(10,3210)RF,THRD,PHRL,THINC,PHINC,IR312,	ESP02220
2 NFF,NFZI,INDZI	ESP02230
3210 FORMAT(1X,E11.5,4(1X,F6.1),1X,6I4)	ESP02240
II2LST=2	ESP02250
FNDFE=1.0	ESP02260
FNDFA=1.0	ESP02270
FNDST=1.0	ESP02280
FNDSE=1.0	ESP02290
ENDIF	ESP02300
IF(INWR.EQ.0)THEN	ESP02310
NH=0	ESP02320
NP=0	ESP02330
NAT=0	ESP02340
NWR=0	ESP02350
NFPT=0	ESP02360
NFS1=0	ESP02370
NFS2=0	ESP02380
ENDIF	ESP02390
IF(INT.GT.0)INT=2*((INT+1)/2)	ESP02400
INTP=2*((INTP+1)/2)	ESP02410
INTD=2*((INTD+1)/2)	ESP02420
270 FORMAT(2I1,2I3)	ESP02430
C	ESP02440
C READ IN PARAMETERS OF ELEVATION AND AZIMUTH PATTERNS	ESP02450
C SET ALL TO 0 IF INDZI > 0	ESP02460
C	ESP02470
IF(INDZI.EQ.0)THEN	ESP02480
C READ(11,*)IFE,IPFE,FNDFE,PHFE	ESP02490
C READ(11,*)IFA,IPFA,FNDFA,THFA	ESP02500
C READ(11,*)ISE,IPSE,FNDSE,PHSE,THIN,PHIN	ESP02510
C READ(11,*)ISA,IPSA,FNDSA,THSA	ESP02520
CC***DEFAULT NAMELIST PATTRN VALUES FOR AZRANG,ELRANG,AZMIN,ELMIN,...	
AZRANG=360.	
ELRANG=360.	
AZMIN=0.	
ELMIN=0.	
IBISC=0	
BETA=0.	
NPTBIS=1	
BANGRG=0.	
READ(11,PATTRN)	
IF(IBISC.EQ.0)NPTBIS=1	
IF(IBISC.EQ.1)ELRANG=0.	
ELSE	ESP02530
IFE=0	ESP02540
IPFE=0	ESP02550
FNDFE=1.0	ESP02560
PHFE=0.0	ESP02570
IFA=0	ESP02580
IPFA=0	ESP02590
FNDFA=1.0	ESP02600

	THFA=0.0	ESP02610
	ISE=0	ESP02620
	IPSE=0	ESP02630
	FNDSE=1.0	ESP02640
	PHSE=0.0	ESP02650
	THIN=0.0	ESP02660
	PHIN=0.0	ESP02670
	ISA=0	ESP02680
	IPSA=0	ESP02690
	FNDSA=1.0	ESP02700
	THSA=0.0	ESP02710
	ENDIF	ESP02720
312	FORMAT(3I2,F10.5)	ESP02730
	IMAGE=0	ESP02740
	IF(INDZI.EQ.0)THEN	ESP02750
	IF(ISE.LT.0.OR.ISA.LT.0)IMAGE=1	ESP02760
	ELSE	ESP02770
	IF(IRS12.LT.0)IMAGE=1	ESP02780
	ENDIF	ESP02790
	ISE=IABS(ISE)	ESP02800
	ISA=IABS(ISA)	ESP02810
	IFF=0	ESP02820
	ISCAT=0	ESP02830
	IF(INDZI.EQ.0)THEN	ESP02840
	IF(IFE+IFA+ISE+ISA.GE.1)IFF=1	ESP02850
	IF(ISE.EQ.1.OR.ISA.EQ.1)ISCAT=1	ESP02860
	IF(ISE.EQ.2.OR.ISA.EQ.2)ISCAT=2	ESP02870
	IF(ISE.EQ.3.OR.ISA.EQ.3)ISCAT=3	ESP02880
	ELSE	ESP02890
	IFF=1	ESP02900
	IF(IABS(IRS12).EQ.2)THEN	ESP02910
	ISCAT=2	ESP02920
	IF(ABS(THINC-THRD)+ABS(PHINC-PHRD).LT.0.001)ISCAT=1	ESP02930
	ISE=1	ESP02940
	ISA=0	ESP02950
	ENDIF	ESP02960
	IF(IABS(IRS12).EQ.1)THEN	ESP02970
	ISCAT=0	ESP02980
	IFE=1	ESP02990
	IFA=0	ESP03000
	ENDIF	ESP03010
	ENDIF	ESP03020
C	NPLOTS = THE NUMBER OF PATTERN PLOTS	ESP03030
C	IRS12 = 1 OR 2 FOR RADIATION OR SCATTERING PATTERNS	ESP03040
	NPLOTS=0	ESP03050
	IF(ISCAT.EQ.0)THEN	ESP03060
	IF(IFE.NE.0.AND.IPFE.EQ.1)NPLOTS=NPLOTS+1	ESP03070
	IF(IFA.NE.0.AND.IPFA.EQ.1)NPLOTS=NPLOTS+1	ESP03080
	ELSE	ESP03090
	IF(ISE.NE.0.AND.IPSE.EQ.1)NPLOTS=NPLOTS+1	ESP03100
	IF(ISA.NE.0.AND.IPSA.EQ.1)NPLOTS=NPLOTS+1	ESP03110
	ENDIF	ESP03120
	IF(INDZI.EQ.0)THEN	ESP03130
	IRS12=1	ESP03140
	IF(ISCAT.NE.0)IRS12=2	ESP03150
	ENDIF	ESP03160
	DO 700 NRUN=1,NRUNS	ESP03170
C		ESP03180
C	READ FREQUENCY, WIRE CONDUCTIVITY, AND WIRE RADIUS	ESP03190
C		ESP03200

C	READ(11,*)FMC,CMM,A	ESP03210
	READ(11,FWIRET)	
	IF(INDZI.NE.O)FMC=FMC2	ESP03220
	IF(NPLOTS.GT.O.AND.INDZI.EQ.O.AND.NGO.NE.O)	ESP03230
2	WRITE(6,337)NPLOTS,IRS12,FMC,RF	ESP03240
337	FORMAT(1X,2(13,1X),2(F11.4,2X))	ESP03250
	WV=300.0/FMC	ESP03260
	TOUCH=0.001*WV	ESP03270
	IOK=1	ESP03280
C		ESP03290
C	READ IN THE NUMBER OF PLATES	ESP03300
C		ESP03310
C	READ(11,*)NPLTS	ESP03320
	SEGMX=-1.0	ESP03330
	IF(NPLTS.GT.IPL)THEN	ESP03340
	WRITE(6,330)NPLTS	ESP03350
330	FORMAT(' ***** INCREASE PARAMETER IPL TO ',I4)	ESP03360
	STOP	ESP03370
	ENDIF	ESP03380
	NOVT=0	ESP03390
	NPLTM=0	ESP03400
	IF(NPLTS.EQ.O)GOTO462	ESP03410
	IOKT=1	ESP03420
C		ESP03430
C	IF NPLTS < 0, GENERATE PLATE GEOMETRY IN CGEOM	ESP03440
C		ESP03450
	IF(NPLTS.LT.C)THEN	ESP03460
C		ESP03470
C	PLATE GEOMETRY GENERATED IN SUBROUTINE CALL BELOW	ESP03480
C	SUBROUTINE PGEOM IS CONTAINED IN ESP4PGM FORTRAN.	ESP03490
C		ESP03500
	CALL PGEOM(IPL,ICN,NPLTS,NCNRS,SEGM,IRES,IPN,IGS,ZSHT,PCN)	ESP03510
	IF(NPLTS.GT.IPL)THEN	ESP03520
	WRITE(6,330)NPLTS	ESP03530
	STOP	ESP03540
	ENDIF	ESP03550
	ELSE	ESP03560
C		ESP03570
C	READ IN THE PLATE GEOMETRY	ESP03580
C		ESP03590
	DO 464 NPL=1,NPLTS	ESP03600
C	READ(11,*)NCNRS(NPL),SEGM(NPL),IRES(NPL),IPN(NPL),IGS(NPL),	ESP03610
C	2 ZSHT(NPL)	ESP03620
	READ(11,PLATEG)	
	WRITE(6,PLATEG)	
	IF(SEGM(NPL).GT.SEGMX)SEGMX=SEGM(NPL)	ESP03630
	IF(NCNRS(NPL).EQ.4)IGS(NPL)=0	ESP03640
	IF(NCNRS(NPL).GT.ICN)THEN	ESP03650
	WRITE(6,331)NCNRS(NPL)	ESP03660
331	FORMAT(' ***** INCREASE PARAMETER ICN TO AT LEAST ',I4)	ESP03670
	STOP	ESP03680
	ENDIF	ESP03690
	DO 466 NCNR=1,NCNRS(NPL)	ESP03700
C	READ(11,*)PCN(1,NCNR,NPL),PCN(2,NCNR,NPL),PCN(3,NCNR,NPL)	ESP03710
C	***FILL-IN PCN ARRAY FROM NAMELIST DATA	
	PCN(1,NCNR,NPL)=XP(NCNR)	
	PCN(2,NCNR,NPL)=YP(NCNR)	
	PCN(3,NCNR,NPL)=ZP(NCNR)	
466	CONTINUE	ESP03720
464	CONTINUE	ESP03730

END IF	ESP03740
DO 465 NPL=1,NPLTS	ESP03750
CALL PLPLCK(PCN,IPL,ICN,NCNRS(NPL),TOUCH,NPL,IOK)	ESP03760
IF (IOK.EQ.0) IOKT=0	ESP03770
465 CONTINUE	ESP03780
IF(IOKT.EQ.0) GOTO 9374	ESP03790
DO 467 NPL=1,NPLTS	ESP03800
NCNS=NCNRS(NPL)	ESP03810
SEG=SEGM(NPL)	ESP03820
IRE=IREC(NPL)	ESP03830
IP=IPN(NPL)	ESP03840
IG=IGS(NPL)	ESP03850
DO 468 NC=1,NCNS	ESP03860
DO 468 I=1,3	ESP03870
468 PC(I,NC)=PCN(I,NC,NPL)	ESP03880
C	ESP03890
C	ESP03900
C	ESP03910
CALL PLATES(PC,NCNS,ICN,NPL,NDNPLT,PA,PB,IPLM,SEG,	ESP03920
1 IQUAD,WV,IRE,IP,MPL1,MPL2,IOK,NM12,NM23,IG)	ESP03930
IF(NPL.EQ.NPLTS)NPLTM=NDNPLT(NPLTS)	ESP03940
NPL11(NPL)=MPL1	ESP03950
NPL22(NPL)=MPL2	ESP03960
C*****	ESP03970
NM12N(NPL)=NM12	ESP03980
NM23N(NPL)=NM23	ESP03990
C*****	ESP04000
467 CONTINUE	ESP04010
C	ESP04020
C	ESP04030
C	ESP04040
CALL POPLOV(NPLTS,PCN,NCNRS,TOUCH,	ESP04050
* SEGM,PA,PB,NOVT,NPLTM,IPL,IPLM,ICN,IOVT,DOVL,ITK,NOPL,	ESP04060
* IQUAD,WV,NDNPLT,OVEP)	ESP04070
462 CONTINUE	ESP04080
NPLTM=NPLTM+NOVT	ESP04090
DO 600 NWC=1,NWGS	ESP04100
I12=1	ESP04110
CALL GETCP2(JCPU)	ESP04120
IWRZM=0	ESP04130
IRDZM=0	ESP04140
C	ESP04150
C	ESP04160
C	ESP04170
C	ESP04180
READ(11,*)IWRZM,IRDZM	
READ(11,SAVE2)	
C	ESP04190
IF(INDZ1.GT.0)THEN	
C	ESP04200
IWRZM=0	
C	ESP04210
IRDZM=0	
C	ESP04220
ENDIF	
WV=300.0/FMC	ESP04230
INM2=2*INM	ESP04240
DO 2774 I=1,INM2	ESP04250
ZLD(I)=CMPLX(0.0,0.0)	ESP04260
VG(I)=CMPLX(0.0,0.0)	ESP04270
IF(I.GT.IAT)GOTO2774	ESP04280
VGA(I)=CMPLX(0.0,0.0)	ESP04290
ZLDA(I)=CMPLX(0.0,0.0)	ESP04300
2774 CONTINUE	ESP04310
IF(INWA.EQ.0) NWA=0	ESP04320

IF(INWR.EQ.O) NAT=0	ESP04330
IF(INWR.EQ.O)GOTO2773	ESP04340
IF(IRGM.EQ.O)GOTO2800	ESP04350
C	ESP04360
C SET UP POINTS AND SEGMENTS.	ESP04370
C	ESP04380
C READ(11,*)NM,NP,NAT,NFPT,NFS1,NFS2	ESP04390
READ(11,WIREAG)	
IF(NAT.GT.IAT)THEN	ESP04400
WRITE(6,332)NAT	ESP04410
332 FORMAT(' ***** INCREASE PARAMETER IAT TO AT LEAST ',I4)	ESP04420
STOP	ESP04430
ENDIF	ESP04440
C	ESP04450
C READ IN COOR. OF NP POINTS	ESP04460
C	ESP04470
DO 2810 I=1,NP	ESP04480
C READ(11,*)X(I),Y(I),Z(I)	ESP04490
2810 CONTINUE	ESP04500
C	ESP04510
C READ IN ENDPOINTS OF NM SEGMENTS	ESP04520
C	ESP04530
DO 2820 I=1,NM	ESP04540
C READ(11,*)IA(I),IB(I)	ESP04550
2820 CONTINUE	ESP04560
C	ESP04570
C READ IN WIRE GENERATORS AND LOADS	ESP04580
C	ESP04590
READ(11,GENLOD)	
DO 2830 I=1,NFPT	ESP04600
C IF(NFPT.GE.1)READ(11,*)IFM,IAB,VLG,ZL	ESP04610
C II=IFM+IAB*NM	ESP04620
II=IFM(I)+IAB(I)*NM	
VG(II)=VLGG(I)	ESP04630
ZLD(II)=ZLL(I)	ESP04640
2830 CONTINUE	ESP04650
C	ESP04660
C READ IN ATTACHMENT POINT GEOMETRY	ESP04670
C	ESP04680
IF(NAT.EQ.O)GOTO2850	ESP04690
READ(11,ATTACH)	
DO 2840 I=1,NAT	ESP04700
C READ(11,*)NAS,IAB,NPLA(I),VGA(I),ZLDA(I),BDSK(I)	ESP04710
C NSA(I)=NAS+IAB*NM	ESP04720
NSA(I)=NASAT(I)+IABAT(I)*NM	
2840 CONTINUE	ESP04730
GOTO2850	ESP04740
C	ESP04750
C IF IRGM = 0, GENERATE WIRE GEOMETRY IN SUBROUTINE WGEOM	ESP04760
C	ESP04770
2800 CALL WGEOM(IA,IB,X,Y,Z,NM,NP,NAT,NSA,NPLA,VGA,BDSK,	ESP04780
2 ZLDA,NVG,VG,ZLD,WV,NFS1,NFS2)	ESP04790
2850 CONTINUE	ESP04800
IF(IFIL.EQ.1.AND.NAT.GT.O)THEN	ESP04810
WRITE(6,2852)	ESP04820
2852 FORMAT(/3X,'ERROR: FILAMENT TESTING CAN NOT BE USED IF ',	ESP04830
2 'GEOMETRY CONTAINS A WIRE/PLATE ATTACHMENT'/3X,	ESP04840
3 'SET IFIL = 0 IN READ 1')	ESP04850
STOP	ESP04860
ENDIF	ESP04870

C		ESP04880
C	PLACE MODES ON THE WIRE	ESP04890
C		ESP04900
	CALL SORT(IA,IB,I1,I2,I3,JA,JB,MD,ND,NM,NP,NWR,MAX,MIN,ICJ,INM)	ESP04910
	NDWR=MAXO(NM,NP,NWR)	ESP04920
	IF(NDWR.GT.IDWR)THEN	ESP04930
	WRITE(6,335)NDWR	ESP04940
335	FORMAT(' ***** INCREASE PARAMETER IDWR TO AT LEAST ',I4)	ESP04950
	STOP	ESP04960
	ENDIF	ESP04970
2773	CONTINUE	ESP04980
C		ESP04990
C	DETERMINE ON WHICH PLATES SURFACE PATCH MODES LIE	ESP05000
C		ESP05010
	DO 2048 I=1,NPLTM	ESP05020
	CALL WCHPLT(I,NPLTS,NOPL,NDNPLT,IOVT,ITK,ITOT,MPLA,MPLB)	ESP05030
2048	CONTINUE	ESP05040
	NTOT=NWR+NPLTM+NAT	ESP05050
	IF(NTOT.GT.ITOT)THEN	ESP05060
	WRITE(6,334)NTOT	ESP05070
334	FORMAT(' ***** INCREASE PARAMETER ITOT TO AT LEAST ',I5)	ESP05080
	STOP	ESP05090
	ENDIF	ESP05100
	N1=NPLTM-NOVT+1	ESP05110
	N2=NPLTM	ESP05120
	IF(NOVT.GT.0)THEN	ESP05130
	DO 665 I=N1,N2	ESP05140
665	IQUAD(I)=0	ESP05150
	ENDIF	ESP05160
	NZT=(NTOT**2+NTOT)/2	ESP05170
	FHZ=FMC*1.0E6	ESP05180
	ETA=(376.7,0.)	ESP05190
	GAM=CMPLX(0.,2.*PI/WV)	ESP05200
	XK=2.*PI/WV	ESP05210
	Q=.001*WV	ESP05220
	IF(NWR.EQ.0)A=Q	ESP05230
C		ESP05240
C	SET UP SLEEVES, NO SLEEVES (1, 0) ON THE SEGMENTS.	ESP05250
C		ESP05260
	DO 125 I=1,INM	ESP05270
	ISC(I)=0	ESP05280
125	CONTINUE	ESP05290
	IF(NGO.EQ.0)THEN	ESP05300
C		ESP05310
C	WRITE OUT WIRE/PLATE/OVERLAP GEOMETRY FOR GKS PLOTTING	ESP05320
C		ESP05330
	WRITE(9,*)NPLTS,NPLTM,NM,NP,NWR,NAT,WV,NOPL,NOVT	ESP05340
	DO 158 I=1,NP	ESP05350
	WRITE(9,*)X(I),Y(I),Z(I)	ESP05360
158	CONTINUE	ESP05370
	DO 159 I=1,NM	ESP05380
	WRITE(9,*)IA(I),IB(I)	ESP05390
159	CONTINUE	ESP05400
	DO 161 NPL=1,NPLTS	ESP05410
161	WRITE(9,*)NCNRS(NPL),NPL11(NPL),NPL22(NPL),NDNPLT(NPL),IPN(NPL)	ESP05420
	DO 162 I=1,NPLTM	ESP05430
	DO 163 J=1,4	ESP05440
	WRITE(9,*)PA(I,J,1),PA(I,J,2),PA(I,J,3),PB(I,J,1),PB(I,J,2),	ESP05450
2	PB(I,J,3)	ESP05460
163	CONTINUE	ESP05470

152	CONTINUE	ESP05480
	DO 156 NPL=1,NPLTS	ESP05490
	NCNR=NCNRS(NPL)	ESP05500
	DO 157 NC=1,NCNR	ESP05510
	WRITE(9,*)PCN(1,NC,NPL),PCN(2,NC,NPL),PCN(3,NC,NPL)	ESP05520
157	CONTINUE	ESP05530
156	CONTINUE	ESP05540
	DO 156 I=1,NOPL	ESP05550
	WRITE(9,*)IOVT(I,1),IOVT(I,2),IOVT(I,3),IOVT(I,4),ITK(I)	ESP05560
166	CONTINUE	ESP05570
	ENDIF	ESP05580
C	END GKS PLOTTING OUTPUT	ESP05590
	IF(NPRINT.NE.O.AND.NPRINT.NE.2)GOTO610	ESP05600
C		ESP05610
C	WRITE OUT INPUT DATA.	ESP05620
C		ESP05630
	WRITE(6,621)FMC,WV,A,INTP,INTD,INT,IFIL	ESP05640
621	FORMAT(/3X,'OHIO STATE UNIVERSITY ELECTROMAGNETIC SURFACE '	ESP05650
2	'PATCH (ESP) CODE: VERSION IV'	ESP05660
2	//10X,'INPUT DATA'//3X,'FREQ.(MHZ)=' ,F10.3,3X,'WAVE(M)=' ,	ESP05670
2	F10.3,3X,'WIRE RAD(M)=' ,F9.6,/,	ESP05680
33X	,INTP=' ,I4,3X,'INTD=' ,I4,3X,'INT=' ,I4,3X,'IFIL=' ,I2)	ESP05690
	WRITE(6,623) CMM	ESP05700
623	FORMAT(3X,'WIRE CONDUCTIVITY =' ,F6.2,' MEGAMHOS/M')	ESP05710
	WRITE(6,3006)IDWR,ITW2,ICN,IPL,IAT,ITOT,IDZT,IDZTF,IDMI,	ESP05720
2	IDZTI,IDZTFI,IDMZI	ESP05730
3006	FORMAT(/3X,'SUMMARY OF ARRAY DIMENSIONS'/3X,'IDWR =' ,I4/	ESP05740
2	3X,'ITW2 =' ,I4/3X,'ICN =' ,I4/3X,'IPL =' ,I4/	ESP05750
3	3X,'IAT =' ,I4/3X,'ITOT =' ,I4/3X,'IDZT =' ,I7/	ESP05760
4	3X,'IDZTF =' ,I4/3X,'IDMI =' ,I4/3X,'IDZTI =' ,I7/	ESP05770
5	3X,'IDZTFI =' ,I4/3X,'IDMZI =' ,I2)	ESP05780
	WRITE(6,3006)IWRZM,IRDZM	ESP05790
3006	FORMAT(/3X,'MATRIX WRITE AND READ Z FROM DISK INDICATORS:/'	ESP05800
2	3X,'IWRZM =' ,I2,5X,'IRDZM =' ,I2)	ESP05810
C		ESP05820
C	WRITE OUT PLATE GEOMETRY.	ESP05830
C		ESP05840
520	FORMAT(2X,'X,Y,Z COOR. (METERS) OF CORNER ',I2,' =' ,3F12.5)	ESP05850
526	FORMAT(/3X,'COOR. (METERS) OF ',I3,' MODES ON PLATE ',I3,/)	ESP05860
526	FORMAT(/3X,'THERE ARE ',I3,' MODES ON PLATE ',I3,/)	ESP05870
530	FORMAT(3X,'I XA1 YA1 ZA1 XA2 YA2 ZA2 ',	ESP05880
2	' XA3 YA3 ZA3 XB1 YB1 ZB1 XB2 ',	ESP05890
3	' YB2 ZB2 XD3 YB3 ZB3 '/')	ESP05900
550	FORMAT(1X,I3,1X,18(F4.2))	ESP05910

```

WRITE(6,471)NPLTS
471 FORMAT(/3X,'GEOMETRY FOR THE ',I3,' PLATES')
IF(NPLTS.LE.0)GOTO610
DO 472 NPL=1,NPLTS
IF(IREC(NPL).EQ.1)WRITE(6,473)NPL,NCNRS(NPL),SEGM(NPL),
1 IPN(NPL),IGS(NPL),ZSHT(NPL)
473 FORMAT(/25X,'PLATE NUMBER ',I3,' (RECTANGULAR)'
1 /3X,'NUMBER OF CORNERS = ',I3/3X,'MAXIMUM SEGMENT SIZE',
2 2X,'(WAVELENGTH) = ',F10.5/3X,'POLARIZATION INDICATOR = ',I3/3X,
3 'GENERATING SIDE INDICATOR = ',I3/
4 3X,'SHEET IMPEDANCE (OHMS/SQ.) = ',E11.4,'+J ',E11.4)
IF(IREC(NPL).EQ.0)WRITE(6,444)NPL,NCNRS(NPL),SEGM(NPL),
1 IPN(NPL),IGS(NPL),ZSHT(NPL)
444 FORMAT(/25X,'PLATE NUMBER ',I3,' (POLYGONAL)'
1 /3X,'NUMBER OF CORNERS = ',I3/3X,'MAXIMUM SEGMENT SIZE',
2 2X,'(WAVELENGTH) = ',F10.5/3X,'POLARIZATION INDICATOR = ',I3/3X,
3 'GENERATING SIDE INDICATOR = ',I3/
4 3X,'SHEET IMPEDANCE (OHMS/SQ.) = ',E11.4,'+J ',E11.4)
DO 474 NCNR=1,NCNRS(NPL)
474 WRITE(6,520)NCNR,PCN(1,NCNR,NPL),PCN(2,NCNR,NPL),PCN(3,NCNR,NPL)
N2=NDNPLT(NPL)
N1=NPL-1
NA=1
IF(NPL.GT.1) NA=NDNPLT(N1)+1
IF(NPL.GT.1) NN=N2-NA+1
IF(NPL.EQ.1) NN=N2
IF(IWR.GE.1)THEN
WRITE(6,525)NN,NPL
ELSE
WRITE(6,526)NN,NPL
ENDIF
IF(IWR.LE.0)GO TO 472
WRITE(6,531)
531 FORMAT(1X,'MONOPOLE MODE X1 Y1 Z1 X2',
1 ' Y2 Z2 X3 Y3 Z3 X4',
2 ' Y4 Z4 '/)
DO 541 I=NA,N2
WRITE(6,551) I,((PA(I,J,K),K=1,3),J=1,4)
551 FORMAT(4X,' A ',3X,I3,2X,12(F9.5))
WRITE(6,552) I,((PB(I,J,K),K=1,3),J=1,4)
552 FORMAT(4X,' B ',3X,I3,2X,12(F9.5)/)
541 CONTINUE
472 CONTINUE
C
C WRITE OUT OVERLAP MODES
C
IF (NOVT .EQ. 0) GOTO 610
IMX=0
DO 2039 I=1,NOPL
IF(IOVT(I,2) .EQ. 0)
& WRITE(6,2031)ITK(I),IOVT(I,1),IOVT(I,3),IOVT(I,4)
IF(IOVT(I,4) .EQ. 0)
& WRITE(6,2031)ITK(I),IOVT(I,3),IOVT(I,1),IOVT(I,2)
IF((IOVT(I,2) .EQ. 0 .OR. IOVT(I,4) .EQ. 0) .AND.
& DOVL(I) .LT. 0.1*WV) WRITE(6,2032)DOVL(I)
IF(IOVT(I,2) .NE. 0 .AND. IOVT(I,4) .NE. 0)THEN
IF(IWR.LE.0)THEN
WRITE(6,2033)ITK(I),IOVT(I,1),IOVT(I,2),IOVT(I,3),IOVT(I,4)
ELSEIF(IWR.GE.1)THEN
WRITE(6,2030)ITK(I),IOVT(I,1),IOVT(I,2),IOVT(I,3),IOVT(I,4)

```


ENDIF	ESPO66520
ENDIF	ESPO66530
IF(IWR.LE.0.OR.ITK(I).EQ.0)GOTO2039	ESPO66540
IMN=IMX+1	ESPO66550
IMX=IMX+ITK(I)	ESPO66560
DO2040ICT=IMN,IMX	ESPO66570
II=NPLTM-NOVT+ICT	ESPO66580
2041 IF(ICT.EQ.IMN)WRITE(6,531)	ESPO66590
WRITE(6,551)II,((PA(II,J,K),K=1,3),J=1,4)	ESPO66600
WRITE(6,552)II,((PB(II,J,K),K=1,3),J=1,4)	ESPO66610
2040 CONTINUE	ESPO66620
2039 CONTINUE	ESPO66630
2030 FORMAT(/3X,'COORD. (METERS) OF ',I3,' OVERLAP MODES',	ESPO66640
& ' BETWEEN'/3X,'PLATE',I3,', SIDE',I2,' AND PLATE',I3,	ESPO66650
& ', SIDE',I2//)	ESPO66660
2033 FORMAT(/3X,'THERE ARE ',I3,' OVERLAP MODES',	ESPO66670
& ' BETWEEN'/3X,'PLATE',I3,', SIDE',I2,' AND PLATE',I3,	ESPO66680
& ', SIDE',I2//)	ESPO66690
2031 FORMAT(/3X,'COORD. (METERS) OF ',I3,' OVERLAP MODES',	ESPO67000
& ' BETWEEN FACE OF PLATE',I3,' AND PLATE ',I3,' SIDE ',I2//)	ESPO67100
2032 FORMAT(3X,'***** WARNING: LENGTH OF OVERLAP MODE = ',	ESPO67200
& 1PE10.2,' LESS THAN 0.1*WAVELENGTH')	ESPO67300
610 CONTINUE	ESPO67400
C	ESPO67500
C WRITE OUT LIST OF PLATE SURFACE PATCH MODE LOCATIONS	ESPO67600
C	ESPO67700
IF(IWR.GE.1)THEN	ESPO67800
WRITE(6,2045)	ESPO67900
2045 FORMAT(/3X,'LIST OF PLATES ON WHICH SURFACE PATCH MODES LIE'	ESPO68000
2 /4X,'N',3X,'N-NWR',3X,'MON. A',3X,'MON. B'//)	ESPO68100
DO2046IL=1,NPLTM	ESPO68200
I=IL+NWR	ESPO68300
WRITE(6,2047)I,IL,MPLA(IL),MPLB(IL)	ESPO68400
2047 FORMAT(1X,I4,3X,I4,5X,I3,7X,I3)	ESPO68500
2046 CONTINUE	ESPO68600
ENDIF	ESPO68700
IF(NPRINT.NE.1.AND.NPRINT.NE.2)GOTO620	ESPO68800
IF(NWR.EQ.0)GOTO726	ESPO68900
C	ESPO69000
C WRITE OUT POINTS AND SEGMENTS.	ESPO69100
C	ESPO69200
WRITE(6,130)NP	ESPO69300
130 FORMAT(/5X,I3,' POINTS ON THE WIRE (METERS)',/5X,'I',9X,	ESPO69400
2'X(I)',9X,'Y(I)',9X,'Z(I)',/)	ESPO69500
DO140I=1,NP	ESPO69600
WRITE(6,150)I,X(I),Y(I),Z(I)	ESPO69700
150 FORMAT(3X,I3,3(2X,E11.4,2X))	ESPO69800
140 CONTINUE	ESPO69900
160 FORMAT(/5X,I3,' SEGMENTS ON THE WIRE',/5X,'J',4X,'IA(J)',	ESPO70000
23X,'IB(J)',2X,'D(J) (METERS)'//)	ESPO70100
WRITE(6,190)MAX,MIN,NWR	ESPO70200
190 FORMAT(/5X,'MODES ON THE WIRE STRUCTURE',/5X,'MAXIMUM NUMBER	ESPO70300
2 OF MODES AT ONE POINT = ',I2/5X,'MINIMUM NUMBER OF MODES AT ONE	ESPO70400
3POINT = ',I2/5X,'NUMBER OF WIRE MODES = ',I3//)	ESPO70500
IF(IWR.LE.0)GOTO729	ESPO70600
WRITE(6,200)	ESPO70700
200 FORMAT(5X,'I',2X,'I1(I)',2X,'I2(I)',2X,'I3(I)',2X,'JA(I)',2X,	ESPO70800
2'JB(I)',/)	ESPO70900
DO210I=1,NWR	ESPO71000
WRITE(6,220)I,I1(I),I2(I),I3(I),JA(I),JB(I)	ESPO71100

```

220 FORMAT(2X,6(I3,4X))
210 CONTINUE
729 WRITE(6,160)NM
230 FORMAT(/5X,'SEGMENT LENGTHS(M)',/5X,'J',3X,'IA(J)',3X,'IB(J)',
29X,'D (J)',/)
DO 70 J=1,NM
K=IA(J)
L=IB(J)
D(J)=SQRT((X(K)-X(L))**2+(Y(K)-Y(L))**2+(Z(K)-Z(L))**2)
EGD=CEXP(GAM*D(J))
SGD(J)=(EGD-1.0/EGD)/2.0
CGD(J)=(EGD+1.0/EGD)/2.0
WRITE(6,240)J,IA(J),IB(J),D (J)
240 FORMAT(3X,I3,4X,I3,5X,I3,3X,E13.6)
70 CONTINUE
C
C WRITE OUT ATTACHMENT POINT GEOMETRY.
C
726 IF(NAT.LE.0)GOTO620
WRITE(6,560)NAT
560 FORMAT(///3X,'GEOMETRY FOR THE ',I2,' ATTACHMENT POINTS')
WRITE(6,570)
570 FORMAT(3X,'1 SEGMENT END PLATE B (METERS)')
DO680NA=1,NAT
NND=0
IF(NSA(NA).GT.NM)NND=1
MMD=NND+1
NAS=NSA(NA)-(MMD-1)*NM
WRITE(6,590)NA,NAS,NND,NPLA(NA),BDSK(NA)
590 FORMAT(2X,I2,3X,I4,5X,I1,5X,I2,5X,F8.5)
580 CONTINUE
620 CONTINUE
WRITE(6,722)
722 FORMAT(/5X,'LISTING OF LOADS AND GENERATORS')
DO622J=1,NM
IF(CABS(VG(J)).GT.1.0E-6)WRITE(6,723)VG(J),J
IF(CABS(VG(J)).GT.1.0E-6)IANT=1
IF(CABS(ZLD(J)).GT.1.0E-6)WRITE(6,624)ZLD(J),J
JJ=J+NM
IF(CABS(VG(JJ)).GT.1.0E-6)WRITE(6,625)VG(JJ),J
IF(CABS(VG(JJ)).GT.1.0E-6)IANT=1
IF(CABS(ZLD(JJ)).GT.1.0E-6)WRITE(6,626)ZLD(JJ),J
723 FORMAT(3X,2E13.4,' VOLTS BY PT. A OF SEGMENT ',I3)
624 FORMAT(3X,2E13.4,' OHMS BY PT. A OF SEGMENT ',I3)
625 FORMAT(3X,2E13.4,' VOLTS BY PT. B OF SEGMENT ',I3)
626 FORMAT(3X,2E13.4,' OHMS BY PT. B OF SEGMENT ',I3)
622 CONTINUE
DO627J=1,NAT
IF(NAT.EQ.0)GOTO627
IF(CABS(VGA(J)).GT.1.0E-6)WRITE(6,628)VGA(J),J
IF(CABS(VGA(J)).GT.1.0E-6)IANT=1
IF(CABS(ZLDA(J)).GT.1.0E-6)WRITE(6,629)ZLDA(J),J
628 FORMAT(3X,2E13.4,' VOLTS AT ATTACHMENT ',I2)
629 FORMAT(3X,2E13.4,' OHMS AT ATTACHMENT ',I2)
627 CONTINUE
WRITE(6,633)NWR,NPLTH,NAT
633 FORMAT(/5X,'NWR = NUMBER OF WIRE MODES = ',I4/5X,
2 'NPLTH = NUMBER OF PLATE MODES = ',I4/5X,
3 'NAT = NUMBER OF ATTACHMENT MODES = ',I4//)
ICP=0

```

```

ESP07120
ESP07130
ESP07140
ESP07150
ESP07160
ESP07170
ESP07180
ESP07190
ESP07200
ESP07210
ESP07220
ESP07230
ESP07240
ESP07250
ESP07260
ESP07270
ESP07280
ESP07290
ESP07300
ESP07310
ESP07320
ESP07330
ESP07340
ESP07350
ESP07360
ESP07370
ESP07380
ESP07390
ESP07400
ESP07410
ESP07420
ESP07430
ESP07440
ESP07450
ESP07460
ESP07470
ESP07480
ESP07490
ESP07500
ESP07510
ESP07520
ESP07530
ESP07540
ESP07550
ESP07560
ESP07570
ESP07580
ESP07590
ESP07600
ESP07610
ESP07620
ESP07630
ESP07640
ESP07650
ESP07660
ESP07670
ESP07680
ESP07690
ESP07700
ESP07710

```

	IF(NFS1.GT.0.AND.NFS2.CT.0)ICP=1	ESP07720
	IF(ICP.EQ.0)GO TO 1226	ESP07730
	WRITE(6,141)	ESP07740
141	FORMAT(/3X,'DEFINITION OF PORTS FOR MUTUAL COUPLING DATA'/)	ESP07750
	DO127NF=1,2	ESP07760
	NFM=0	ESP07770
	SN=1.0	ESP07780
	NFS=NFS1	ESP07790
	IF(NF.EQ.2)NFS=NFS2	ESP07800
	DO128I=1,NWR	ESP07810
	IF(NFS.GT.NM)GOTO129	ESP07820
	IF(I2(I).NE.IA(NFS))GOTO128	ESP07830
	NFM=I	ESP07840
	IF(JA(I).EQ.NFS)SN=-1.0	ESP07850
	WRITE(6,142)NF,NFS	ESP07860
142	FORMAT(3X,'PORT ',I2,' IS BY PT. A OF SEGMENT',I4)	ESP07870
	GOTO128	ESP07880
129	IF(I2(I).NE.IB(NFS-NM))GOTO128	ESP07890
	NFM=I	ESP07900
	IF(JB(I).EQ.NFS-NM)SN=-1.0	ESP07910
	NFSNM=NFS-NM	ESP07920
	WRITE(6,143)NF,NFSNM	ESP07930
143	FORMAT(3X,'PORT ',I2,' IS BY PT. B OF SEGMENT',I4)	ESP07940
128	CONTINUE	ESP07950
	IF(NFM.GT.0.OR.NAT.EQ.0)GOTO131	ESP07960
	DO132I=1,NAT	ESP07970
	IF(NFS.NE.NSA(I))GOTO132	ESP07980
	NFM=NWR+NPLTM+I	ESP07990
	WRITE(6,144)NF,I	ESP08000
144	FORMAT(3X,'PORT ',I2,' IS BY ATTACHMENT',I3)	ESP08010
132	CONTINUE	ESP08020
131	CONTINUE	ESP08030
	IF(NF.EQ.1)NFM1=NFM	ESP08040
	IF(NF.EQ.2)NFM2=NFM	ESP08050
	IF(NF.EQ.1)SN1=SN	ESP08060
	IF(NF.EQ.2)SN2=SN	ESP08070
127	CONTINUE	ESP08080
1226	CONTINUE	ESP08090
C		ESP08100
C	WRITE OUT PARAMETERS OF FREQUENCY SWEEP	ESP08110
C		ESP08120
	IF(INDZI.NE.0)THEN	ESP08130
	WRITE(6,3030)INDZI,FMC1,FMC2,DFZI,DFI	ESP08140
3030	FORMAT(/6X,'PARAMETERS OF FREQUENCY SWEEP COMPUTATION'/	ESP08150
2	3X,'INTERPOLATION METHOD: INDZI = ',I3/	ESP08160
2	3X,'BEGINNING FREQUENCY (MHZ) = ',F9.3/	ESP08170
3	3X,'ENDING FREQUENCY (MHZ) = ',F9.3/	ESP08180
4	3X,'FREQUENCY INTERVAL FOR COMPUTATION OF Z (MHZ) = ',F9.3/	ESP08190
5	3X,'FREQUENCY INTERVAL FOR MM FIELD COMPUTATIONS (MHZ) = ',F9.3)	ESP08200
	IF(IABS(IRS12).EQ.1)WRITE(6,3080)THRD,PHRD	ESP08210
3080	FORMAT(3X,'RADIATION ANGLE: THETA =',F6.1,' PHI =',F6.1,' DEG')	ESP08220
	IF(IABS(IRS12).EQ.2)WRITE(6,3090)THINC,PHINC	ESP08230
3090	FORMAT(3X,'INCIDENT ANGLE: THETA =',F6.1,' PHI =',F6.1,' DEG')	ESP08240
	IF(IABS(IRS12).EQ.2)WRITE(6,3100)THRD,PHRD	ESP08250
3100	FORMAT(3X,'SCATTERING ANGLE: THETA =',F6.1,' PHI =',F6.1,	ESP08260
	&' DEG')	ESP08270
	ENDIF	ESP08280
	IF(NGO.EQ.0)GOTO600	ESP08290
	NF2=0	ESP08300
3010	IF(INDZI.NE.0)THEN	ESP08310

	NFZ=NFZ+1	ESP08320
	FMC=FMC1*(NFZ-1)*DFZI	ESP08330
	WV=300.0/FMC	ESP08340
	XK=2.0*PI/WV	ESP08350
	FHZ=FMC+1.0E6	ESP08360
	GAM=CMPLX(0.0,XK)	ESP08370
	Q=0.001*WV	ESP08380
	ENDIF	ESP08390
C		ESP08400
C	COMPUTE IMPEDANCE MATRIX	ESP08410
C		ESP08420
C	READ IN IMPEDANCE MATRIX IF IRDZM NOT ZERO	ESP08430
	IF(IRDZM.LT.1)GOTO631	ESP08440
	IF(IFIL.EQ.0)READ(12)(ZT(I),I=1,NZT)	ESP08450
	IF(IFIL.EQ.1)THEN	ESP08460
	DO 777 J=1,NTOT	ESP08470
	DO 777 I=1,NTOT	ESP08480
777	READ(12)ZTF(I,J)	ESP08490
	END IF	ESP08500
631	CONTINUE	ESP08510
	IF(IRDZM.EQ.3)GOTO276	ESP08520
C		ESP08530
C	IF A FREQUENCY SWEEP IS BEING MADE SCALE THE IMAGINARY PART OF	ESP08540
C	THE PLATE SHEET ADMITTANCE BY THE FREQUENCY	ESP08550
C		ESP08560
	DO636NPL=1,NPLTS	ESP08570
	ZSHTF(NPL)=ZSHT(NPL)	ESP08580
	IF(INDZI.EQ.0)GOTO636	ESP08590
	IF(ABS(AIMAG(ZSHT(NPL)))>.LE.1.0E-34)GOTO636	ESP08600
	YSHT=1.0/ZSHT(NPL)	ESP08610
	FRATIO=FMC/FMC1	ESP08620
	YSHTF=CMPLX(REAL(YSHT),FRATIO*AIMAG(YSHT))	ESP08630
	ZSHTF(NPL)=1.0/YSHTF	ESP08640
636	CONTINUE	ESP08650
C	SUBROUTINE ZTOTZ: COMPUTES IMPEDANCE MATRIX ZT, OR ZTF, AND IS	ESP08660
C	LOCATED IN ESP4SUBS FORTRAN	ESP08670
	CALL ZTOTZ(IA,IB,INM,ISC,I1,I2,I3,JA,JB,MD,NVR,ND,	ESP08680
	2NM,NP,CGD,SGD,D,X,Y,Z,ZLD,NPLTS,NAT,ZS,IRDZM,ZLDA,	ESP08690
	3PA,PB,NSA,NPLA,PCN,IPL,IPLM,BDSK,ZT,ZTF,NM12N,NM23N,ICN,	ESP08700
	4NDNPLT,NOVT,INT,INTP,INTD,CMM,ERVSR,RMIN,DR,IAT,IPN,	ESP08710
	5IQUAD,NCNRS,IFIL,IREF,ICC,IERSVR,PDIST,MPLA,MPLB,PSZ,ZSHTF,SEGMX)	ESP08720
276	CONTINUE	ESP08730
C		ESP08740
C	IF INDZI = 3, FORM AND STORE EFFECTIVE INVERSE OF Z	ESP08750
C		ESP08760
C	IF(INDZI.EQ.3)THEN	ESP08770
C	CJ(1)=(1.0,0.0)	ESP08780
C	IF(IFIL.EQ.0) CALL SQROT(ZT,CJ,0,1,NTOT)	ESP08790
C	CJ(1)=(1.0,0.0)	ESP08800
C	IF(IFIL.EQ.1) CALL CROUT(ZTF,CJ,1DZTF,1,0,1,NTOT)	ESP08810
C	ENDIF	ESP08820
	IF(INDZI.NE.0)THEN	ESP08830
	IF(I2468.EQ.0)IZC(NFZ)=NFZ	ESP08840
	IF(I2468.EQ.2468)THEN	ESP08850
	DO3250III=1,3	ESP08860
	IF(IZC(III).EQ.1)THEN	ESP08870
	IZMT=III	ESP08880
	IZC(III)=3	ESP08890
	ELSE	ESP08900
	IZC(III)=IZC(III)-1	ESP08910

	ENDIF	ESP08920
3250	CONTINUE	ESP08930
	ENDIF	ESP08940
C		ESP08950
C	I2C(I) = INTERPOLATING POINT NUMBER OF I ENTRY IN ZT OR ZTF ARRAY	ESP08960
C		ESP08970
	DO3020J=1,NTOT	ESP08980
	IF(IFIL.EQ.0)JJ=J	ESP08990
	IF(IFIL.EQ.1)JJ=1	ESP09000
	DO3020I=JJ,NTOT	ESP09010
	IF(IFIL.EQ.0)THEN	ESP09020
	IJN=IJ(I,J,NTOT)	ESP09030
	IF(I2468.EQ.0)ZTIN(NFZ,IJN)=ZT(IJN)	ESP09040
	IF(I2468.EQ.2468)ZTIN(I2NXT,IJN)=ZT(IJN)	ESP09050
	END IF	ESP09060
	IF(IFIL.EQ.1.AND.I2468.EQ.0)ZTFIN(NFZ,I,J)=ZTF(I,J)	ESP09070
	IF(IFIL.EQ.1.AND.I2468.EQ.2468)ZTFIN(I2NXT,I,J)=ZTF(I,J)	ESP09080
3020	CONTINUE	ESP09090
	ENDIF	ESP09100
C	WRITE OUT IMPEDANCE MATRIX.	ESP09110
	IF(IWRZM.LE.0)GOTO632	ESP09120
C	OPEN(UNIT=1,NAME='ZMAT.DAT',TY.2='UNKNOWN',FORM= 'UNFORMATTED')	ESP09130
	IF(IFIL.EQ.0)WRITE(12)(ZT(I),I=1,NZT)	ESP09140
	IF(IFIL.EQ.1)THEN	ESP09150
	DO 778 J=1,NTOT	ESP09160
	DO 778 I=1,NTOT	ESP09170
778	WRITE(12)ZTF(I,J)	ESP09180
	END IF	ESP09190
C	CLOSE(UNIT=1)	ESP09200
632	CONTINUE	ESP09210
	IF(IWRZT.GT.0.AND.IFIL.EQ.0)WRITE(6,634)FMC	ESP09220
634	FORMAT(/3X,'LOWER TRIANGULAR PART OF SYMMETRIC IMPEDANCE',	ESP09230
2	' MATRIX AT ',F9.3,' (MHZ)'/5X,'I',6X,'J',12X,'Z(I,J)'/)	ESP09240
	IF(IWRZT.GT.0.AND.IFIL.EQ.1)WRITE(6,635)FMC	ESP09250
635	FORMAT(/5X,'IMPEDANCE MATRIX AT ',F9.3,' (MHZ)'/	ESP09260
2	5X,'I',6X,'J',12X,'Z(I,J)'/)	ESP09270
	DO1234J=1,NTOT	ESP09280
	IF(IFIL.EQ.0)JJ=J	ESP09290
	IF(IFIL.EQ.1)JJ=1	ESP09300
	DO1234I=JJ,NTOT	ESP09310
	IF(IFIL.EQ.0)THEN	ESP09320
	IJN=IJ(I,J,NTOT)	ESP09330
	IF(IWRZT.GT.0)WRITE(6,1233)I,J,ZT(IJN)	ESP09340
	END IF	ESP09350
	IF(IFIL.EQ.1.AND.IWRZT.GT.0.AND.J.EQ.J)WRITE(6,1233)I,J,ZTF(I,J)	ESP09360
1233	FORMAT(2I6,2E15.5)	ESP09370
1234	CONTINUE	ESP09380
	IF(I2468.EQ.2468)GOTO3260	ESP09390
	IF(INDZI.NE.0.AND.NFZ.LT.3)GOTO3010	ESP09400
	NFFS=0	ESP09410
	NFFS=NFFS+1	ESP09420
3260	CONTINUE	ESP09430
3050	IF(INDZI.NE.0)THEN	ESP09440
	IF(NFFS.EQ.1)THEN	ESP09450
	IF(IRS12.EQ.1.AND.RF.LT.0.0)THEN	ESP09460
	WRITE(6,3110)	ESP09470
3110	FORMAT(/3X,'FREQUENCY SWEEP OF ANTENNA IMPEDANCE, '	ESP09480
2	'EFFICIENCY, AND FAR-ZONE GAIN'/	ESP09490
2	2X,'F(MHZ)',12X,'ZIN(OMHS)',8X,'% EFF',3X,'GTHETA',2X,	ESP09500
3	' GPHI ',2X,'GTHETA',2X,' GPHI ')	ESP09510

	WRITE(6,3112)	ESP09520
3112	FORMAT(46X,'***MAG. (DB)*** **PHASE (DEG)**')	ESP09530
	ENDIF	ESP09540
	IF(IRS12.EQ.1.AND.RF.GE.0.0)THEN	ESP09550
	WRITE(6,3113)RF	ESP09560
3113	FORMAT(/3X,'FREQUENCY SWEEP OF ANTENNA IMPEDANCE, '	ESP09570
2	'EFFICIENCY, AND NEAR-ZONE GAIN'/	ESP09580
3	3X,'PATTERN RADIUS, RF = ',F11.5,' METERS'/	ESP09590
2	2X,'F(MHZ)',12X,'ZIN(OHMS)',8X,'% EFF',3X,'GTHETA',2X,	ESP09600
3	' GPHI ',2X,' GRAD ',2X,'GTHETA',2X,' GPHI ',2X,' GRAD '	ESP09610
	WRITE(6,3114)	ESP09620
3114	FORMAT(46X,'***MAG. (DB)***** **PHASE (DEG)*****')	ESP09630
	ENDIF	ESP09640
	ENDIF	ESP09650
C		ESP09660
C	QUADRATIC INTERPOLATE ZTIN OR ZTFIN IMPEDANCE MATRIX ARRAYS	ESP09670
C	TO FIND THE IMPEDANCE MATRIX AT THIS FMC	ESP09680
C		ESP09690
	II2=1	ESP09700
C	IF(INDZI.EQ.3)II2=2	ESP09710
	DFFT=(H.F'S-1)*DFF	ESP09720
	FMC=FMC1+DFFT	ESP09730
C	TYPE=,NFFS,FMC	ESP09740
C	RE-COMPUTE FREQ. DEPENDENT QUANTITIES	ESP09750
	WV=300.0/FMC	ESP09760
	IK=2.0*PI/WV	ESP09770
	FHZ=FMC*1.0E6	ESP09780
	GAM=CMPLX(0.0,IK)	ESP09790
	Q=0.001*WV	ESP09800
	DO 3180 J=1,NM	ESP09810
	IF(N' EQ.0)GOTO3180	ESP09820
	K=1A(J)	ESP09830
	L=1B(J)	ESP09840
	D(J)=SQRT((X(K)-X(L))**2+(Y(K)-Y(L))**2+(Z(K)-Z(L))**2)	ESP09850
	EGD=CEXP(GAM*D(J))	ESP09860
	SGD(J)=(EGD-1.0/EGD)/2.0	ESP09870
	CGD(J)=(EGD+1.0/EGD)/2.0	ESP09880
3180	CONTINUE	ESP09890
C		ESP09900
	II2=1.50+DFFT/DFZI	ESP09910
	IF(II2.LT.2)II2=2	ESP09920
	IF(II2.GT.NFZI-1)II2=NFZI-1	ESP09930
	IF(II2.NE.II2LST)THEN	ESP09940
	I2468=2468	ESP09950
	II2LST=II2	ESP09960
	GUT03010	ESP09970
	ENDIF	ESP09980
	II1=II2-1	ESP09990
	II3=II2+1	ESP10000
	DO3270III=1,3	ESP10010
	IF(IZC(III).EQ.1)JJ1=III	ESP10020
	IF(IZC(III).EQ.2)JJ2=III	ESP10030
	IF(IZC(III).EQ.3)JJ3=III	ESP10040
3270	CONTINUE	ESP10050
	FM1=FMC1+(II1-1)*DFZI	ESP10060
	FM2=FMC1+(II2-1)*DFZI	ESP10070
	FM3=FMC1+(II3-1)*DFZI	ESP10080
	CL1=ALOG(FM1)	ESP10090
	CL2213=-ALOG(FM2**2/(FM1*FM3))	ESP10100
	CL21=ALOG(FM2/FM1)	ESP10110

	WV1=300.0/FM1	ESP10120
	XK1=2.0*PI/WV1	ESP10130
	WV2=300.0/FM2	ESP10140
	XK2=2.0*PI/WV2	ESP10150
	WV3=300.0/FM3	ESP10160
	XK3=2.0*PI/WV3	ESP10170
	DFZI2=DFZI**2	ESP10180
	EL1=0.6*(FMC-FM2)*(FMC-FM3)/DFZI2	ESP10190
	EL2=-(FMC-FM1)*(FMC-FM3)/DFZI2	ESP10200
	EL3=0.6*(FMC-FM1)*(FMC-FM2)/DFZI2	ESP10210
	IF(IWRZT.GT.0.AND.IFIL.EQ.0)WRITE(6,634)FMC	ESP10220
	IF(IWRZT.GT.0.AND.IFIL.EQ.1)WRITE(6,635)FMC	ESP10230
	WVMIN=300.0/FMC2	ESP10240
	RIJ=0.0	ESP10250
	D03060J=1,NTOT	ESP10260
	IF(INDZI.EQ.2)THEN	ESP10270
C	FIND CENTER COOR. OF MODE J	ESP10280
	IF(J.LE.NWR)THEN	ESP10290
	I2J=I2(J)	ESP10300
	XCJ=X(I2J)	ESP10310
	YCJ=Y(I2J)	ESP10320
	ZCJ=Z(I2J)	ESP10330
	ENDIF	ESP10340
	IF(J.GT.NWR.AND.J.LE.NWR+NPLTM)THEN	ESP10350
	JJJ=J-NWR	ESP10360
	XCJ=0.6*(PA(JJJ,1,1)+PA(JJJ,4,1))	ESP10370
	YCJ=0.6*(PA(JJJ,1,2)+PA(JJJ,4,2))	ESP10380
	ZCJ=0.6*(PA(JJJ,1,3)+PA(JJJ,4,3))	ESP10390
	ENDIF	ESP10400
	IF(J.GT.NWR+NPLTM)THEN	ESP10410
	JJJ=J-NPLTM-NWR	ESP10420
	JSG=NSA(JJJ)	ESP10430
	IF(JSG.LE.NM)I2J=IA(JSG)	ESP10440
	IF(JSG.GT.NM)I2J=JB(JSG-NM)	ESP10450
	XCJ=X(I2J)	ESP10460
	YCJ=Y(I2J)	ESP10470
	ZCJ=Z(I2J)	ESP10480
	ENDIF	ESP10490
	ENDIF	ESP10500
	IF(IFIL.EQ.0)JJ=J	ESP10510
	IF(IFIL.EQ.1)JJ=1	ESP10520
	D03060I=JJ,NTOT	ESP10530
C		ESP10540
C	IF INDZI = 2, FACTOR OUT THE EXP(-J*K*R) DEPENDENCE OF THE	ESP10550
C	ELEMENTS IN THE IMPEDANCE MATRIX BEFORE INTERPOLATING	ESP10560
C		ESP10570
	CEXP1=(1.0,0.0)	ESP10580
	CEXP2=(1.0,0.0)	ESP10590
	CEXP3=(1.0,0.0)	ESP10600
	CEXP4=(1.0,0.0)	ESP10610
	IF(INDZI.EQ.2)THEN	ESP10620
C	FIND CENTER COOR. OF MODE I	ESP10630
	IF(I.LE.NWR)THEN	ESP10640
	I2J=I2(I)	ESP10650
	XCI=X(I2J)	ESP10660
	YCI=Y(I2J)	ESP10670
	ZCI=Z(I2J)	ESP10680
	ENDIF	ESP10690
	IF(I.GT.NWR.AND.I.LE.NWR+NPLTM)THEN	ESP10700
	JJJ=I-NWR	ESP10710

XCI=0.5*(PA(JJJ,1,1)+PA(JJJ,4,1))	ESP10720
YCI=0.5*(PA(JJJ,1,2)+PA(JJJ,4,2))	ESP10730
ZCI=0.5*(PA(JJJ,1,3)+PA(JJJ,4,3))	ESP10740
ENDIF	ESP10750
IF(I.GT.NWR-NPLTM)THEN	ESP10760
JJJ=I-NPLTM-NWR	ESP10770
JSG=NSA(JJJ)	ESP10780
IF(JSG.LE.NM)I2J=IA(JSG)	ESP10790
IF(JSG.GT.NM)I2J=IB(JSG-NM)	ESP10800
XCI=X(I2J)	ESP10810
YCI=Y(I2J)	ESP10820
ZCI=Z(I2J)	ESP10830
ENDIF	ESP10840
RIJ=SQRT((XCJ-XCI)**2+(YCI-YCJ)**2+(ZCI-ZCJ)**2)	ESP10850
IF(RIJ/WVMIN.GT.0.501)THEN	ESP10860
CEXP1=CEXP(-XJ*(XK1-XK2)*RIJ)	ESP10870
CEXP2=CEXP(-XJ*(XK2-XK2)*RIJ)	ESP10880
CEXP3=CEXP(-XJ*(XK3-XK2)*RIJ)	ESP10890
CEXP4=CEXP(-XJ*(XK-XK2)*RIJ)	ESP10900
ENDIF	ESP10910
ENDIF	ESP10920
IF(IFIL.EQ.0)THEN	ESP10930
IJN=IJ(I,J,NTOT)	ESP10940
FAC1=CEXP1	ESP10950
FAC2=CEXP2	ESP10960
FAC3=CEXP3	ESP10970
FACK=CEXP4	ESP10980
ZT(IJN)=EL1*ZTIN(JJ1,IJN)/FAC1+EL2*ZTIN(JJ2,IJN)/FAC2+	ESP10990
2 EL3*ZTIN(JJ3,IJN)/FAC3	ESP11000
ZT(IJN)=ZT(IJN)*FACK	ESP11010
IF(INDZI.EQ.2.AND.RIJ/WVMIN.LE.0.501.AND.I.LE.NWR.AND.J.LE.NWR)	ESP11020
2 THEN	ESP11030
XXX1=AIMAG(ZTIN(JJ1,IJN))	ESP11040
XXX2=AIMAG(ZTIN(JJ2,IJN))	ESP11050
XXX3=AIMAG(ZTIN(JJ3,IJN))	ESP11060
BBB=(XXX2-XXX1-XXX3)/CL2213	ESP11070
CCC=(XXX2-XXX1-BBB*CL21)/DFZI	ESP11080
AAA=XXX1-BBB*CL1-CCC*FM1	ESP11090
XXX=AAA+BBB*ALOG(FMC)+CCC*FMC	ESP11100
ZT(IJN)=CMPLX(REAL(ZT(IJN)),XXX)	ESP11110
ENDIF	ESP11120
IF(IWRZT.GT.0)WRITE(6,1233)I,J,ZT(IJN)	ESP11130
END IF	ESP11140
IF(IFIL.EQ.1)THEN	ESP11150
FAC1=CEXP1	ESP11160
FAC2=CEXP2	ESP11170
FAC3=CEXP3	ESP11180
FACK=CEXP4	ESP11190
ZTF(I,J)=EL1*ZTFIN(JJ1,I,J)/FAC1+EL2*ZTFIN(JJ2,I,J)/FAC2+	ESP11200
2 EL3*ZTFIN(JJ3,I,J)/FAC3	ESP11210
ZTF(I,J)=ZTF(I,J)*FACK	ESP11220
IF(INDZI.EQ.2.AND.RIJ/WVMIN.LE.0.501)THEN	ESP11230
IF(IWRZT.GT.0)WRITE(6,1233)I,J,ZTF(I,J)	ESP11240
XXX1=AIMAG(ZTFIN(JJ1,I,J))	ESP11250
XXX2=AIMAG(ZTFIN(JJ2,I,J))	ESP11260
XXX3=AIMAG(ZTFIN(JJ3,I,J))	ESP11270
BBB=(XXX2-XXX1-XXX3)/CL2213	ESP11280
CCC=(XXX2-XXX1-BBB*CL21)/DFZI	ESP11290
AAA=XXX1-BBB*CL1-CCC*FM1	ESP11300
XXX=AAA+BBB*ALOG(FMC)+CCC*FMC	ESP11310


```
ZTF(I,J)=CMPLX(REAL(ZTF(I,J)),XIX)
ENDIF
IF(IWRZT.GT.0)WRITE(6,1233)I,J,ZTF(I,J)
ENDIF
3060 CONTINUE
ENDIF
```

```
ESP11320
ESP11330
ESP11340
ESP11350
ESP11360
ESP11370
```

C		ESP11380
C	COMPUTE COUPLING BETWEEN TWO WIRE PORTS	ESP11390
C		ESP11400
	IF(ICP.EQ.1) CALL COUPLE(ZT,ZTF,NFM1,NFM2,SN1,SN2,I12,V,	ESP11410
	2 NTOT,IFIL,ICC)	ESP11420
	IF(ISCAT.GE.1) GOTO 501	ESP11430
C	COMPUTE CONSTANT VECTOR & SOLVE SYSTEM	ESP11440
	IF(IWR.GT.0)WRITE(6,576)	ESP11450
576	FORMAT(/5X,'ANTENNA MODAL CURRENTS'/3X,'MODE',3X,	ESP11460
	2 'REL MAG',6X,'ABS MAG',5X,'PHASE',10X,'*** COMPLEX ***'/)	ESP11470
	IF(IANT.EQ.0)GOTO600	ESP11480
		ESP11490
C	FOR ANTENNA PROBLEMS, SET UP RHS VECTOR AND SOLVE FOR CURRENTS	ESP11500
C		ESP11510
	CALL ANTV(I1,I2,I3,IA,IB,IWR,JA,JB,NM,ZT,IFIL,	ESP11520
	& ICC,ZTF,CJP,CG,VG,Y11,Z11,VIN,NGEN,NWR,NPLTM,NAT,VGA,PIN,	ESP11530
	2 A,CMM,D,DISS,GAM,SGD,ZLD,ZS,ZLDA,INM,MD,ND,HSA,I12)	ESP11540
C		ESP11550
C	IF THERE IS ONLY ONE GENERATOR COMPUTE INPUT IMPEDANCE	ESP11560
C		ESP11570
	ZIN=(0.0,0.0)	ESP11580
	YIN=(0.0,0.0)	ESP11590
	IF(NGEN.EQ.1)THEN	ESP11600
	YIN=Y11/(CABS(VIN))**2	ESP11610
	ZIN=1.0/YIN	ESP11620
	ENDIF	ESP11630
	I12=2	ESP11640
	PRAD=PIN-DISS	ESP11650
	EFF=100.0*PRAD/PIN	ESP11660
C	IF(INDZI.EQ.0)WRITE(6,513) Y11,Z11,EFF	ESP11670
513	FORMAT(/3X,'INPUT ADMITTANCE(MHOS) = ',F10.6,' J ',F10.6/	ESP11680
	2 3X,'INPUT IMPEDANCE(OHMS) = ',F10.3,' J ',F10.3/,	ESP11690
	3 3X,'EFFICIENCY (PERCENT) = ',F7.3/)	ESP11700
	IF(INDZI.EQ.0.AND.NGEN.EQ.1)WRITE(6,513) YIN,ZIN,EFF	ESP11710
	IF(INDZI.EQ.0.AND.NGEN.NE.1)WRITE(6,514)NGEN,EFF	ESP11720
514	FORMAT(/3X,'INPUT IMPEDANCE AND ADMITTANCE ONLY COMPUTED IF',	ESP11730
	2 ' WIRE HAS ONE GENERATOR'/3X,'NUMBER OF GENERATORS = ',I4/	ESP11740
	3 3X,'EFFICIENCY (PERCENT) = ',F7.3/)	ESP11750
	501 CONTINUE	ESP11760
	IF(IFF.NE.1) GOTO 599	ESP11770
572	FORMAT(/3X,'ANTENNA PROBLEM, ISCAT = ',I6)	ESP11780
573	FORMAT(/3X,'BACKSCATTERING, ISCAT = ',I6)	ESP11790
574	FORMAT(/3X,'BISTATIC SCATTERING, ISCAT = ',I6)	ESP11800
577	FORMAT(/3X,'FORWARD SCATTERING, ISCAT = ',I6)	ESP11810
	IF(INDZI.EQ.0)THEN	ESP11820
	IF(ISCAT.EQ.0)WRITE(6,572)ISCAT	ESP11830
	IF(ISCAT.EQ.1)WRITE(6,573)ISCAT	ESP11840
	IF(ISCAT.EQ.2)WRITE(6,574)ISCAT	ESP11850
	IF(ISCAT.EQ.3)WRITE(6,577)ISCAT	ESP11860
	ENDIF	ESP11870
	IF(ISCAT.NE.0)GO TO 601	ESP11880
		ESP11890
C		ESP11900
C	GET INPUT FOR PATTERNS	ESP11910
C	ANTENNA PROBLEM ISCAT=0	ESP11920
C		ESP11930
	960 DTH=PI/180.	ESP11940
	IF (IFE .NE. 1) GOTO 901	ESP11950
C		ESP11960
C	PERFORM ELEVATION PLANE RADIATION PLANE PATTERN	ESP11970
C		ESP11970

	PHI=PHFE*DTH	ESP11980
CC	NPTS=360/FNDFE+1.5	ESP11990
CC	XNDFE=360/(NPTS-1)	ESP12000
	NPTS=ELRANG/FNDFE+1.5	
CC=	SET XNDFE=0. INITIALLY AND CHECK NPTS.GT.1 (AJF)	
	XNDFE=0.	
	IF(NPTS.GT.1)XNDFE=ELRANG/(NPTS-1)	
	IEA=1	ESP12010
	IF(NPLOTS.GT.0.AND.INDZI.EQ.0)WRITE(8,338)IEA,NPTS,PHFE	ESP12020
338	FORMAT(1X,2(I3,1X),2X,F7.2)	ESP12030
	IF(INDZI.NE.0)THEN	ESP12040
	PHI=PHRD*DTH	ESP12050
	NPTS=1	ESP12060
	ENDIF	ESP12070
	DO 903 I=1,NPTS	ESP12080
CC=	ADDED ELMIN TO THETA IN NEXT LINE TO START AT ARB. OBS. PT.	
	THETA=ELMIN*DTH+(I-1)*DTH*XNDFE	ESP12090
	IF(THETA.GT.1.00001*PI)THEN	ESP12100
	THETA=2.0*PI-THETA	ESP12110
	IF(I9999.NE.9999)PHI=PHI+PI	ESP12120
	I9999=9999	ESP12130
	ENDIF	ESP12140
	IF(INDZI.NE.0)THETA=THRD*DTH	ESP12150
C	CALL SORTB(IA,IB,I1,I2,I3,NWR,NM,A,CGD,SGD,FHZ,D,	ESP12160
C	& O,I12,ISCAT,ZTF,ZT,IFIL,ICC,ETT,EPP,	ESP12170
C	& X,Y,Z,NPLTS,NAT,PA,PB,NSA,NFLA,PCN,BDSK,IQUAD,	ESP12180
C	& NPLTM,IPL,IPLM,CJP,CJT,ETTS,EPPS,ETPS,EPTS,THETA,PHI,JA,JB,	ESP12190
C	& SCSP,SCST,SPPM,SPTM,STPM,STTM,IMAGE,ICN,NDNPLT)	ESP12200
	CALL SORTBN(IA,IB,I1,I2,I3,NWR,NM,A,CGD,SGD,FHZ,D,	ESP12210
	& O,I12,ISCAT,ZTF,ZT,IFIL,ICC,ETT,EPP,INTP,INTD,	ESP12220
	& X,Y,Z,NPLTS,NAT,PA,PB,NSA,NPLA,PCN,BDSK,IQUAD,	ESP12230
	& NPLTM,IPL,IPLM,CJP,CJT,ETTS,EPPS,ETPS,EPTS,THETA,PHI,JA,JB,	ESP12240
	& SCSP,SCST,SPPM,SPTM,STPM,STTM,IMAGE,ICN,NDNPLT,	ESP12250
	& RF,EXN,EYN,EXN,EXT,EYT,EZT,EXP,EYP,EZP,ERRS,ETRS,EPRS,STRM,SPRM)	ESP12260
	PET(I)=PHS(ETTS)	ESP12270
	PEP(I)=PHS(EPPS)	ESP12280
	ETE(I)=CABS(ETTS)**2/((1.0,0.0)*30.0*PIN)	ESP12290
	EPE(I)=CABS(EPPS)**2/((1.0,0.0)*30.0*PIN)	ESP12300
	AET=AMP(ETE(I))	ESP12310
	AEP=AMP(EPE(I))	ESP12320
	AER=0.0	ESP12330
	PER(I)=0.0	ESP12340
	IF(RF.GT.0.0)THEN	ESP12350
	PER(I)=PHS(ERRS)	ESP12360
	ERE(I)=CABS(ERRS)**2/((1.0,0.0)*30.0*PIN)	ESP12370
	AER=AMP(ERE(I))	ESP12380
	ENDIF	ESP12390
	IF(NPLOTS.GT.0.AND.INDZI.EQ.0)WRITE(8,333)DB(AET),PET(I),	ESP12400
2	DB(AEP),PEP(I),DB(AER),PER(I)	ESP12410
	II=I	ESP12420
903	CONTINUE	ESP12430
	IF(INDZI.NE.0.AND.RF.LT.0.0)THEN	ESP12440
	WRITE(6,3120)FMC,ZIN,EFF,DB(AET),DB(AEP),PET(II),PEP(II)	ESP12450
	WRITE(10,3125)FMC,ZIN,EFF,DB(AET),DB(AEP),PET(II),PEP(II)	ESP12460
3120	FORMAT(1X,F9.3,2X,E10.4,' J ',E10.4,2X,F6.1,2(2X,F6.2),	ESP12470
2	2(2X,F6.1))	ESP12480
3125	FORMAT(1X,F9.3,2X,E10.4,2X,E10.4,2X,F6.1,2(2X,F6.2),	ESP12490
2	2(2X,F6.1))	ESP12500
	GOTO3070	ESP12510
	ENDIF	ESP12520

```

      IF(INDZI.NE.0.AND.RF.GE.0.0)THEN
      WRITE(6,3121)FMC,ZIN,EFF,DB(AET),DB(AEP),DB(AER),
2    PET(II),PEP(II),PER(II)
      WRITE(10,3126)FMC,ZIN,EFF,DB(AET),DB(AEP),DB(AER),
2    PET(II),PEP(II),PER(II)
3121  FORMAT(1X,F9.3,2X,E10.4,' J ',E10.4,2X,F6.1,3(2X,F6.2),
2    3(2X,F6.1))
3126  FORMAT(1X,F9.3,2X,E10.4,2X,E10.4,2X,F6.1,3(2X,F6.2),
2    3(2X,F6.1))
      GOTO3070
      ENDIF
      IF(RF.LE.0.0)THEN
      WRITE(6,904) PHFE
904   FORMAT(///,' FAR-ZONE GAIN ELEVATION PLANE PATTERN. PHI =',F6.1,
2     ' DEG. '//)
      WRITE(6,902)
902   FORMAT(' (DEG) **MAG (DB)** *PHASE (DEG)*'//
2     ' THETA GTHETA GPHI GTHETA GPHI'//)
      ELSE
      WRITE(6,804) RF,PHFE
804   FORMAT(///,' NEAR-ZONE GAIN ELEVATION PLANE PATTERN.'//3X,
2     ' R = ',F11.6,1X,' METERS PHI =',F6.1,' DEG. '//)
      WRITE(6,805)
805   FORMAT(' (DEG) *****MAG (DB)***** *PHASE (DEG)*****'//
2     ' THETA GTHETA GPHI GR GTHETA GPHI GR'//)
      ENDIF
      DO 906 I=1,NPTS
CC***ADDED ELMIN IN NEXT LINE TO START AT ARB. OBS. PT.
      XII=ELMIN+(I-1)*XNDFE
      AET=AMP(ETE(I))
      AEP=AMP(EPE(I))
      AET=DB(AET)
      AEP=DB(AEP)
      IF(RF.GT.0.0)THEN
      AER=AMP(ERE(I))
      AER=DB(AER)
      WRITE(6,807)XII,AET,AEP,AER,PET(I),PEP(I),PER(I)
807   FORMAT(1X,F5.1,3(2X,F6.2),3(2X,F6.1))
      ELSE
      WRITE(6,907) XII,AET,AEP,PET(I),PEP(I)
907   FORMAT(1X,F5.1,2X,F6.2,2X,F6.2,2X,F6.1,2X,F6.1)
      ENDIF
      ETE(I)=CSQRT(1.0E-20+ETE(I))
      EPE(I)=CSQRT(1.0E-20+EPE(I))
      IF(RF.GT.0.0)ERE(I)=CSQRT(1.0E-20+ERE(I))
906   CONTINUE
901   CONTINUE
      IF(IPA.NE.1) GOTO 599
C
C   PERFORM AZIMUTH PLANE RADIATION PATTERN
C
      THETA=THFA+DTH
C**NOTE: IN NEXT TWO LINES CHANGED 360 TO AZRANG
      NPTS=AZRANG/FNDFA+1.5
CC***SET INDFA=0. AND CHECK NPTS.GT.1
      INDFA=0.
      IF(NPTS.GT.1)INDFA=AZRANG/(NPTS-1)
      IEA=2
      IF(NPLOTS.GT.0.AND.INDZI.EQ.0)WRITE(6,336)IEA,NPTS,THFA
      DO 911 I=1,NPTS

```

```

ESP12530
ESP12540
ESP12550
ESP12560
ESP12570
ESP12580
ESP12590
ESP12600
ESP12610
ESP12620
ESP12630
ESP12640
ESP12650
ESP12660
ESP12670
ESP12680
ESP12690
ESP12700
ESP12710
ESP12720
ESP12730
ESP12740
ESP12750
ESP12760
ESP12770
ESP12780
ESP12790
ESP12800
ESP12810
ESP12820
ESP12830
ESP12840
ESP12850
ESP12860
ESP12870
ESP12880
ESP12890
ESP12900
ESP12910
ESP12920
ESP12930
ESP12940
ESP12950
ESP12960
ESP12970
ESP12980
ESP12990
ESP13000
ESP13010
ESP13020
ESP13030
ESP13040
ESP13050
ESP13060
ESP13070
ESP13080

```

```

CC***ADDED AZMIN IN NEXT LINE
      PHI=AZMIN*DTH+(I-1)*DTH*XNDFA
C*****
C      CALL SORTB(IA,IB,I1,I2,I3,NWR,NM,A,CGD,SGD,FHZ,D,
C      & 0,I12,ISCAT,ZTF,ZT,IFIL,ICC,ETT,EPP,
C      &X,Y,Z,NPLTS,NAT,PA,PB,NSA,NPLA,PCN,BDSK,IQUAD,
C      &NPLTM,IPL,IPLM,CJP,CJT,ETTS,EPPS,ETPS,EPTS,THETA,PHI,JA,JB,
C      & SCSP,SCST,SPPM,SPTM,STPM,STTH,IMAGE,ICN,NDNPLT)
      CALL SORTBN(IA,IB,I1,I2,I3,NWR,NM,A,CGD,SGD,FHZ,D,
      & 0,I12,ISCAT,ZTF,ZT,IFIL,ICC,ETT,EPP,INTP,INTD,
      &X,Y,Z,NPLTS,NAT,PA,PB,NSA,NPLA,PCN,BDSK,IQUAD,
      &NPLTM,IPL,IPLM,CJP,CJT,ETTS,EPPS,ETPS,EPTS,THETA,PHI,JA,JB,
      & SCSP,SCST,SPPM,SPTM,STPM,STTH,IMAGE,ICN,NDNPLT,
      & RF,EXN,EYN,EZN,EXT,EYT,EZT,EAP,EYP,EZP,ERRS,ETRS,EPRS,STRM,SPRM)
      PET(I)=PHS(ETTS)
      PEP(I)=PHS(EPPS)
      ETAZ(I)=CABS(ETTS)**2/((1.0,0.0)*30.0*PIN)
      EPAZ(I)=CABS(EPPS)**2/((1.0,0.0)*30.0*PIN)
      AET=AMP(ETAZ(I))
      AEP=AMP(EPAZ(I))
      AER=0.0
      PER(I)=0.0
      IF(RF.GT.0.0)THEN
      PER(I)=PHS(ERRS)
      ERAZ(I)=CABS(ERRS)**2/((1.0,0.0)*30.0*PIN)
      AER=AMP(ERAZ(I))
      ENDIF
      IF(NPLOTS.GT.0.AND.INDZI.EQ.0)WRITE(8,333)DB(AET),PET(I),
2      DB(AEP),PEP(I),DB(AER),PER(I)
911      CONTINUE
      IF(RF.LE.0.0)THEN
      WRITE(6,912) THFA
912      FORMAT(///2X,'FAR-ZONE GAIN AZIMUTH PLANE PATTERN. THETA =',F6.1,
2,' DEG. '//)
      WRITE(6,906)
906      FORMAT(' (DEG) **MAC (DB) ** *PHASE (DEG)* '//
2 ' PHI GTHETA GPHI GTHETA GPHI '//)
C      WRITE(6,914)
C914      FORMAT(' PHI(DEG) GTHETA(DB) GPHI(DB)')
      ELSE
      WRITE(6,808) RF,THFA
808      FORMAT(///,' NEAR-ZONE GAIN AZIMUTH PLANE PATTERN. '//3X,
2 ' R = ',F11.5,1X,' METERS THETA =',F6.1,' DEG. '//)
      WRITE(6,809)
809      FORMAT(' (DEG) *****MAC (DB)***** *****PHASE (DEG)*****'//
2 ' PHI GTHETA GPHI GR GTHETA GPHI GR')
      ENDIF
      DO 913 I=1,NPTS
      XII=AZMIN+(I-1)*XNDFA
      AET=AMP(ETAZ(I))
      AEP=AMP(EPAZ(I))
      AET=DB(AET)
      AEP=DB(AEP)
      IF(RF.GT.0.0)THEN
      AER=AMP(ERAZ(I))
      AER=DB(AER)
      WRITE(6,807)XII,AET,AEP,AER,PET(I),PEP(I),PER(I)
      ELSE
      WRITE(6,907) XII,AET,AEP,PET(I),PEP(I)
      ENDIF

```

```

ESP13090
ESP13100
ESP13110
ESP13120
ESP13130
ESP13140
ESP13150
ESP13160
ESP13170
ESP13180
ESP13190
ESP13200
ESP13210
ESP13220
ESP13230
ESP13240
ESP13250
ESP13260
ESP13270
ESP13280
ESP13290
ESP13300
ESP13310
ESP13320
ESP13330
ESP13340
ESP13350
ESP13360
ESP13370
ESP13380
ESP13390
ESP13400
ESP13410
ESP13420
ESP13430
ESP13440
ESP13450
ESP13460
ESP13470
ESP13480
ESP13490
ESP13500
ESP13510
ESP13520
ESP13530
ESP13540
ESP13550
ESP13560
ESP13570
ESP13580
ESP13590
ESP13600
ESP13610
ESP13620
ESP13630
ESP13640
ESP13650
ESP13660
ESP13670

```

	ETAZ(I)=CSQRT(1.0E-20+ETAZ(I))	ESP13680
	EPAZ(I)=CSQRT(1.0E-20+EPAZ(I))	ESP13690
	ERAZ(I)=CSQRT(1.0E-20+ERAZ(I))	ESP13700
913	CONTINUE	ESP13710
	GOTO599	ESP13720
601	CONTINUE	ESP13730
C		ESP13740
C	BACK OR BISTATIC OR FORWARD SCATTERING ISCAT = 1 OR 2 OR 3.	ESP13750
C		ESP13760
	IF(INDZI.EQ.0)THEN	ESP13770
	IF(RF.LE.0.0)WRITE(6,721)	ESP13780
721	FORMAT(3X,'FAR-ZONE PATTERN')	ESP13790
	IF(RF.GT.0.0)WRITE(6,731)RF	ESP13800
731	FORMAT(3X,'NEAR-ZONE PATTERN: R = ',F11.5)	ESP13810
	IF(IMAGE.EQ.1)WRITE(6,714)	ESP13820
714	FORMAT(3X,'IMAGE WAVE INCLUDED')	ESP13830
	IF(ISCAT.EQ.2)WRITE(6,713)THIN,PHIN	ESP13840
713	FORMAT(3X,'THETA INC.(DEG.) = ',F6.1/3X,'PHI INC.(DEG.) = ',F6.1	ESP13850
2	//)	ESP13860
	ELSE IF(NFFS.EQ.1) THEN	ESP13870
	IF(IRS12.EQ.-2)WRITE(6,714)	ESP13880
	WRITE(6,3200)	ESP13890
3200	FORMAT(//3X,'FREQUENCY SWEEP OF TARGET RCS '//	ESP13900
2	12X,'***** MAG. (DB/M**2) *****',	ESP13910
3	5X,'***** PHASE (DEG) *****'/	ESP13920
4	2X,'F(MHZ)',4X,'STTH',4X,'SPPH',4X,'STPM',4X,'SPTM',	ESP13930
5	5X,'STTH',4X,'SPPH',4X,'STPM',4X,'SPTM'/)	ESP13940
	ENDIF	ESP13950
	ISP=0	ESP13960
	DTH=PI/180.0	ESP13970
C	I12=1	ESP13980
	IEA=1	ESP13990
	IF(ISE.EQ.0)GOTO916	ESP14000
	PHDG=PHSE	ESP14010
	PANG=PHDG	ESP14020
	NANG=0.5*(ELRANG/FNDSE)	ESP14030
	ANGRAN=ELRANG	
	GOTO917	ESP14040
918	IEA=2	ESP14050
	IF(ISA.EQ.0)GOTO916	ESP14060
	THDG=THSA	ESP14070
	PANG=THDG	ESP14080
	NANG=0.5*(AZRANG/FNDSA)	ESP14090
	ANGRAN=AZRANG	
917	CONTINUE	ESP14100
	C**IN LINE BELOW SUBSTITUTED ANGRAN (DEFINED ABOVE) FOR 360.	
	CC***SET DANG=0. AND CHECK NANG.GT.0	
	DANG=0.	
	IF(NANG.GT.0)DANG=ANGRAN/NANG	ESP14110
	IA1=1	ESP14120
	ISP=ISP+1	ESP14130
	IF(ISCAT.EQ.2.AND.ISP.EQ.1)IA1=0	ESP14140
	IA2=1+NANG	ESP14150
	NPTS=IA2	ESP14160
	IF(NPLOTS.GT.0.AND.INDZI.EQ.0)WRITE(8,336)IEA,NPTS,ISCAT,	ESP14170
2	PANG,THIN,PHIN	ESP14180
336	FORMAT(1X,3(I3,1X),3(F7.2,2X))	ESP14190
	IF(INDZI.NE.0)IA2=1	ESP14200
	C**NEW LINES TO IMPLEMENT CONSTANT BISTATIC ANGLE OPTION (TARGET ROT.)	
	C**IT IS ASSUMED THAT THE REFERENCE ANGLE IS THE BISECTOR OF THE	

```

C**BISTATIC ANGLE. NOTE THAT THE SUM OF THE INCIDENT AND OUTGOING
C**ANGLES DIVIDED BY 2 GIVES THE TARGET ROTATION ANGLE.
  DANGB=0.
  IF(NPTBIS.GT.1)DANGB=BANGRC/(NPTBIS-1)
  DO 1920 IBIS=1,NPTBIS
  IF(IBISC.EQ.1)THIN=-BETA/2.+DANGB*(IBIS-1)
  IF(IBISC.EQ.1)WRITE(6,9278)IBIS,THIN
9278  FORMAT(1X,'IBIS=',I4,' THIN=',F12.3)
  DO 701 IANG=IA1,IA2
  CALL GETCP2(ICPUB)
  CPU=ICPUB-ICPU
  WRITE(6,9552)IANG,CPU
9552  FORMAT(1X,'IANG=',I4,2X,'CPU=',F11.2,2X,'SEC. ')
CC**ADDED ELMIN,AZMIN TO THDG,PHDG IN NEXT TWO LINES
  IF(IEA.EQ.1)THDG=ELMIN+(IANG-1)*DANG
  IF(IEA.EQ.2)PHDG=AZMIN+(IANG-1)*DANG
  IF(IBISC.EQ.1.AND. IEA.EQ.1)THDG=BETA/2.+DANGB*(IBIS-1)
  IF(IBISC.EQ.1.AND. IEA.EQ.2)PHDG=BETA/2.+DANGB*(IBIS-1)
  THETA=THDG*DTH
  PHI=PHDG*DTH
  IF(ISCAT.LE.2)ISCT=ISCAT
  IF(IANG.EQ.0)ISCT=1
  IF(IANG.EQ.0)THETA=THIN*DTH
  IF(IANG.EQ.0)PHI=PHIN*DTH
  IF(IWR.GT.0.AND. ISCT.EQ.1)WRITE(6,576)
C    III=1
  IF(ISCAT.EQ.3)III=2
  DO711IIS=1,III
  IF(ISCAT.LE.2)GOTO716
  IF(IIS.EQ.1)THEN
    IF(THDG.GT.180.0)THDGI=THDG-180.0
    IF(THDG.LE.180.0)THDGI=THDG+180.0
    PHDGI=PHDG
    THETA=THDGI*DTH
    PHI=PHDGI*DTH
    ENDIF
    IF(IIS.EQ.2)THEN
      THETA=THDG*DTH
      PHI=PHDG*DTH
    ENDIF
    ISCT=IIS
716  CONTINUE
    IF(INDZI.NE.0)THEN
      IF(IANG.EQ.0)THEN
        THETA=THINC*DTH
        PHI=PHINC*DTH
      ENDIF
      IF(IANG.EQ.1)THEN
        THETA=THRD*DTH
        PHI=PHRD*DTH
      ENDIF
    ENDIF
  IF(THETA.GT.1.00001*PI)THEN
C    INSURE THAT (THETA,PHI) IS IN THE PROPER RANGE
C
C    THETAP=THETA
    PHIP=PHI
    THDGO=THETAP/DTH
    PHDGO=PHIP/DTH
    IF(THETA.GT.1.00001*PI)THEN

```

ESP14210

ESP14220

ESP14230

ESP14240

ESP14250

ESP14260

ESP14270

ESP14280

ESP14290

ESP14300

ESP14310

ESP14320

ESP14330

ESP14340

ESP14350

ESP14360

ESP14370

ESP14380

ESP14390

ESP14400

ESP14410

ESP14420

ESP14430

ESP14440

ESP14450

ESP14460

ESP14470

ESP14480

ESP14490

ESP14500

ESP14510

ESP14520

ESP14530

ESP14540

ESP14550

ESP14560

ESP14570

ESP14580

ESP14590

ESP14600

ESP14610

ESP14620

ESP14630

ESP14640

ESP14650

	THETAP=2.0*PI-THETA	ESP14660
	PHIP=PHI+PI	ESP14670
	IF(PHIP.GT.2.00001*PI)PHIP=PHIP-2.0*PI	ESP14680
	THDGO=THETAP/DTH	ESP14690
	PHDGO=PHIP/DTH	ESP14700
	ENDIF	ESP14710
C	TYPE1111,THETA/DTH,PHI/DTH,THETAP/DTH,PHIP/DTH	ESP14720
1111	FORMAT(1X,4F10.3)	ESP14730
C	CALL SORTB(IA,IB,I1,I2,I3,NWR,NM,A,CGD,SGD,FHZ,D,	ESP14740
C	& IWR,I12,ISCT,ZTF,ZT,IFIL,ICC,ETT,EPP,	ESP14750
C	& X,Y,Z,NPLTS,NAT,PA,PB,NSA,NPLA,PCN,BDSK,IQUAD,	ESP14760
C	& NPLTM,IPL,IPLM,CJP,CJT,ETTS,EPPS,ETPS,EPTS,THETAP,PHIP,JA,JB,	ESP14770
C	& SCSP,SCST,SPPM,SPTM,STPM,STTM,IMAGE,ICN,NDNPLT)	ESP14780
	CALL SORTBN(IA,IB,I1,I2,I3,NWR,NM,A,CGD,SGD,FHZ,D,	ESP14790
	& IWR,I12,ISCT,ZTF,ZT,IFIL,ICC,ETT,EPP,INTP,INTD,	ESP14800
	& X,Y,Z,NPLTS,NAT,PA,PB,NSA,NPLA,PCN,BDSK,IQUAD,	ESP14810
	& NPLTM,IPL,IPLM,CJP,CJT,ETTS,EPPS,ETPS,EPTS,THETAP,PHIP,JA,JB,	ESP14820
	& SCSP,SCST,SPPM,SPTM,STPM,STTM,IMAGE,ICN,NDNPLT,	ESP14830
	& RF,EXN,EYN,EZN,EXT,EYT,EZT,EXP,EYP,EZP,ERRS,ETRS,EPRS,STRM,SPRM)	ESP14840
711	CONTINUE	ESP14850
	IF(IANG.EQ.0)GOTO701	ESP14860
710	FORMAT(1X,F10.2,2X,E20.6)	ESP14870
712	FORMAT(/,3X,'SCATTERING PARAMETERS')	ESP14880
175	FORMAT(2X,' THETA=',F10.2,' PHI=',F10.2,' SPPM=',E20.6,	ESP14890
	2' STTM=',E20.6,' IN SQUARE-WAVES')	ESP14900
176	FORMAT(2X,'SPPM=',E20.6,' DB OVER WAVELENGTH-SQUARED')	ESP14910
173	FORMAT(2X,'STTM=',E20.6,' DB OVER WAVELENGTH-SQUARED')	ESP14920
	PHTT=BTAN2(AIMAG(ETTS),REAL(ETTS))*180.0/PI	ESP14930
	PHPP=BTAN2(AIMAG(EPPS),REAL(EPPS))*180.0/PI	ESP14940
	PHTP=BTAN2(AIMAG(ETPS),REAL(ETPS))*180.0/PI	ESP14950
	PHPT=BTAN2(AIMAG(EPTS),REAL(EPTS))*180.0/PI	ESP14960
	PHTR=BTAN2(AIMAG(ETRS),REAL(ETRS))*180.0/PI	ESP14970
	PHPR=BTAN2(AIMAG(EPRS),REAL(EPRS))*180.0/PI	ESP14980
	IF(IANG.NE.0.AND.NPLOTS.GT.0.AND.INDZI.EQ.0)WRITE(8,333)	ESP14990
2	DB(STTM),PHTT,DB(SPPM),PHPP,DB(STPM),PHTP,DB(SPTM),PHPT,	ESP15000
3	DB(STRM),PHTR,DB(SPRM),PHPR	ESP15010
333	FORMAT(6(1X,F6.1,1X,F6.1))	ESP15020
	ETAZ(IANG)=CMPLX(SQRT(STTM),1.0E-20)	ESP15030
	EPAZ(IANG)=CMPLX(SQRT(SPPM),1.0E-20)	ESP15040
	STTM=DB(STTM)	ESP15050
	SPPM=DB(SPPM)	ESP15060
	STPM=DB(STPM)	ESP15070
	SPTM=DB(SPTM)	ESP15080
	STRM=DB(STRM)	ESP15090
	SPRM=DB(SPRM)	ESP15100
	IF(IANG.EQ.0.AND.INDZI.NE.0)GOTO701	ESP15110
	IF(IANG.EQ.1.AND.INDZI.NE.0)THEN	ESP15120
	WRITE(6,3190)FMC,STTM,SPPM,STPM,SPTM,PHTT,PHPP,PHTP,PHPT	ESP15130
3190	FORMAT(1X,F8.2,4(2X,F6.2),4(2X,F6.1))	ESP15140
	IF(RF.LT.0.0)WRITE(10,3195)FMC,STTM,SPPM,STPM,SPTM,	ESP15150
2	PHTT,PHPP,PHTP,PHPT	ESP15160
3195	FORMAT(1X,F8.2,4(2X,F6.2),4(2X,F6.1))	ESP15170
	IF(RF.GE.0.0)WRITE(10,3196)FMC,STTM,SPPM,STPM,SPTM,STRM,SPRM,	ESP15180
2	PHTT,PHPP,PHTP,PHPT,PHTR,PHPR	ESP15190
3196	FORMAT(1X,F8.2,6(2X,F6.2)/9X,6(2X,F6.1))	ESP15200
	GOTO701	ESP15210
	ENDIF	ESP15220
	IF(IANG.EQ.1)THEN	ESP15230
	IF(RF.LE.0.0)THEN	ESP15240
	WRITE(6,182)	ESP15250


```

182 FORMAT(/,2X,'** (DEG)** ** CROSS SECTION (DB/M**2) ** ', ESP15260
2 '***** PHASE (DEG) *****' ESP15270
WRITE(6,181) ESP15280
181 FORMAT(3X,'TH PHI STTM SPPM STPM SPTM STTM', ESP15290
2 ' SPPM STPM SPTM') ESP15300
ENDIF ESP15310
IF(RF.GT.0.0)THEN ESP15320
WRITE(6,179) ESP15330
179 FORMAT(/,3X,'** (DEG)** ***** NEAR-ZONE CROSS SECTION ', ESP15340
2 '(DB/M**2) *****' ESP15350
WRITE(6,178) ESP15360
178 FORMAT(3X,'TH PHI STTM SPPM STPM SPTM STRM', ESP15370
2 ' SPRM') ESP15380
ENDIF ESP15390
ENDIF ESP15400
IF(IANG.GE.1)THEN ESP15410
IF(RF.LE.0.0)WRITE(6,183)THDGO,PHDGO,STTM,SPPM,STPM, ESP15420
2 SPTM,PHTT,PHPP,PHTP,PHPT ESP15430
183 FORMAT(1X,F6.1,1X,F5.1,4(2X,F6.2),4(2X,F6.1)) ESP15440
IF(RF.GT.0.0)WRITE(6,184)THDGO,PHDGO,STTM,SPPM,STPM, ESP15450
2 SPTM,STRM,SPRM ESP15460
184 FORMAT(1X,F5.1,1X,F5.1,6(2X,F6.2)) ESP15470
ENDIF ESP15480
701 CONTINUE ESP15490
1920 CONTINUE
C***END OF NEW FIXED BISTATIC ANGLE OPTION
IF(INDZI.NE.0)GOTO3070 ESP15500
916 CONTINUE ESP15510
IF(IEA.EQ.1)GOTO918 ESP15520
599 CONTINUE ESP15530
CALL GETCP2(KCPU) ESP15540
CC CPU=(KCPU-JCPU)/100.0 ESP15550
CPU=(KCPU-JCPU)
WRITE(6,508)NRUN,NWG,CPU ESP15560
508 FORMAT(/,3X,'CPU RUN TIME FOR RUN',1X,I3,' GEOMETRY',1X, ESP15570
2 I3,' = ',F11.2,' SECONDS'/) ESP15580
3070 CONTINUE ESP15590
IF(INDZI.NE.0)THEN ESP15600
NFFS=NFFS+1 ESP15610
IF(NFFS.LE.NFF)GOTO3050 ESP15620
ENDIF ESP15630
600 CONTINUE ESP15640
700 CONTINUE ESP15650
CALL GETCP2(LCPU) ESP15660
CPU=(LCPU-ICPU)
CC CPU=(LCPU-ICPU)/100.0 ESP15670
WRITE(6,507)CPU ESP15680
507 FORMAT(/,3X,'TOTAL CPU RUN TIME = ',F11.2,' SECONDS'/) ESP15690
9374 STOP ESP15700
END ESP15710
SUBROUTINE GETCP(ICPU) ESP15720
C CALL TIMES(DATE,TIME,IVCPU,ITCPU) ESP15730
ICPU=ITCPU*0.0013 ESP15740
RETURN ESP15750
END ESP15760
SUBROUTINE GETCP2(ICPU)
REAL ETIME,TARRAY(2)
TIME=ETIME(TARRAY)
ICPU=TARRAY(1)
RETURN

```

END

```
****data file   filename esp4nam.ratrplate (untitled plate)
&RNCTRL
NGO=1,NPRINT=2,NAUNS=1,NWGS=1,IWR=0,IWRZT=0,INT=4,INTP=6,INTD=18,
INWR=0,IRGM=1,IFIL=0,RF=-1.0,INDZI=0,
&
&FSWEEP
&
&PATTRN
IFE=0,IPFE=1,FNDFE=3.0,PHFE=90.0,
IFA=0,IPFA=1,FNDFE=3.0,THFA=90.0,
ISE=2,IPSE=1,FNDSE=3.0,PHSE=0.0,THIN=90.0,PHIN=0.0,ELRANG=0.,
ISA=0,IPSA=1,FNDSA=3.0,THSA=90.0,
IBISC=1,BETA=120.,NPTBIS=121,BANGRG=-360.,
&
&FWIRET
FMC=1300.0,CMM=38.0,A=0.001,NPLTS=1,
&
&PLATEG
NCNRS(1)=4,SEGM(1)=0.2,IREC(1)=0,IPN(1)=3,IGS(1)=0,ZSHT(1)=(0.0,0.0),
XP(1)=-.4445,0.,.4445,0.,
YP(1)=0.,-.3429,0.,.3429,
ZP(1)=0.0,0.0,0.0,0.0,
&PLATEG
&
&SAVEZ
IWRZM=0,IRDEM=3,
&
&WIREAG
NM=3,NP=4,NAT=1,NFPT=1,NFS1=0,NFS2=0,
X(1)=0.0,0.0,0.0,0.0,-0.3,
Y(1)=0.0,0.0,0.0,0.0,0.0,
Z(1)=0.0,0.25,0.5,0.25,
IA(1)=1,2,2,
IB(1)=2,3,4,
&
&GENLOD
IFMM(1)=3,IABB(1)=0,VLOG(1)=(0.0,0.0),ZLL(1)=(50.0,0.0),
&
&ATTACH
NASAT(1)=1,IABAT(1)=0,NPLA(1)=1,
VGA(1)=(1.0,0.0),ZLDA(1)=(0.0,0.0),BDSK(1)=0.4,
&
****data file   filename esp4nam.ratrtiltp (tilted plate)
```

```
&RNCTRL
NGO=1,NPRINT=2,NAUNS=1,NWGS=1,IWR=0,IWRZT=0,INT=4,INTP=6,INTD=18,
INWR=0,IRGM=1,IFIL=0,RF=-1.0,INDZI=0,
&
&FSWEEP
&
&PATTRN
IFE=0,IPFE=1,FNDFE=3.0,PHFE=90.0,
IFA=0,IPFA=1,FNDFE=3.0,THFA=90.0,
ISE=2,IPSE=1,FNDSE=3.0,PHSE=0.0,THIN=90.0,PHIN=0.0,ELRANG=0.,
ISA=0,IPSA=1,FNDSA=3.0,THSA=90.0,
IBISC=1,BETA=120.,NPTBIS=121,BANGRG=-360.,
&
```

```

&FWIRET
PWC=1300.0,CMM=38.0,A=0.001,NPLTS=1,
*
&PLATEG
NCNRS(1)=4,SEGH(1)=0.2,IREC(1)=0,IPN(1)=3,IGS(1)=0,ZSHT(1)=(0.0,0.0),
XP(1)=-.4445,0.,.4445,0.,
YP(1)=0.,-.2425,0.,.2425,
ZP(1)=0.0,.2425,0.0,-.2425,
*
&PLATEG
*
&SAVEZ
IWRZM=0,IRDZM=3,
*
&WIKEAG
NM=3,NP=4,NAT=1,NFPT=1,NFS1=0,NFS2=0,
X(1)=0.0,0.0,0.0,-0.3,
Y(1)=0.0,0.0,0.0,0.0,
Z(1)=0.0,0.25,0.5,0.25,
IA(1)=1,2,2,
IB(1)=2,3,4,
*
&GENLOD
IFMM(1)=3,IABB(1)=0,VLGG(1)=(0.0,0.0),ZLL(1)=(50.0,0.0),
*
&ATTACH
NASAT(1)=1,IABAT(1)=0,NPLA(1)=1,
VGA(1)=(1.0,0.0),ZLDA(1)=(0.0,0.0),BDSK(1)=0.4,
*

```

REPORT DOCUMENTATION PAGE			Form Approved OMB No. 0704-0188	
<small>Public reporting burden for this collection of information is estimated to average 1 hour per response, including the time for reviewing instructions, searching existing data sources, gathering and maintaining the data needed, and completing and reviewing the collection of information. Send comments regarding this burden estimate or any other aspect of this collection of information, including suggestions for reducing this burden, to Washington Headquarters Services, Directorate for Information Operations and Reports, 1215 Jefferson Davis Highway, Suite 1204, Arlington, VA 22202-4302, and to the Office of Management and Budget, Paperwork Reduction Project (0704-0188), Washington, DC 20503.</small>				
1. AGENCY USE ONLY (Leave blank)	2. REPORT DATE 2 May 1990	3. REPORT TYPE AND DATES COVERED Technical Report		
4. TITLE AND SUBTITLE Bistatic Radar Cross Section of a Perfectly Conducting Rhombus-Shaped Flat Plate		6. FUNDING NUMBERS C -- F19628-90-C-0002 PE -- 63741D PR -- 280		
6. AUTHOR(S) Alan J. Fenn				
7. PERFORMING ORGANIZATION NAME(S) AND ADDRESS(ES) Lincoln Laboratory, MIT P.O. Box 73 Lexington, MA 02173-9108		8. PERFORMING ORGANIZATION REPORT NUMBER TR-880		
9. SPONSORING/MONITORING AGENCY NAME(S) AND ADDRESS(ES) HQ AF Space Systems Division SD/XRS Los Angeles AFB, CA 90009-2960		10. SPONSORING/MONITORING AGENCY REPORT NUMBER ESD-TR-90-008		
11. SUPPLEMENTARY NOTES				
12a. DISTRIBUTION/AVAILABILITY STATEMENT Approved for public release; distribution is unlimited.		12b. DISTRIBUTION CODE		
13. ABSTRACT (Maximum 200 words) The bistatic radar cross section of a perfectly conducting flat plate that has a rhombus shape (equilateral parallelogram) is investigated. The Ohio State University electromagnetic surface patch code (ESP version 4) is used to compute the theoretical bistatic radar cross section of a 35- X 27-in rhombus plate at 1.3 GHz over the bistatic angles 15° to 142°. The ESP-4 computer code is a method of moments FORTRAN-77 program which can analyze general configurations of plates and wires. This code has been installed and modified at Lincoln Laboratory on a SUN 3 computer network. Details of the code modifications are described. Comparisons of the method of moments simulations and measurements of the rhombus plate are made. It is shown that the ESP-4 computer code provides a high degree of accuracy in the calculation of copolarized and cross-polarized bistatic radar cross section patterns.				
14. SUBJECT TERMS bistatic radar cross section prediction rhombus-shaped flat plate perfectly conducting plate		method of moments electromagnetic surface patch code radar cross section measurements		15. NUMBER OF PAGES 90
17. SECURITY CLASSIFICATION OF REPORT Unclassified		18. SECURITY CLASSIFICATION OF THIS PAGE Unclassified		16. PRICE CODE
17. SECURITY CLASSIFICATION OF REPORT Unclassified		19. SECURITY CLASSIFICATION OF ABSTRACT Unclassified		20. LIMITATION OF ABSTRACT SAR